Spring 2007

Development of a 20-ton capacity open ocean aquaculture feed buoy

Chad A. Turmelle
University of New Hampshire, Durham

DEVELOPMENT OF A 20-TON CAPACITY OPEN OCEAN AQUACULTURE FEED BUOY

BY

CHAD A. TURMELLE

B.S., University of New Hampshire, 1999

THESIS

Submitted to the University of New Hampshire

in Partial Fulfillment of

the Requirements for the Degree of

Master of Science

in

Mechanical Engineering

May, 2007

This thesis has been examined and approved.

Thesis Director, M. R. Swift, Professor of Mechanical Engineering and Ocean Engineering

Kenneth C. Baldwin, Professor of Mechanical Engineering and Ocean Engineering

Barbaros Celikkol, Professor of Mechanical Engineering and Ocean Engineering

Date

DEDICATION

This thesis is dedicated to my wife, Amy, for her support and love throughout the entire project.

ACKNOWLEDGEMENTS

I would like to thank the members of my thesis committee for their continued involvement in the project and my education. My special thanks go to M. Robinson Swift. His time and patience in working with me and the project has been invaluable.

My appreciation is extended to the many individuals involved with the Open Ocean Aquaculture project for their generous input and assistance with the buoy. Those individuals that had a direct and substantial impact on the buoy include: Judson DeCew, for his vast amounts of work with the numerical modeling of the buoy and mooring design, Kim Leung, for the FE analysis performed on the buoy mooring plate design. Paul Lavoie, for his great input and fabrication/design assistance with numerous parts located inside the buoy, Glen Rice, for his continued patience with all manner of questions that were directed at him, Michael Chambers, for his input with the design criteria for the feeding systems, Stanley Boduch, for his involvement with the complex electrical system on the buoy, Kurt Swanson, for his input into the hull stiffeners.

My thanks to you all.

Partial funding for this project was obtained by Ocean Spar LLC (formerly Net Systems Inc.) from the National Oceanographic and Atmospheric Administration (NOAA) through their small business innovation research (SBIR) Phase II program under contract number DG133R04CN0156. Additional funding was obtained by NOAA through the University of New Hampshire Cooperative Institute for New England Mariculture and Fisheries (CINEMAR) under grant number NA040AR4600155.

TABLE OF CONTENTS

LIST OF TABLES

LIST OF FIGURES

NOMENCLATURE

A_{wp}	Cross-sectional buoy waterplane area
CG	Center of gravity
f_{fs}	Frequency full scale
f_m	Frequency model scale
F_{fs}	Force full scale
F_m	Force model scale
Fr	Froude number
g	Gravitational constant
GM	Metacentric height
GZ	Righting arm
h	Water depth
H	Wave height
H_{fs}	Wave height full scale
H_m	Wave height model scale
$HeaveAmp_{buoy}$	Heave amplitude buoy
$HeaveAmp_{wave}$	Heave amplitude wave
HeaveRAO	Heave motion response amplitude operator
k	Spring constant
L	Length
L_{fs}	Length full scale
L_m	Length model scale
$PitchAmp_{buoy}$	Pitch amplitude buoy
PitchRAO	Pitch motion response amplitude operator
RAO	Response amplitude operator
$SurgeAmp_{buoy}$	Surge amplitude buoy
$SurgeAmp_{wave}$	Surge amplitude wave
SurgeRAO	Surge motion response amplitude operator
T_{fs}	Period full scale
T_m	Period model scale
Td	Damped natural period
Td_{fs}	Damped natural period full scale
Td_m	Damped natural period model scale
U	Velocity
VCG	Vertical center of gravity
α	Scale factor for model construction
∇	Volumetric displacement
λ	Wavelength
λ_{fs}	Wavelength full scale
λ_m	Wavelength model scale

ABSTRACT

DEVELOPMENT OF A 20-TON CAPACITY

OPEN OCEAN AQUACULTURE FEED BUOY

by

Chad A. Turmelle

University of New Hampshire, May, 2007

A design for a 20-ton capacity buoy was developed to feed fish in up to four submerged cages at an exposed site south of the Isles of Shoals, New Hampshire. The buoy was designed to contain all the equipment necessary to accomplish the feed dispensing tasks as well as have the strength and stability to remain on location in a variety of sea states. New feed handling and distribution systems were developed and tested. To evaluate seakeeping response a Froude scaled physical model was constructed and tested at the Ocean Engineering wave/tow tank at the University of New Hampshire. Construction of the buoy in New Brunswick near the Bay of Fundy is nearing completion, and deployment is scheduled for the summer of 2007.

CHAPTER I

INTRODUCTION

1. Buoy Development

A prototype finfish aquaculture feed buoy, with a 20-ton feed capacity, was developed to supply feed to four submerged net-pens at an exposed site south of the Isles of Shoals, New Hampshire, USA. This type of feeding system is needed because such a commercial system is not available in the United States for exposed sites using submerged cages. A collaborative agreement was made between Ocean Spar LLC and the Open Ocean Aquaculture (OOA) operations and engineering groups at the University of New Hampshire (UNH) to develop a 20-ton capacity feed buoy. The design of the buoy's systems and construction has been ongoing since 2004 and the buoy is scheduled for launch, deployment, and testing in the summer of 2007.

2. Background

a. Aquaculture

Aquaculture is defined as the cultivation of sea products, including fish, shellfish, algae, or other items that come from the sea. While aquaculture is not a novel concept, as can be seen throughout history, open ocean aquaculture is relatively unexplored.

Because the population of the world is increasing and the amount of available arable land decreasing, other sources of food production need to be explored. With over 70% of the earth's surface covered in water, the oceans of the world present an excellent location for expanding food production. With production of capture fisheries at a plateau, new areas of fish production need to be investigated.

One successful arena of fish production is aquaculture. Due to the fact that coastal waters are finite and many competing uses occur there, aquaculture activities need to be further away from the coast. However, the deeper waters away from the coast typically exhibit harsher and more extreme ocean currents and waves. These environmental factors greatly influence the type of fish containment systems as well as their associated mooring systems. The fish feeding systems are also affected by the harsher environment.

A consequence of relocating aquaculture sites further offshore will be a decrease in the frequency with which fish farmers can access the site. Poor weather, an increase in the time required for travel to the site, and other factors will make the journey to and from the site more cumbersome. These difficulties may cause the fish to be fed and the site to be maintained only sporadically, resulting in suboptimal growing conditions. These inconsistent feeding conditions increase the fish grow-out time as well as impact the quality of the fish flesh. However, remotely operated automatic feeding would obviate the problems associated with sporadic travel to the site. Using such a feeding operation, the fish should be fed regardless of the environmental conditions.

b. Project and Site Description

UNH has operated an OOA site in 52 meters of water approximately 10 km from the New Hampshire coast, since 1999 (see Figure 1.1). The site is permitted to perform research related to the operational, engineering, biological, and environmental aspects

of open ocean aquaculture. For over seven years, the site and its associated systems have been the focus of an intense engineering and operational analysis program (see Tsukrov et al., 2000; Fredriksson et al., 2000; Baldwin et al., 2000, Celikkol et al., 2006). Studies were conducted to investigate the dynamics of cage, buoy, and mooring systems so that numerical and physical modeling techniques could be developed to cost-effectively engineer and specify equipment suitable for deployment at the OOA site (see Palczynski, 2000; Tsukrov et al., 2002; Fredriksson et al., 2004a; Fredriksson et al., 2004b).

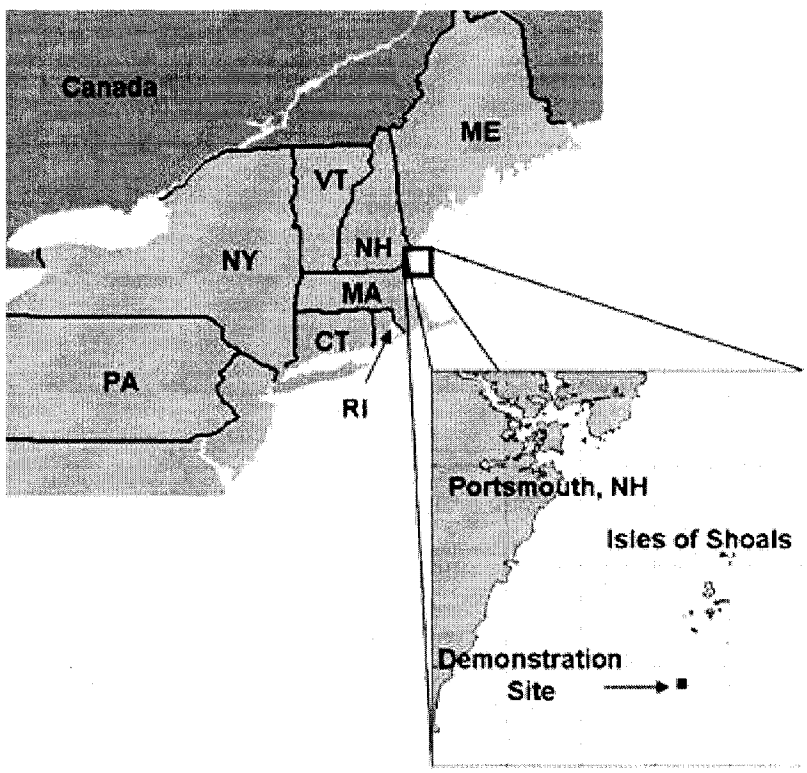

Figure 1.1: Location of OOA Demonstration site off the coast of New Hampshire, USA.

The OOA grid is currently in the second generation of development and testing. The first generation grid was a submerged grid with only one bay, while the second and current generation grid is a four-bay submerged grid (see Figure 1.2). The grid is secured to the seafloor using 9 plow embedment anchors. The grid lines are submerged 65 feet below the surface of the water. The grid lines facilitate attachment of the cages,

marker buoys, and the smaller feed buoys. Each grid line is 220 feet in length, creating individual bays that are square. This grid configuration allows the attachment of a variety of fish containment systems providing the flexibility for the site to be a testing ground for a variety of organizations.

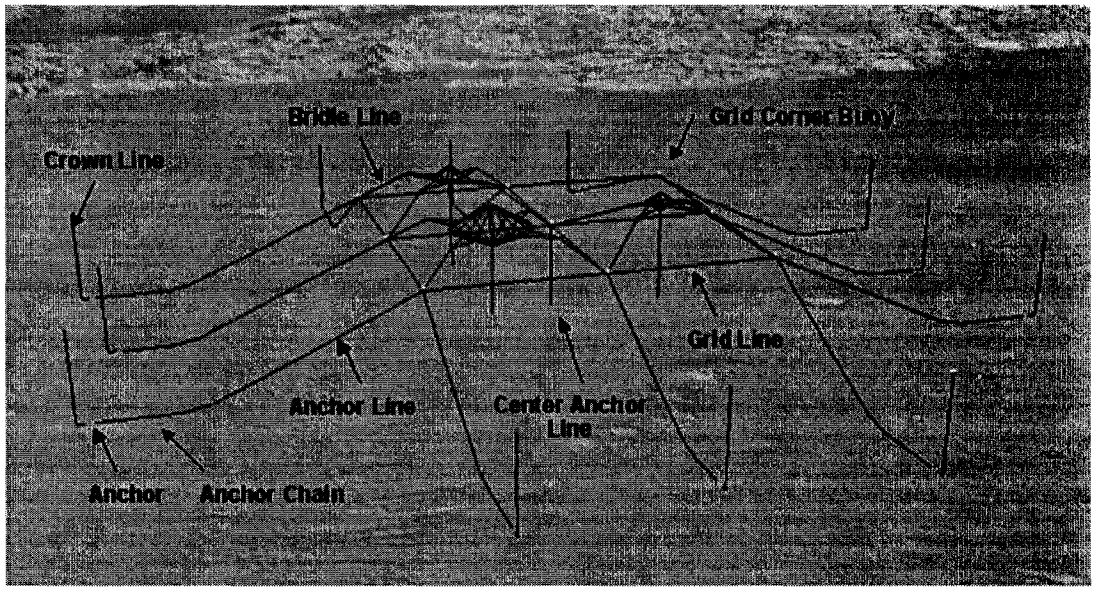

Figure 1.2: Graphical representation of the current UNH OOA grid. The current grid system is a four bay grid.

c. Previous UNH Feeder Designs

Two prototype feed buoys have been developed previously at UNH: a 1/4-ton and a 1-ton feed capacity buoy. Both buoys were designed to feed one submerged cage using water as the medium to transport feed. The 1/4-ton capacity feed buoy has an overall height of 17 feet, a diameter of 5 feet, and an approximate weight of 4,500 pounds full of feed (see Rice et al., 2003, Fullerton et al., 2004). The 1/4-ton buoy hull is constructed entirely of aluminum. The feed is stored high in the buoy, above the waterline. The major internal components are labeled in Figure 1.3.

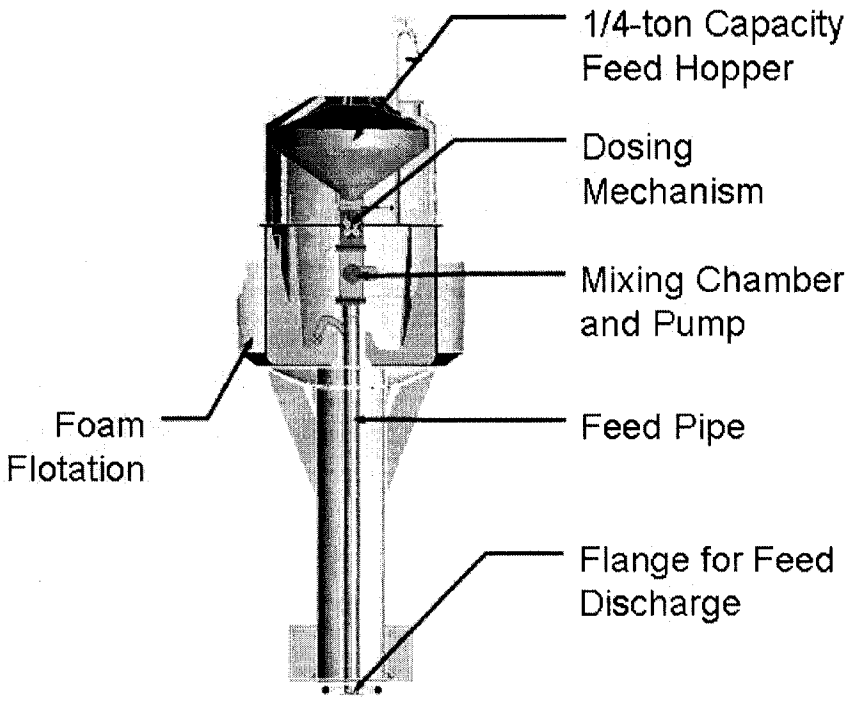

Figure 1.3: Cross-section of 1/4-ton capacity feed buoy. Major internal components are labeled.

The 1-ton capacity feed buoy has an overall height of 33.5 feet, diameter of 8.2 feet, and an approximate weight of 17,200 pounds full of feed. The lower section of the 1-ton buoy is constructed of steel, while the upper section is of aluminum. Similar to the 1/4-ton buoy, the feed is stored high in the buoy, above the waterline. The major internal components are labeled in Figure 1.4.

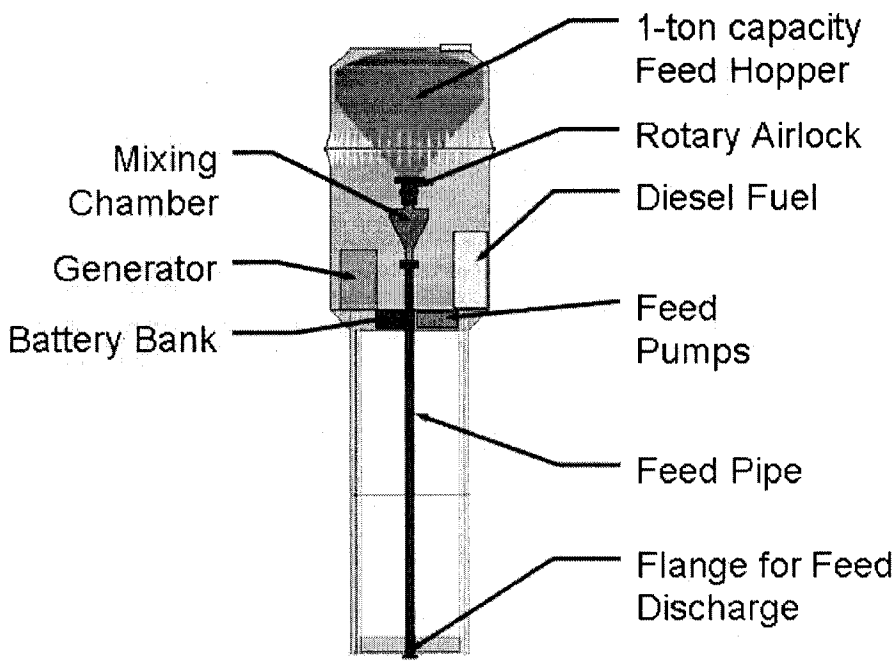

Figure 1.4: Cross-section of 1-ton capacity feed buoy. Major internal components are labeled.

Since the 1/4-ton buoy was the first feed buoy designed by UNH, it was kept as simple as possible. Due to its low power usage, the buoy is powered exclusively by renewable resources: wind and solar power. However, the 1-ton buoy's power requirements necessitated a diesel generator in addition to solar panels.

The external feeding systems of the 1/4-ton and 1-ton buoy are similar. The mixing chamber is located high above the waterline (along with the feed) to minimize back pressure wetting of the rotary airlock. In both cases, the main feed pump is upstream of the feed/water mixing location.

3. Goals / Objectives

The goal was to design, analyze, and build an open ocean aquaculture 20-ton capacity feed buoy. Some individual goals contained within the overall goal of the buoy include the following:

- Contain four separate feed storage bins and feed four separate submerged cages allowing any feed storage bin to supply any cage.
- Develop a feed delivery system that places the feed storage bins low in the buoy and attains large flow rates over long distances without back pressure problems. Transport feed in a water medium using submerged feed hoses.
- Design a strong hull, with minimal overall size, that allows sufficient space inside the buoy for all power generation, feed systems, and electrical equipment required for operation.
- Possess the hydrodynamic stability to survive the storm conditions normally observed at the OOA site.
- Allow independent operation of the buoy, at the OOA site, for several days.

4. Approach

A design criteria was established for the buoy and its feeding system. Preliminary buoy hull shapes and configurations were generated, and space for components, reserve buoyancy and righting moment, and heave and pitch natural frequencies were investigated. A general layout for the buoy hull, internal components, and ballast configuration was determined. New systems needed for this size of feed buoy were identified and designed, including the internal and external feed transport systems. Full scale experimental testing of new feed systems and their individual components were performed. Physical model testing was done using a Froude scaled physical model in the UNH ocean engineering wave/tow tank. Mooring system design and components were iteratively determined using a finite element analysis model. Construction was undertaken, and deployment is scheduled for late summer of 2007.

CHAPTER II

DESIGN CONFIGURATION

1. Design Criteria / Rationale

With the goal of designing a large feed capacity buoy, a list of design criteria was generated. Two separate sets of design criteria were developed: one for the overall buoy, and a second set focused on the feeding system. These criteria resulted from numerous consultations with all groups involved with the OOA project represented. The majority of the criteria were developed from spring 2004 until the winter of 2005. Throughout the design process new issues that were identified were added into the design criteria.

Overall Buoy Design Criteria

The overall buoy design criteria is a list of desired characteristics that were most influential in shaping the design for the 20-ton buoy. All the items listed below were addressed during the design and development process.

Feed capacity

- 20 tons (40,000 pounds)

Feed storage

- Four separate storage bins, allowing four different species/sizes of fish to be fed
  - Different species require specialized feed
  - Varying stages of development requires different size feed

Wave Response

- Survive design wave/current conditions (9 meter height, 8.8 second period, 1 meter/second current)
- Minimize resonance (especially heave) at storm wave frequencies
- 20 tons (40,000 pounds)

Hydrostatics

- Sufficient reserve buoyancy/freeboard
- Positive righting moment at all angles
  - Including ice build-up
- Watertight integrity
  - Vents and hatches
- Positive buoyancy

Machinery

- Located above waterline whenever possible

Power system

- Power generated for all electrical needs

Control & telemetry

- System to allow user to control feeding systems remotely
- System monitoring to allow viewing of important electrical systems remotely

Mooring

- Buoy outside of grid (due to grid limitations)
- Accommodate water level variations
- Survive design wave/current conditions (9 meter height, 8.8 second period, 1 meter/second current)

Maintenance

- Internal components (systems) must be accessible for routine maintenance while deployed

Safety systems

- Incorporate safety features into the design, including fire suppression systems, air quality monitoring and control, radio communication systems, and abandon ship equipment

Feeding System Design Criteria (External feed transfer)

The feeding system design criteria is a focused set to design goals for the external feed transfer system. These criteria are independent of the main design goals for the overall buoy design.

General

- Any storage bin (silo), total of four, should be able to feed any cage, total of four
- Feed one cage from one silo at a time
- Four separate feed hoses exit the buoy
- Each feed hose is connected to one cage

Feed amounts (flow rates)

- A maxi mum feed transfer rate of 1800 pounds/hour. Assuming an average feed density of 37 pounds/cubic foot, the volume feed rate is approximately 50 cubic feet/hour.
- A time limit of 5 minutes of transport time from buoy to cage

Geometry

- The maximum assumed length of tube from buoy to cage is 800 feet
- Approximate discharge height of feed tubes from buoy is 10 feet above the waterline –or– the feed tubes will be exiting through the bottom of the buoy
- Buoy to cage pipe size diameter is 3 or 4 inches

Size

- Space is limited in the buoy, so size should be minimized
- Because the majority of the system will be located high in the buoy, keeping the weight low is important

Other considerations

- A continuous feeding system is desired over a batch feeding system. This is to minimize the amount of time required to feed.
- Feed transfer rate is most likely to be slower than the water transfer rate due to the feed and pipe wall interaction (including turbulence of flow)
- System should be able to survive all situations that the feed buoy will experience, including storm waves and freezing temperatures. However, feeding will most likely not occur in 'heavy' seas.

Upon completion of the design criteria, the design process was started. Since the buoy's systems are interdependent, no single system could be designed separately. The design process was divided into three major subsystems: Hydrostatics/Hull shape/Wave Response, Internal Feed Transfer System, and External Feed Transfer System. The iterative design process, including development of feed storage, fuel storage, ballast configuration, feeding systems, hull shape, and hydrostatics, began in spring 2004 and was completed in the winter of 2006.

2. General Arrangement

The buoy is comprised of the hull structure and the internal and external feeding systems (see Figures 2.1 and 2.2). The hull shape was developed to survive the environmental conditions expected at the OOA site as well as contain all components necessary for feeding operations. The machine house, the uppermost portion of the buoy, is used to contain the electronics, motors, and diesel generator for buoy control, feed transfer, and power generation. The bulk of the main hull is used for storage of the 20 tons of feed as well as the major external feeding components, including the mixing chamber. The lowest section of the buoy, the ballast can, contains the concrete ballast used for stability of the buoy.

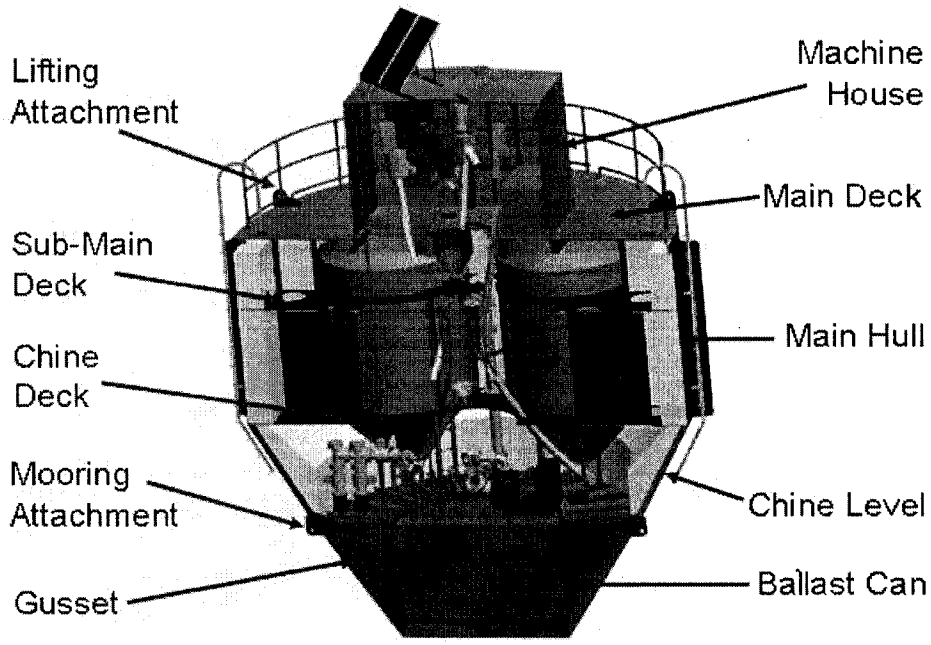

Figure 2.1: Cross-section of 20-ton capacity buoy showing major buoy sections as well as major external components.

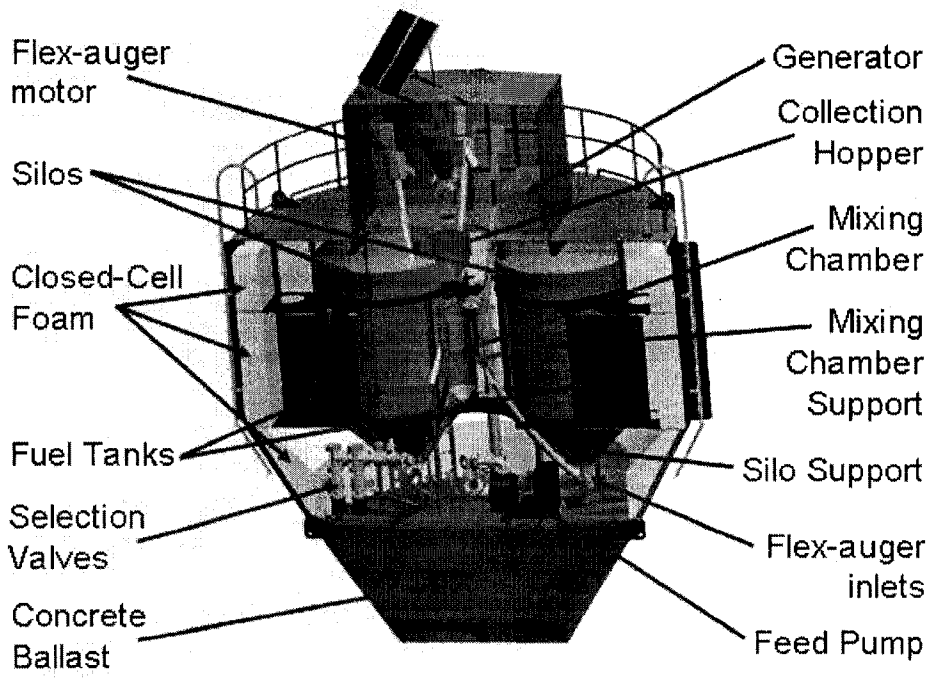

Figure 2.2: Cross-section of 20-ton capacity buoy showing major internal components.

Four mechanical flex-augers, part of the internal feed transfer system, have inlets located beneath each silo and transfer the feed pellets through flexible pipes up to the central collection hopper in the superstructure. Below the hopper is the mixing chamber, where water is introduced to create a mixture which is piped down centrally to the feed pump on the inside base of the buoy. The mixture is then pumped through selection valves to one of four exits located on the buoy bottom – each connected by feed hose to one of four cages.

As the design was developed to the final product described above, iterative hydrostatic analyses were undertaken. The initial design underwent a basic numerical evaluation, and as the design progressed, detailed computer analyses were updated resulting in re-sizing, re-ballasting and modifications in major weight placement. The hydrostatics of the buoy was a driving mechanism in the design and configuration of the buoy.

3. Hydrostatics

Hydrostatics analysis, much like the buoy design, began with a first principles approach, which progressed to a detailed analysis. With each modification to the buoy design, the hydrostatic analysis was revised. Particular interest was given to hull shape and weight distribution to have the following characteristics: reduce heave and pitch response, positive righting moments at various heel angles, as well as sufficient reserve buoyancy under operational environmental conditions.

The first step in determining the hull shape was to investigate the desired buoy wave response characteristics by estimating natural frequencies. In the planning phase, this was done using previous buoy data and a dimensionless parameter called the shape factor (SF). After a general hull shape was determined and approximate weights of major items were positioned, a computer model was created for further detailed hydrostatic analysis.

a. Shape Factor

To estimate the resonant heave and pitch frequencies for the initial design concept, a database of various buoy hull shapes tested at UNH was utilized. These shapes were translated into a dimensionless shape factor (SF), which relates displacement and waterplane area. The SF is defined as

$$SF = \frac{\nabla^{1/3}}{A_{wp}^{1/2}}, \qquad [2.1]$$

where ∇ is the volumetric displacement and A_{wp} is the cross-sectional waterplane area of the buoy. The database includes a range of SFs, including spar type buoys (SF greater than one) to large diameter can type buoys (SF less than one). The database incorporates model data as well as full-scale measurements. These values were Froude-scaled to the same size as the 20-ton design concept for comparison (see Table 2.1).

Table 2.1: Various shape factors known from previous model testing performed at UNH for generation of the 20-ton capacity design.

	Shape Factor	*Heave Period (seconds) **	*Pitch Period (seconds) **
Waverider	0.501	3.797	---
20-Ton:			
load	0.702	4.251	11.826
light	0.706	4.261	11.836
1/4-Ton	0.736	4.327	11.895
1-Ton	0.919	5.232	12.267
100-Ton Spar	1.410	7.317	11.907
30-Ton Spar	1.704	7.705	12.295

* Values were scaled to 20-ton weight so resonant periods could be directly compared.

By using equation 2.1, the SF for the current 20-ton buoy concept was found to be 0.704 (average value). From the SF, the heave and pitch resonant periods were estimated by linear interpolation. Resonant periods resulted for heave and pitch were 4.256 and 11.8 seconds, respectively. These values were considered adequate because, in general, 4 second waves typically do not produce extreme amplitudes (unlike storm waves with periods greater then 8 seconds). Therefore, operational activities would be more manageable. In waves with periods longer than 4 seconds, it is expected that the buoy will be a wave follower. During fair weather operations (3 to 5 second period waves), the buoy is expected to be stable in pitch. Though resonance with long period storm waves is not desirable, at least no one is expected on deck, and pitch/roll motion will be strongly influenced by the mooring system.

With a desirable SF determined for the buoy design, a detailed hydrostatic analysis commenced. However, determining the displacement and waterplane area of the buoy was far from a completed design. With every component of the buoy that was finalized, a more accurate overall weight and center of gravity was obtained. These values in conjunction with the overall hull shape were used to create a computer model that was then used for the iterative hydrostatic analysis.

b. Pro/ENGINEER Solid Model

Mechanical Design

All mechanical design was performed with the aid of the 3D solid modeling computer program Pro/ENGINEER. Generating the buoy design utilizing 3D solid modeling had numerous benefits, including ease of design modifications, observing component physical interaction problems, and the relative ease of generating 2D construction drawings. Solid modeling was an essential asset used in the buoy design process.

All buoy components, from the largest exterior hull sections to the smallest electrical panel, could be located inside the solid model. This allowed for geometric verification that all necessary components were not occupying the same space as another component.

Mass Distribution

In order to perform a detailed hydrodynamic analysis, the mass (weight) distribution needed to be evaluated. Since every mass could not be specified until the design was complete, only the major sources of mass were included for the initial analyses. As weights were determined and components added, additional analyses were performed.

Given shapes and material densities, weights and centers of gravity (CG) of individual components were generated from the 3D solid model. These values were then tallied to obtain the buoy overall weight and CG.

c. Rhino Surface Model

To quickly and easily perform a variety of hydrostatic analyses, a computer program, RhinoMarine, was used. RhinoMarine is a hydrostatic analysis plug-in for the

3D surface modeling program called Rhinoceros® 3D (Rhino). The exterior surface of the buoy was generated using Rhino and then analyzed using RhinoMarine (see Figure 2.3).

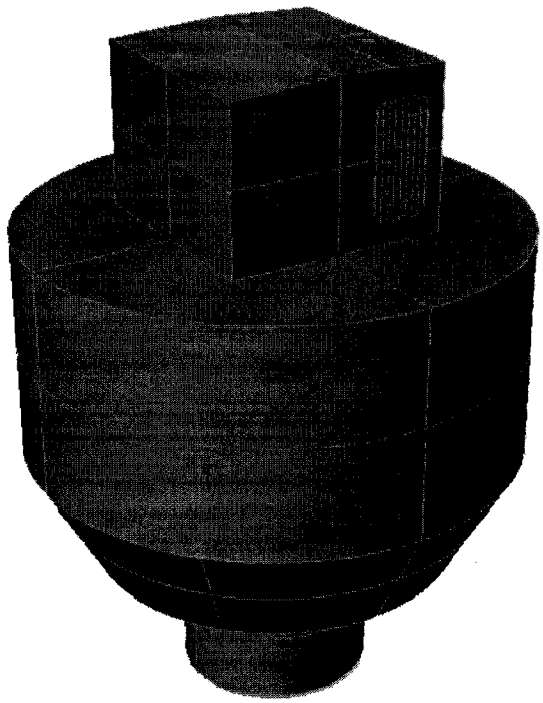

Figure 2.3: Rhino model created for use in the hydrostatic analyses performed using RhinoMarine.

Aside from the exterior surface geometry, the CG and mass (weight) of all components were needed for the hydrostatic analysis. These values were obtained using the 3D solid model.

To simplify the Rhino model, exterior components that displace small amounts of water were omitted, including the gussets that connect the Ballast Can to the bottom of the Main Hull, ladders, fenders, mooring attachment points, and zincs. However, weights and CG values for these items were included in the overall weight and CG of the buoy.

Using the weights and CG values from Pro/ENGINEER, a hydrostatic analysis was performed using Rhino for load and light conditions. The varying overall weight of the buoy is due to the fact that during operation, the feed and fuel inside the buoy will be consumed by the fish and generator, respectively. To bracket the possible operational

conditions, the two extreme loading conditions were analyzed: load and light. The load condition corresponds to a situation were the buoy is full of feed and fuel, while the light condition is without feed or fuel. The hydrostatic analysis included a heel analysis to determine the righting arm for the buoy at different angles of heel under the different loading conditions.

For the hydrostatic analysis, an initial stability design criterion was applied. The initial stability of a floating object depends on its metacentric height (GM) (Tupper, 1996). The GM value is an indication of the initial stability of the buoy: positive values indicate stability; zero values indicate neutral stability; negative values indicate instability. Thus, the larger the positive value of GM, the more stable the buoy.

By observing Figure 2.4, a graphical representation showing values of interest, the physical value of GM is seen as the straight line distance between points G and M. Point G is the CG of the buoy, and point M is the metacenter. The figure shows the Rhino model of the buoy design displaced a small angle from vertical. For the buoy to be stable using the initial stability criterion, point M must be above point G, resulting in a positive value of GM.

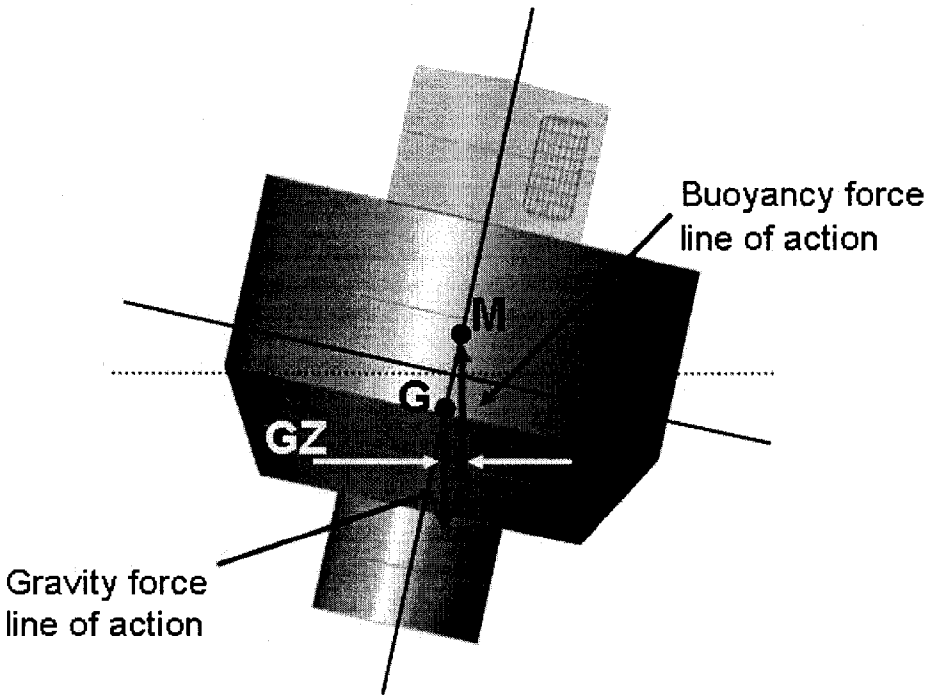

Figure 2.4: Rhino model showing graphical representation of metacentric height (GM). Metacentric height is the distance from point G to M. GZ is the righting arm.

Both the GM values (load and light conditions) are positive and over two feet (see Table 2.2). This is an indication that the buoy is stable. Since there is the possibility that the feed storage bins will be emptied at different rates, a stability calculation was performed for the case that two feed storage bins, on the same side, are empty, while the other two are full. This resulted in a static heel angle of 14 degrees.

Table 2.2: Hydrostatic results for buoy under load and light weight conditions.

	Load	Light
Weight (pounds)	175,366	135,318
Draft (inch)	159.25	140.35
Metacentric height – GM (inch)	26.75	38.35

The Rhino hydrostatic analyses also provided insight into the freeboard and reserve buoyancy for the buoy under the two investigated loading conditions. The minimum freeboard (up to the Main Deck) of the buoy under the load condition was found to be 7.7 feet. The reserve buoyancy/weight to immerse was calculated to be 2,120 pounds/inch. The freeboard and reserve buoyancy were determined to be adequate under the worst case load condition.

All the righting arm (GZ in Figure 2.4) values were found to be positive (see Figure 2.5) as well as increasing through heel angles of up to 90 degrees. This shows that if the buoy heels over, the righting moment (righting arm multiplied by displacement) will work to push the buoy back to a nominal heel angle (more vertical position).

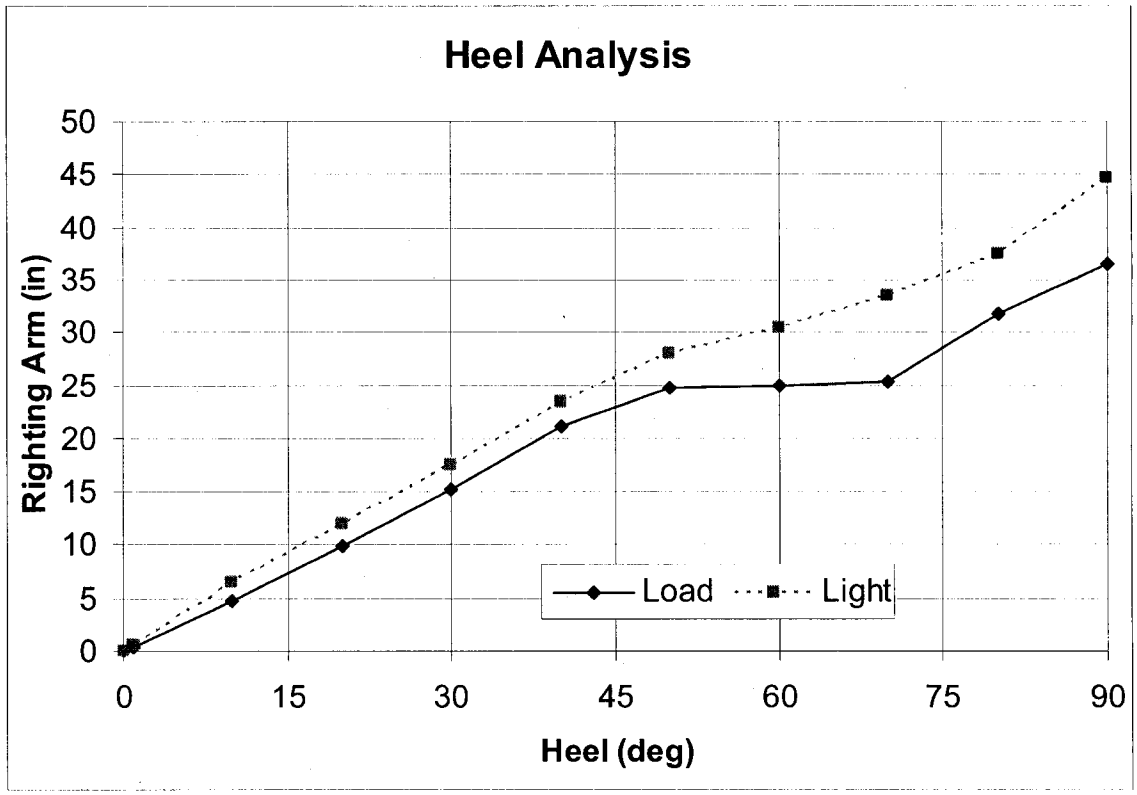

Figure 2.5: Stability heel analysis righting arm (GZ) curves for the final design.

Principles of Naval Architecture, published by the Society of Naval Architects and Marine Engineers (SNAME), provides stability criteria derived from the International Maritime Organization (IMO) for intact stability of fishing vessels and passenger vessels. Stability values for the final buoy configuration were well above the requirements for both types of vessels.

d. Ice Loading

Ice build-up over the winter months on the above-waterline exposed surfaces was identified as a potential problem that needed to be addressed with the 20-ton

design. A basic static ice build-up analysis was performed utilizing a worst case loading condition based upon previous evidence from past winters.

The worst case icing condition was assumed to be 6 inches of ice on all surfaces above the waterline. The ice weight resulted in a 15% increase in the overall buoy weight, reducing the freeboard by approximately 8 inches.

Since ice is most likely not going to be evenly distributed over all surfaces of the buoy, an additional analysis was performed with 6 inches of ice distributed over half the buoy. This analysis assumed 6 inches of ice on half of all exposed surfaces, all on one side. This resulted in a heel angle range of approximately 17-18 degrees.

An updated hydrostatic analyses was performed (based upon design changes) which incorporated ice loading. Table 2.3 shows the results of the hydrostatic analyses performed under ice loading conditions. Again, these GM values are positive, demonstrating the initial stability of the buoy.

Table 2.3: Hydrostatics results under ice loading conditions

	Load		Light	
	Full Load*	**½ Load****	**Full Load***	**½ Load****
Weight (pounds)	205,371	188,129	160,720	143,475
Draft (inch)	167.25	165.6	146.25	144.85
GM (inch)	10	21.9	12.15	25.35
Heel angle (degree)	< 1	16.9	< 1	18.1

* Full Load refers to an ice loading on all exposed surfaces above the waterline.
** ½ Load refers to an ice loading on one side of the buoy's exposed surfaces.

e. Foam Buoyancy

With the buoy's ultimate survivability of utmost importance, it was decided to incorporate internal buoyancy into the design. The absolute need for positive buoyancy became apparent during the design development. It is vital to have positive buoyancy in the case of free flooding to keep the buoy at the surface.

To accomplish the positive buoyancy requirement, foam flotation was incorporated into the buoy. The volume of foam required to keep the buoy at the surface in the event of free flooding is greater than the volume of available free space inside the buoy. However, foam combined with the feed storage silos (sealed at the top and bottom) can provide adequate buoyancy.

f. Evolution of Hydrostatics Analysis

Over the months of design refinement, additional systems were incorporated into the design resulting in a weight increase. These weight increases demanded that new hydrostatic analysis be performed. New GM values were calculated with every new hydrostatic analysis. In an effort to keep the GM as large as possible, a few different strategies were implemented, including increasing the ballast weight and the diameter of the buoy. The initial stability analyses showed positive GM values in all cases tested. This leads to the conclusion that, under the tested conditions, the buoy will be a stable feeding platform.

4. Hull Structure

The hull structure is composed of five main components: Machinery House, Main Deck, Main Hull, Chine Level, and the Ballast Can (see Figure 2.1). Every section of the hull is made of steel ranging in thickness from 1/4 inch to 1/2 inch. The major outside dimensions are shown below in Figures 2.6 and 2.7. Dimensions[1] and specifications of construction of individual components are described in their respective and following sections.

---

[1] All dimensions given in the included dimensioned drawings, in Chapter 2 Section 4, are in inches unless otherwise specified.

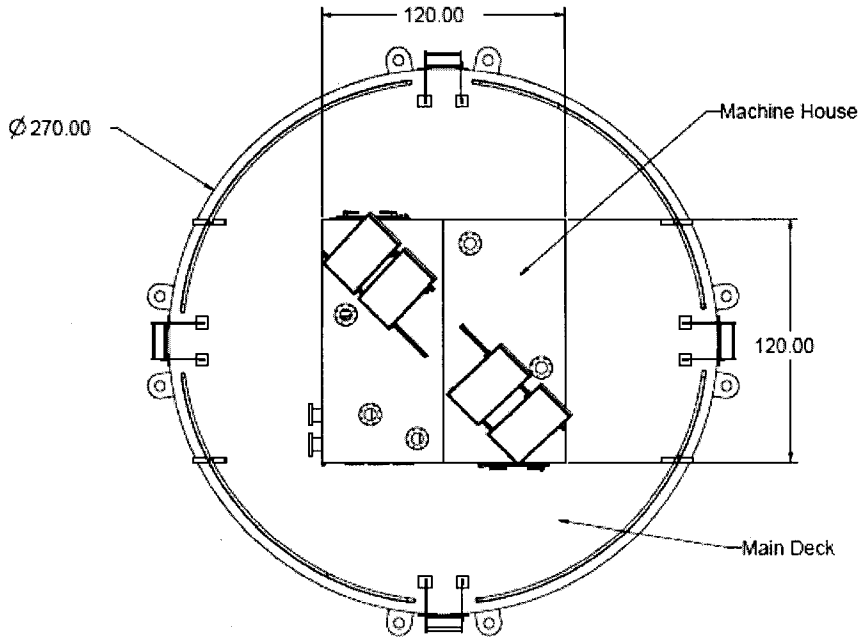

Figure 2.6: Top view of buoy showing major external dimensions (inches).

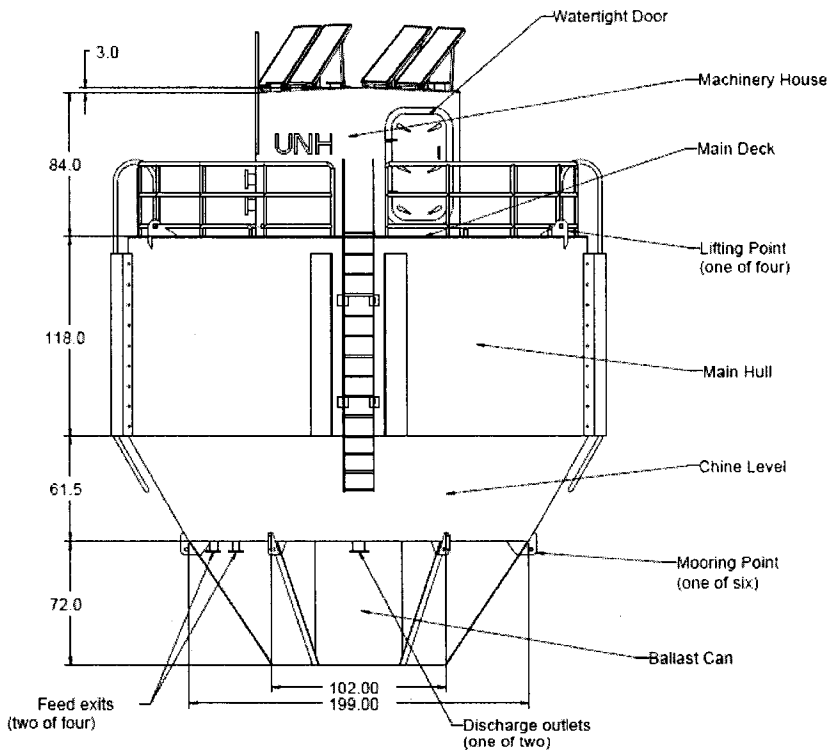

Figure 2.7: Front view of buoy showing external dimensions (inches).

a. Machinery House

The Machinery House (see Figures 2.1, 2.6, and 2.7) encloses the majority of the buoy's electrical system, electric motors, and generator in addition to feed transfer mechanisms. This is the main workstation for personnel on the buoy. The structure is 120 inches long and 120 inches wide with an overall height of 87 inches. It is constructed of 1/4 inch steel plate. The majority of the scantlings are to be 3 x 2 x 1/4 inch steel angle. These are located approximately 18 inches on center for the four walls and roof (see Figure 2.8). In addition, a larger set of scantlings consisting of 6 x 4 x 3/8 inch steel angle is used to support the roof ridge member and run vertically on each opposing end wall. The horizontal steel angle ridge member, of the same size, is welded on top of the two vertical supports.

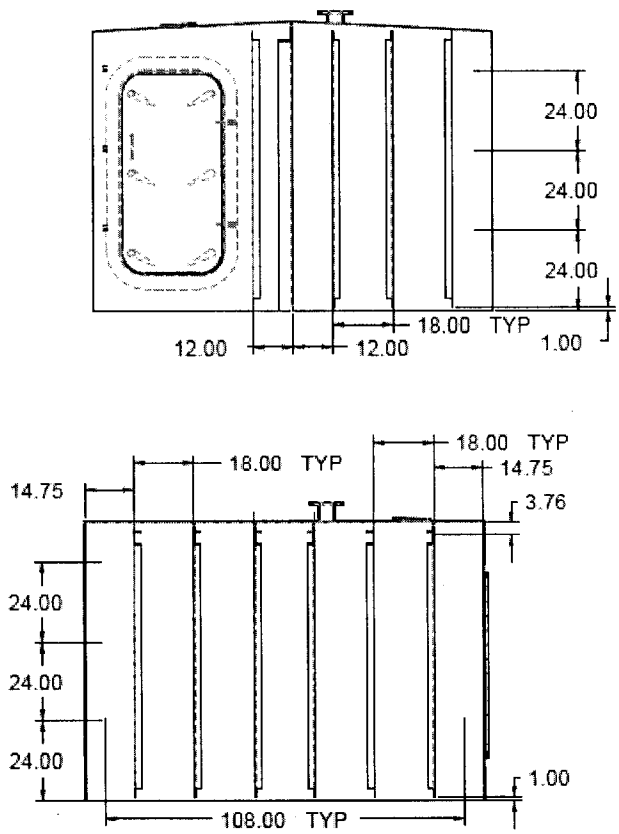

Figure 2.8: Internal section views of the Machinery House showing scantling spacing (inches) and orientation for two different walls. The walls on opposing sides have the same scantling arrangement.

The other major construction items involved with the Machinery House are the two 6-Dog watertight doors that have a clear opening of 60 x 30 inches. There are also nine access hatches. These include four flex-auger installation/removal hatches (located on the roof), four external cage wiring hatches (located on one wall) and one external wiring access hatch (located on the roof). These hatches are constructed of 6 inch Schedule 80 steel pipe with 150 pounds per square inch standard flanges welded to the pipe's exterior end. Blind flanges were then bolted to the access flanges to ensure watertight integrity.

b. Main Deck

The Main Deck (see Figures 2.6, 2.7, and 2.9) is composed of the exterior platform as well as the machinery house interior. Lifting attachments are also incorporated into the Main Deck (see Figures 2.1, 2.7, and 2.9). The deck is constructed of 1/4 inch steel plate, and has an outer diameter of 270 inches. It is supported by four main scantlings, 9 x 4 x 1/2 inch steel angle, that run under the machinery house walls. These are toe-outward to allow a 120 inch square opening below the main deck. One scantling, 6 x 4 x 3/8 inch steel angle, runs inside the square center opening to aid in supporting the generator. Also, inside the square opening are other 3 x 3 x 1/4 inch steel angles (spaced 18 inches on center) that run perpendicular to the 6 x 4 x 3/8 inch angle (notched) and span the full 120 inch interior opening.

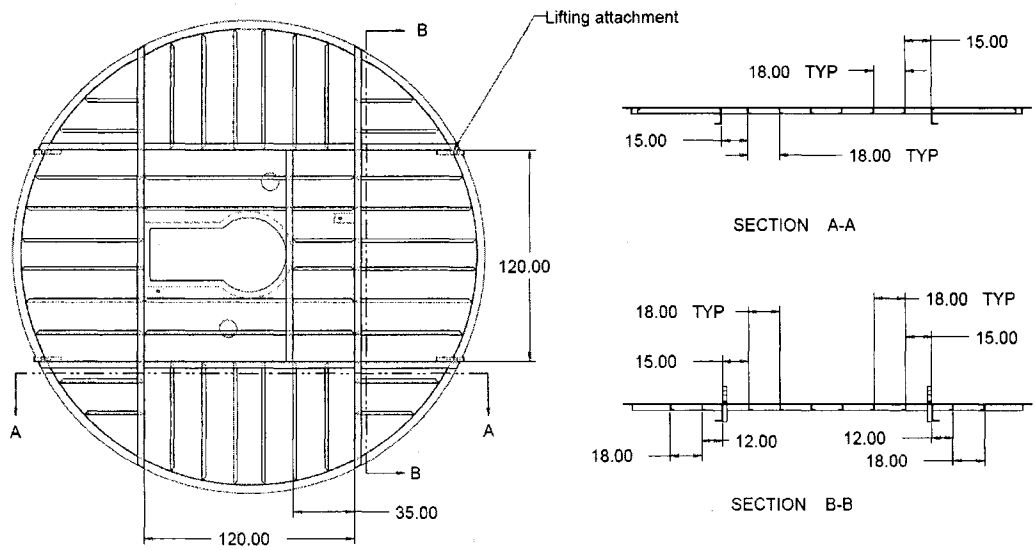

Figure 2.9: Bottom view of Main Deck with scantling spacing detail.

Scantlings for the exterior main deck are also 3 x 3 x 1/4 inch steel angle (spaced 18 inches on center) that start, running perpendicular, from the large main scantlings and proceed to the outer edge of the buoy. These scantlings are terminated at a rolled 3.5 x 1/4 inch flat bar welded to the underside of the deck at a radius 4.5 inches less than the outer radius of the buoy. This allows the vertical scantlings, from the lower sections of the buoy, to extend as close to the deck as possible and still allow access, on the inside, to the outermost deck-hull intersection.

The Main Deck interior has a large 'keyhole' shaped opening to allow personnel access to the lower levels. This hole also has a 2 x 1/4 inch flat bar around the edge to keep water inside the machinery house from penetrating the lower levels. Also on the interior deck are two fuel fill containment barriers. These are made of 3.5 x 1/4 inch flat bar stock. Three sides of the bar and the machinery house wall surround each of the two fuel fill access holes. Miscellaneous access holes were cut in the Machine House floor to allow flex-auger, feed fill lines, keel cooling and fuel lines to penetrate the lower sections. The majority of these holes are 2 inches or smaller in diameter. The flex-auger holes and feed fill lines are no larger than 8 inches.

The lifting attachments (see Figures 2.1, 2.7, and 2.10) are welded to the ends of the four large main deck support beams (see Figure 2.9) as well as the Main Hull section.

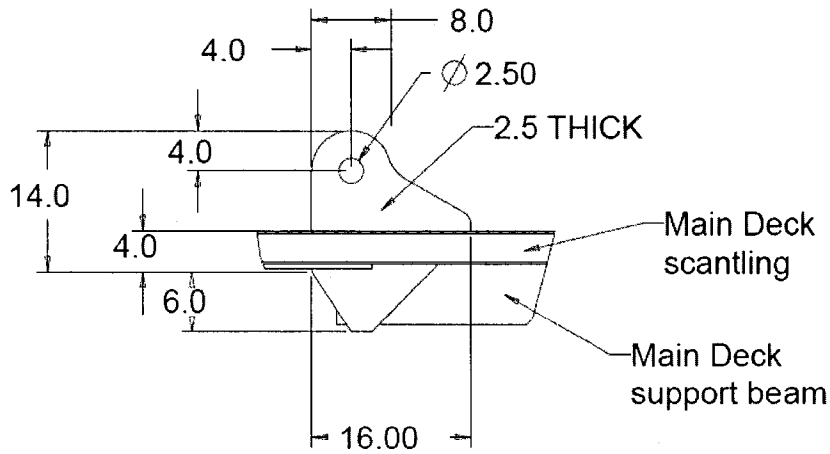

Figure 2.10: Lifting attachment plate detail.

c. Main Hull

The Main Hull (see Figures 2.1, 2.7, and 2.11) encloses the feed storage bins (4 silos), diesel fuel tanks, and the feed/water mixing chamber. Two intermediate decks (see Figure 2.1) are also located inside the Main Hull. Lifting points for the buoy are also incorporated into the Main Hull and Main Deck intersection, as discussed in the previous section.

The shell is constructed of 3/8 inch rolled steel plate. The overall diameter is 270 inches with a height of 117.75 inches. The scantlings are 3 x 3 x 3/8 inch steel angle that run vertically along the hull. They are spaced at 7.5 degrees or approximately 18 inch increments (48 total) around the complete circumference of the inner surface.

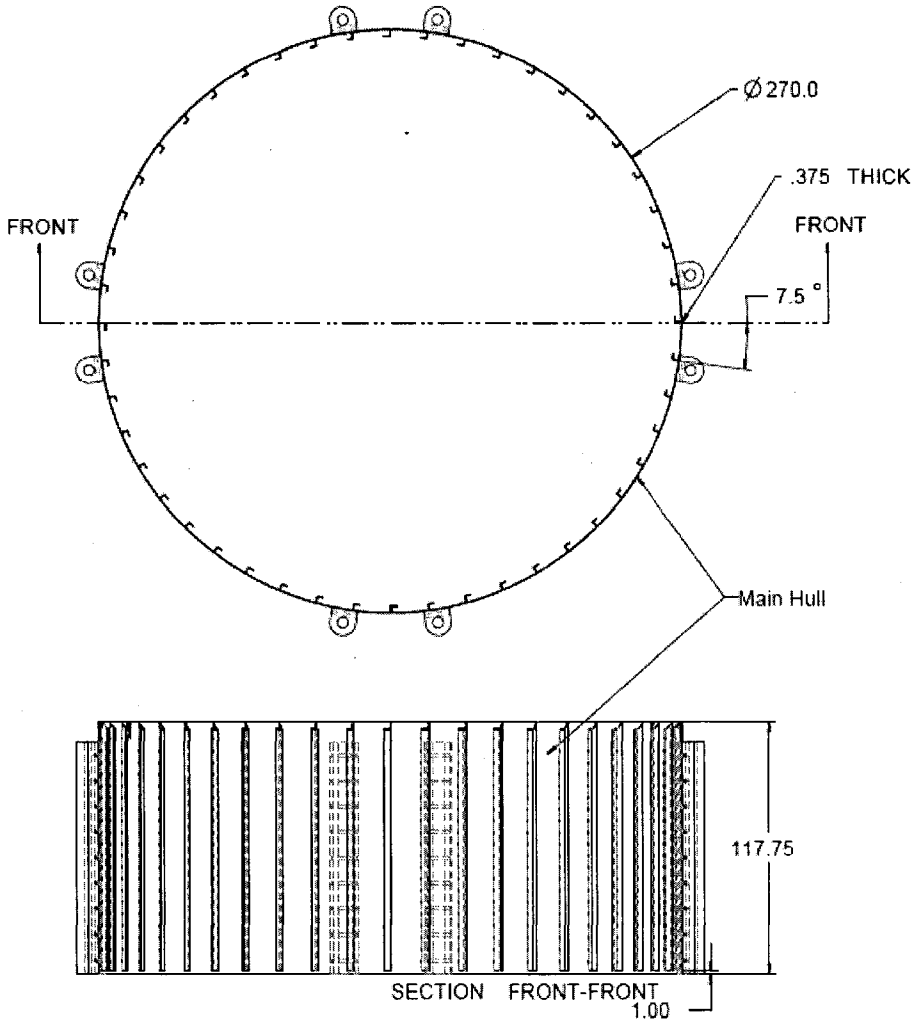

Figure 2.11: Top and Section FRONT-FRONT view of the Main Hull.

The Main Hull cross-section is spanned by two intermediate decks (see Figures 2.12 and 2.13). The location of these decks in the overall buoy structure can be seen in Figure 2.1. They are constructed using 3/8 inch steel plate. They have a diameter of 269.25 inches and contain cutouts for all vertical hull scantlings. The main features of the decks are the large holes to allow the feed silos to pass through them as well as a large center hole to allow personnel access to the lower levels. Smaller holes allowing access through the decks for other systems are also necessary.

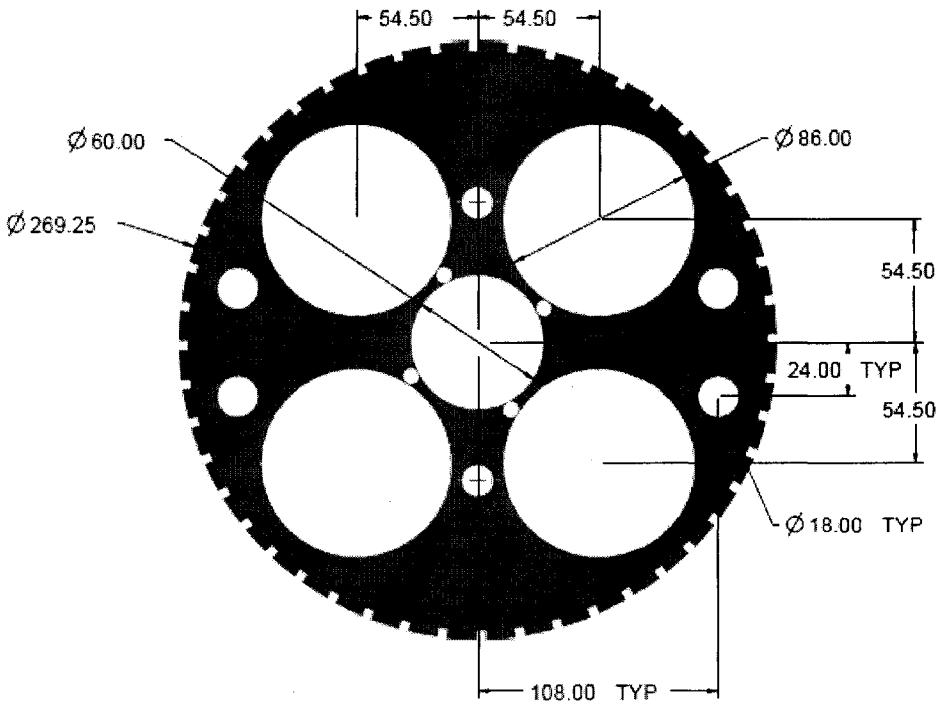

Figure 2.12: Chine deck – located at bottom of Main Hull section.

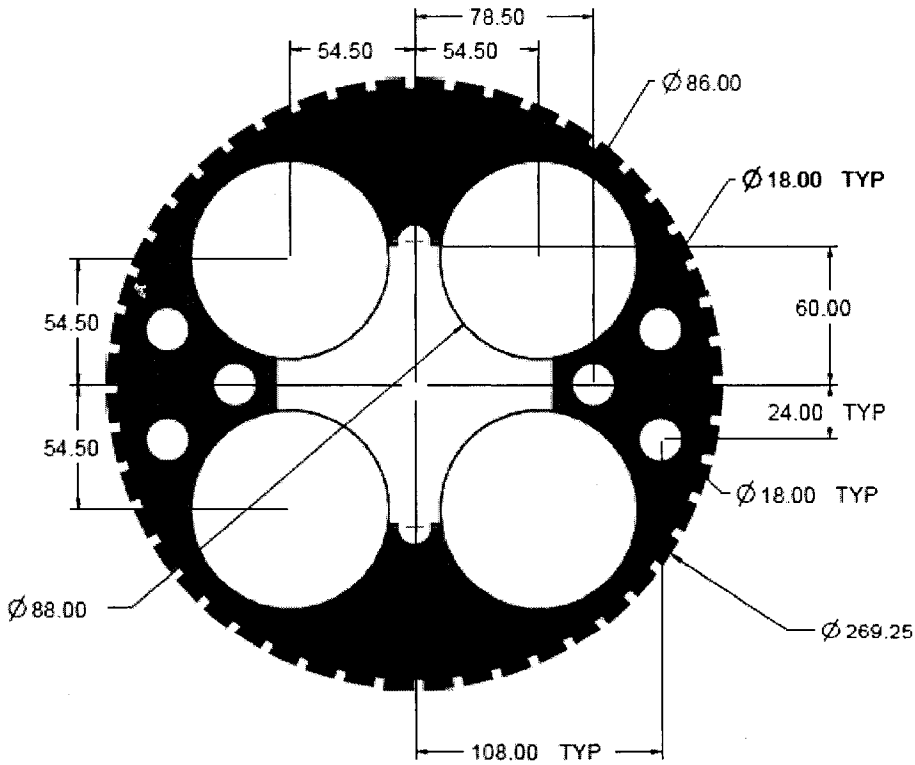

Figure 2.13: Sub-Main Deck – located 72 inches above the Chine Deck.

An additional structural element that is located within the Main Hull section is the Mixing Chamber support structure (see Figures 2.2 and 2.14). It is constructed of a 3/8 inch flat plate ring and assorted lengths of 3 x 3 x 3/8 inch steel angle. The bottom of the support ring is welded to the horizontal supports. The vertical steel angle is welded in between the Chine Deck and Sub-Main Deck. The angled steel angle is to be bolted to the other components to allow removal of the structure, so that removal of larger items is possible.

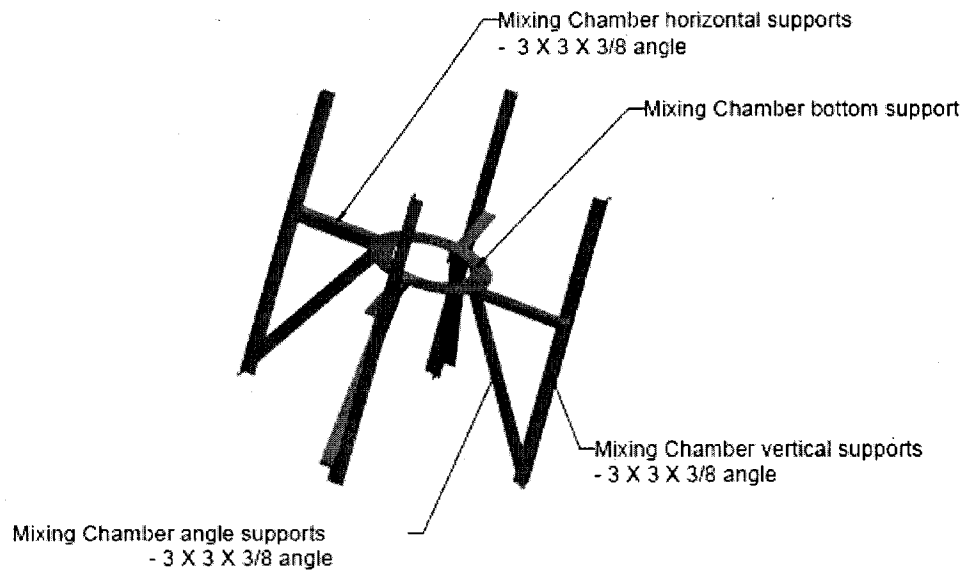

Figure 2.14: Assembly of Mixing Chamber support structure.

Due to the environment that the buoy will be placed in, the silos will require vertical restraints at the top. These consist of a shallow angle cone, made of steel sheet metal (14 gauge), with a 24 inch diameter. Each silo has one cap that was welded above the center of the silo to the Main Deck framing.

One final component in this section is the foam supports. These are constructed of 3 x 3 x 3/8 inch steel angle. The angle was cut to length and welded in-between (vertical orientation) the interior decks, the Chine Deck and Sub-Main Deck. Steel angle was also welded in-between the Sub-Main Deck and Main Deck. The foam supports

were positioned inside the buoy to ensure the foam would remain in its desired position around the periphery of the buoy.

d. Chine Level

The Chine Level is the region between the lower and upper chines (see Figures 2.1, 2.7, 2.15, and 2.16). This section encloses the bulk of the equipment required to transport feed to the cages. All thru-hull fittings are located on the bottom of this level. Pumps, piping, silo supports, and mooring attachments are located in this section.

The actual chine level is comprised of a flat lower 'floor' section and conical wall section. The lower section is made of 1/2 inch steel plate, while the conical section is constructed of 3/8 inch rolled steel plate. The scantlings for this section are the same size and material as that of the Main Hull section, 3 x 3 x 3/8 inch steel angle. They also mate with the vertical scantlings from the adjoining section. The scantlings are joined by a simple plate bracket, to provide continuous support between the sections of the buoy. The lower section of the chine level has half the number (24 total) of scantlings as the mating sections, every other one omitted.

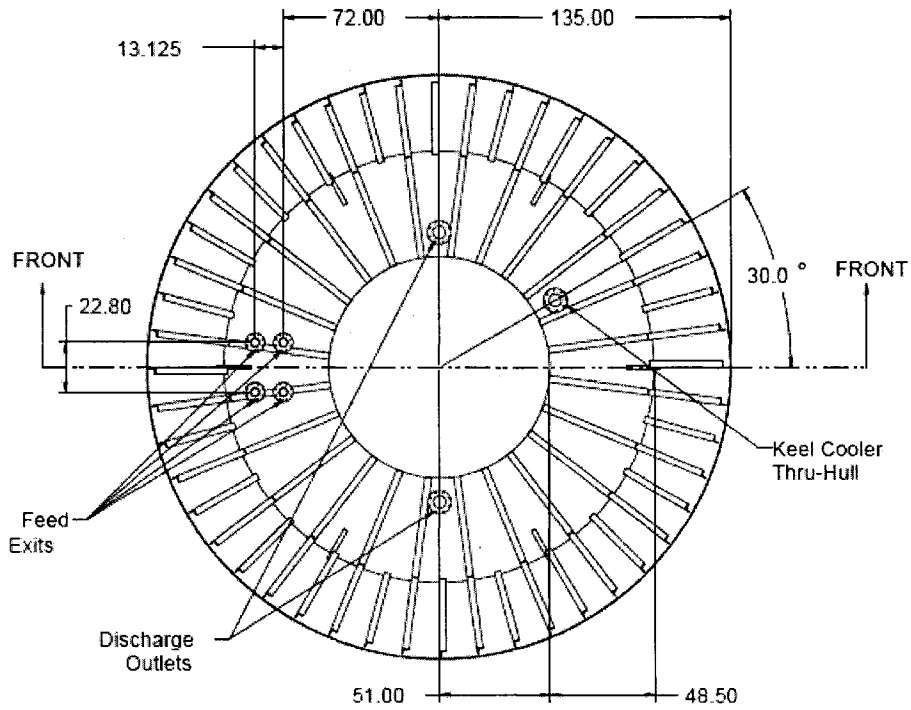

Figure 2.15: Top view of Chine Level.

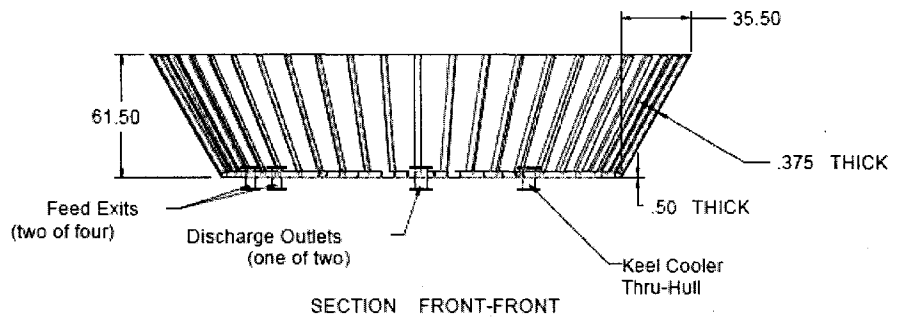

Figure 2.16: Section Front-Front view of Chine Level.

The silo support structures are located in this chine section (see Figures 2.2 and 2.17). There are four of these structures (one per silo). Steel angle, 3 x 2 x 1/4 inch, is welded to the bottom of the Chine Deck and the silo support base. The sheet metal cone (14 gauge) is welded to the angle silo supports. Below the base plate are three short vertical supports, welded to the bottom of the Chine Level. The long vertical supports are welded to the angle silo supports and the bottom of the Chine Level. The base plate is

where the remainder of the feed transfer equipment is mounted, which includes knife gate valves, charging adapters, and the bottom of the flex-auger systems.

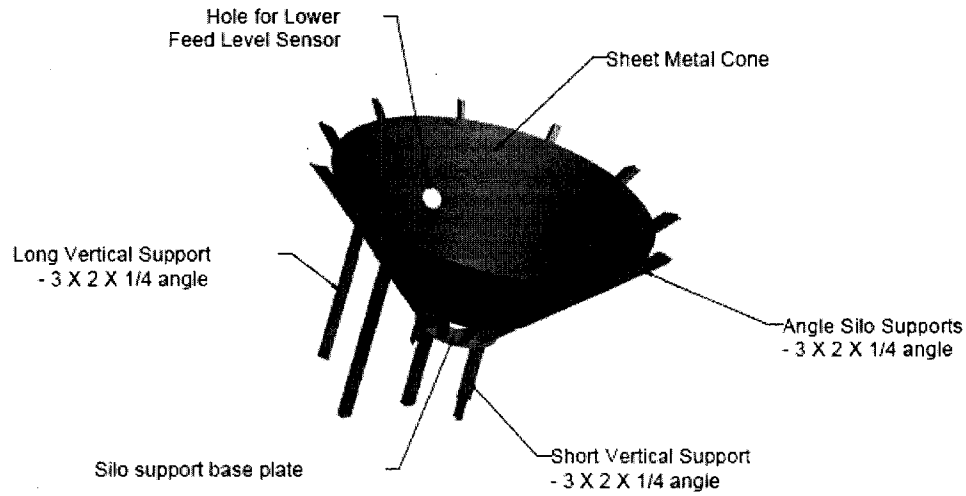

Figure 2.17: Assembly of Silo support structure.

Critical thru-hull fittings are located on the floor of the Chine Level. These fittings are schedule 80 steel pipe with flanges welded to both ends (exterior and interior). There are four 4 inch and three 6 inch fittings. The 4 inch fittings are used for feed transport to the cages, while the 6 inch fittings are for the keel cooler, mixing chamber overflow and pump inlet.

The mooring attachments (see Figures 2.1, 2.7, and2.18) are incorporated into the floor of the Chine Level, the Chine Level scantlings, as well as the six gusset plates for the Ballast Can discussed in the following section. Each gusset plate and Chine Level intersection has a mooring attachment (6 total).

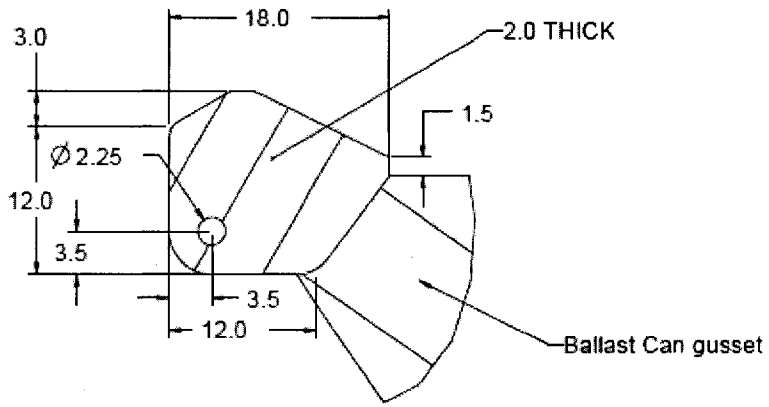

Figure 2.18: Mooring attachment plate dimensions.

e. Ballast Can

The Ballast Can (see Figures 2.1, 2.7, 2.19, and 2.20) holds the concrete ballast for the buoy. Also involved in this section are the gussets from the Ballast Can to the Chine Level. Sumps for bilge pumps and pump mounts are located within this structure.

All steel involved with the construction of the Ballast Can is 1/2 inch thick, including the gussets, sides, and bottom. Support framing is located at the bottom of the Ballast Can. This radial framing, consisting of 1/2 inch thick plate, intersects at a central vertical 6 inch diameter rod which is 12 inches tall. These plates and rod join all the gussets together. The concrete, poured into the buoy during construction, has a final weight of approximately 49,000 pounds with a density of 150 pounds per cubic foot.

The Ballast Can sides protrude into the Chine Level. This allows the scantling ends for the Chine Level to be welded to the Ballast Can. In addition, scuppers were cut into the top of the Ballast Can side to allow water passage from the lower Chine Level to the center of the Ballast Ban where the bilge pumps are located.

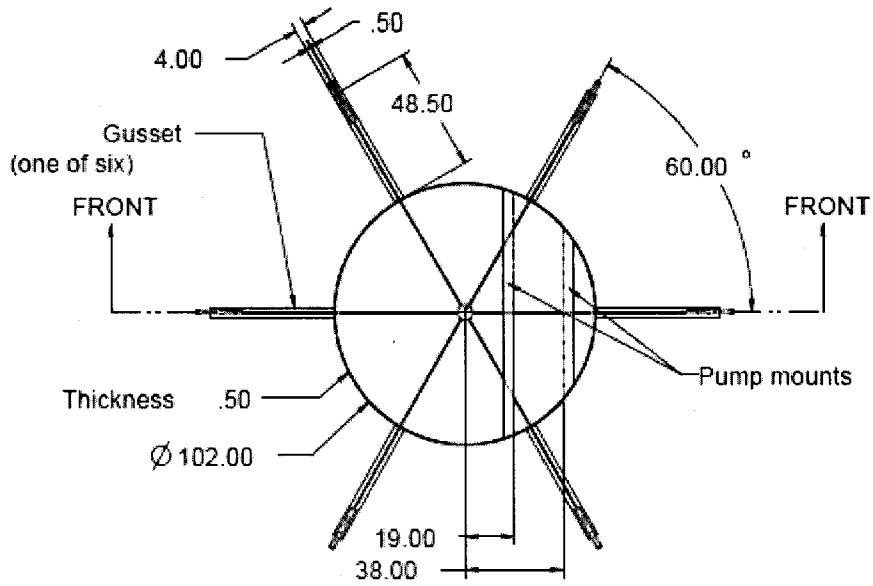

Figure 2.19: Top view of Ballast Can.

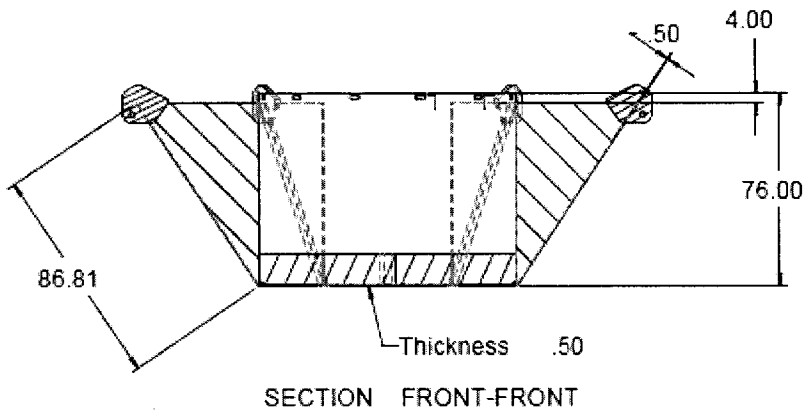

Figure 2.20: Section FRONT-FRONT of Ballast Can.

f. Mooring Plate Analysis

Mooring plates were incorporated into the hull structure of the buoy (see Figure 2.21). In order to maximize the loads the plates could withstand they were incorporated into the intersection of the Chine Level and Ballast Can gussets. This was done to provide the greatest weld area surrounding the mooring plates.

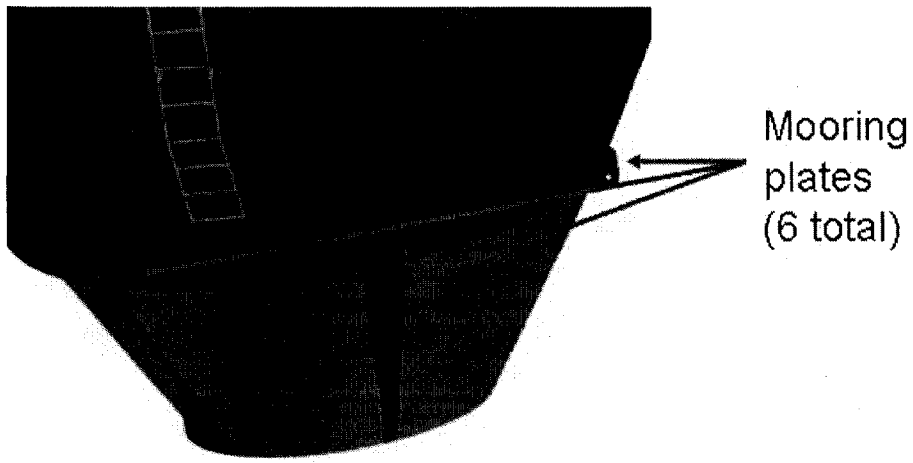

Figure 2.21: Exterior view of buoy showing location of three mooring plates. The remaining mooring plates are on the opposite side of the buoy.

The mooring plate design is shown in Figure 2.22(a) with the dimensions shown in Figure 2.22(b). Though six mooring plates are provided, the buoy is intended to be moored using four legs. The mooring design is discussed in greater detail in Chapter VI.

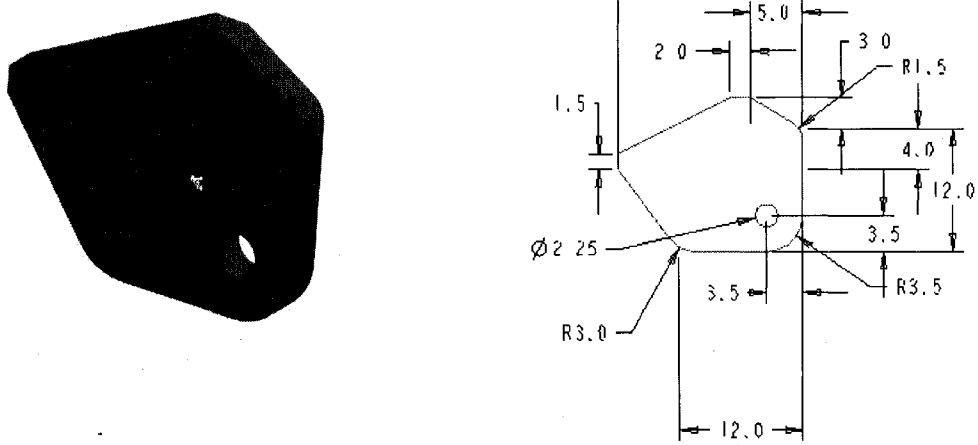

(a) (b)

Figure 2.22: (a) The mooring attachment plate and (b) its dimensions in inches.

A finite element (FE) analysis was performed on the mooring plate design using the software package Marc.Mentat. A worst-case single mooring attachment load value of 40,000 pounds was used for the analysis. The load value was determined using

UNH's analysis program called Aqua-FE, which is capable of analyzing ocean systems involving waves and currents. The load value stated above was calculated using the UNH storm wave that has a 9 meter wave height and an 8.8 second period. One mooring plate was assumed to sustain the entire load (worst case condition).

For analysis purposes, any component of the mooring attachment plate that was to be welded inside the buoy was considered fixed. This yielded the Marc.Mentat model mesh, as tested, shown in Figure 2.23. The load of 40,000 pounds was distributed over the inside of the hole as shown by the arrows in Figure 2.23, while holding the left most line of nodes as fixed.

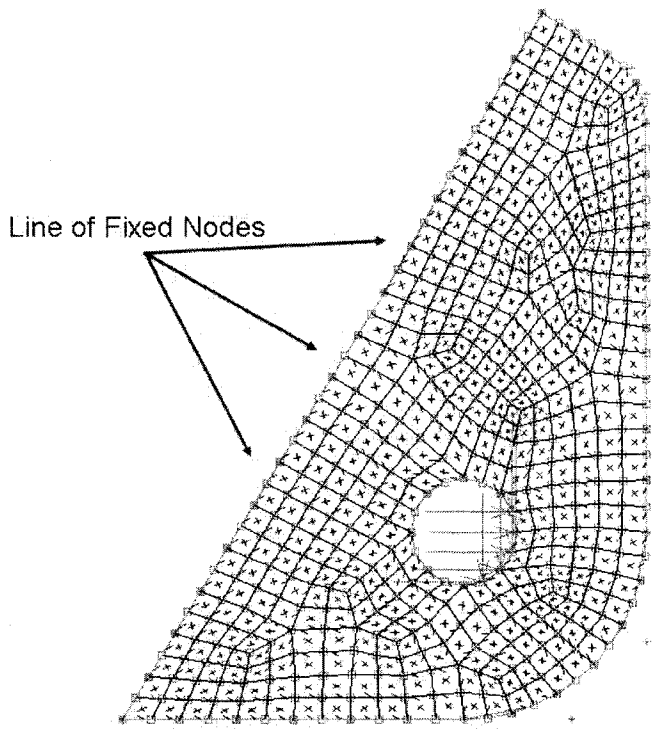

Figure 2.23: Model configuration with hole loading.

The resulting calculated stresses are shown in Figure 2.24. The maximum equivalent von Mises stress was calculated to be 17,566 pounds/square inch and is well below the yield stress for ASTM-36 steel (36,000 pounds/square inch). Thus the mooring plate has a safety factor of two based upon the single point worst-case load.

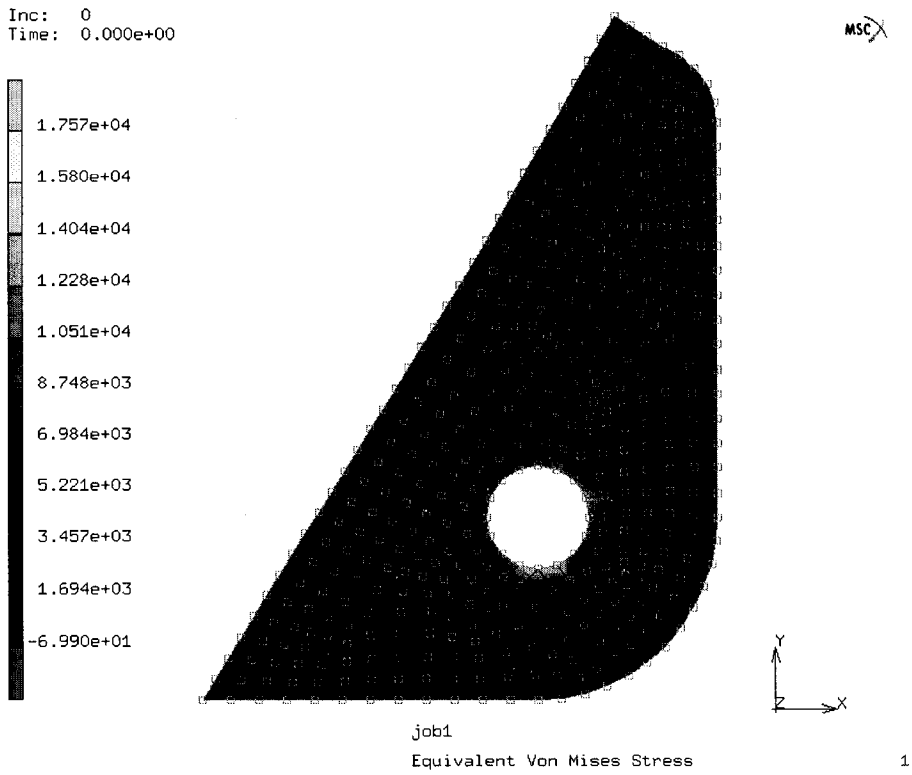

Figure 2.24: Equivalent von Mises stress distribution. Maximum stress observed was 17,566 pounds per square inch.

CHAPTER III

DESIGN OF FEED TRANSFER SYSTEMS

1. Internal Feed Transfer System

One of the main challenges with the larger buoy design is the addition of a major system to handle internal feed transfer. Both the existing ¼-ton and 1-ton UNH feed buoys have not required a system of this type because the feed could be stored high in the buoy. Since a 20-ton feed capacity is required, the feed needs to be located low in the buoy for stability concerns.

Possible types of internal feed transfer systems investigated included: flexible screw augers, straight augers, aero-mechanical conveyors, bucket elevators, cable conveying methods and pneumatic systems. After an extensive review of the options, the search list was narrowed down to flexible augers or pneumatic systems.

a. Pneumatic vs. Flexible auger

Pneumatic transfer systems use moving streams of air within metal piping. A pump circulates the air inside the closed loop piping system; the material to be conveyed is introduced into the air flow and carried by the air stream. Flexible augers typically consist of a flexible plastic pipe with a metal helix (spring coil shape) inside. The helix is connected to an electric motor that spins the helix which transports the material.

A trip to Eastport, ME was conducted to view a pneumatic conveying system, in operation. Pneumatic conveying methods are currently used extensively for fish feed pellet transfer. These systems are used to transfer feed to surface cages as well as for feed transport inside a structure. However, for this buoy design, it is not possible to use a pneumatic system for external transport to cages due to the use of submerged cages. The feed needs to be delivered in a water medium.

Since fish feed pellets have not typically been used in a flexible auger system a field test was conducted at Flexicon Corporation, on 9 September 2004, located in Bethlehem, PA. A system comparable with our needs was setup and tested. Two different sizes of feed were tested: 6.5 millimeter and 13 millimeter. A 4 inch and 3 inch diameter auger system were tested on both feed sizes. The auger motor was operated at 230 revolutions per minute during testing. For the 4 inch auger system, both sizes of feed were conveyed without problem at a transfer rate of over 100 cubic feet/hour (approximately 3700 pounds/hour, depending upon the density of feed being conveyed). The 3 inch auger system performed poorly with the larger diameter feed pellet, resulting in the 4 inch pipe size being selected for use.

Since both types of systems could fulfill the desired task of transporting feed, a meeting was conducted, on 27 September 2004 by engineering and operations personnel, to examine the major differences between the systems. The result of the discussion was that a flexible auger system was the best choice. The major factors in the decision were cost, maintenance, and complexity.

The concept for the internal feed transfer is shown graphically in Figure 3.1. The need for four separate storage bins results in four flexible augers. The augers are curved due to the physical space constraints inside the buoy.

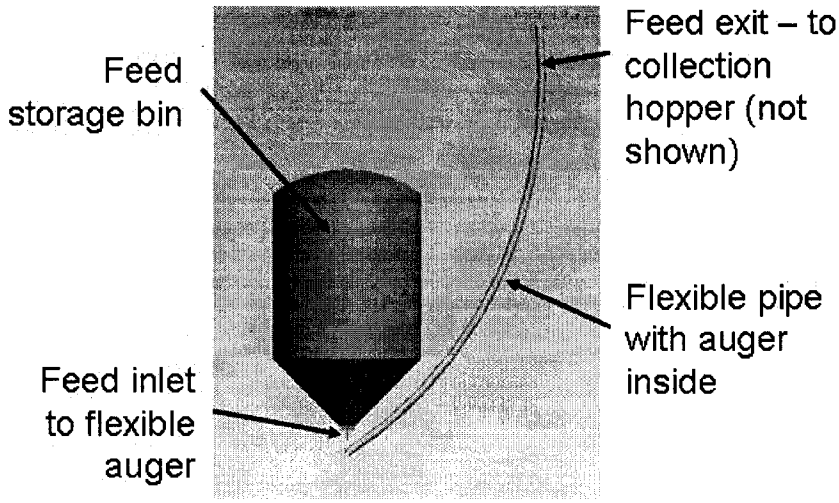

Figure 3.1: Internal feed transfer system for one feed storage bin.

2. External Feed Transport System

a. Concept

Since the UNH aquaculture site uses submerged cages, the feed must be delivered to the cages in a water solution. Due to the size of the proposed buoy design it will have to be moored separately from the grid, resulting in extremely long hoses (approximately 800 feet) running from the buoy to the cages. To best protect the hoses they need to be submerged, further indicating a need for feed delivered in a water solution.

A major design decision was whether to use a batch or continuous feeding system. Since the design criteria specifies a maximum of 1800 pounds/hour needs to be transferred, a batch system cannot be used. This is due to the start/stop time (approximately 15 seconds) required for the pumps to cycle on and off. With limited time to move the large volume of feed the amount of batches is limited, requiring the batches to be much larger. Since a larger batch size is not a desirable characteristic, the decision was made to use a continuous feeding system. For a continuous system to function a

free surface, water to air interface, is needed. Pumping water through a pipe creates back pressure (head pressure) and causes the water level of free surfaces to rise. The continuous feeding system needs to have a method to control the level of the water to eliminate the possibility of flooding the buoy.

The concept for a continuous feeding system uses a mixing chamber, two pumps and piping. A schematic of the concept is shown in Figure 3.2. The external feeding system process begins with valves (not shown in figure), located after the feed pump, opening or closing to direct the feed into the appropriate discharge pipe to feed the desired cage. Then the supply pump turns on to fill the mixing chamber and prime the feed pump. Once the water reaches the desired level all extra water will exit through the two exit (overflow) pipes. These pipes are very large (6 inches) in relation to the inlet pipe (3 inches). The flow rate for the inlet pump is to be twice the exit pump so that the mixing chamber will always have water inside it. Once the water reaches the desired level, the feed pump will be started. Up to this point no feed has been introduced into the system. After the water is moving and the free surfaces are created in the mixing chamber, the feed can be dropped in. A rotary airlock will control the feed introduction into the mixing chamber.

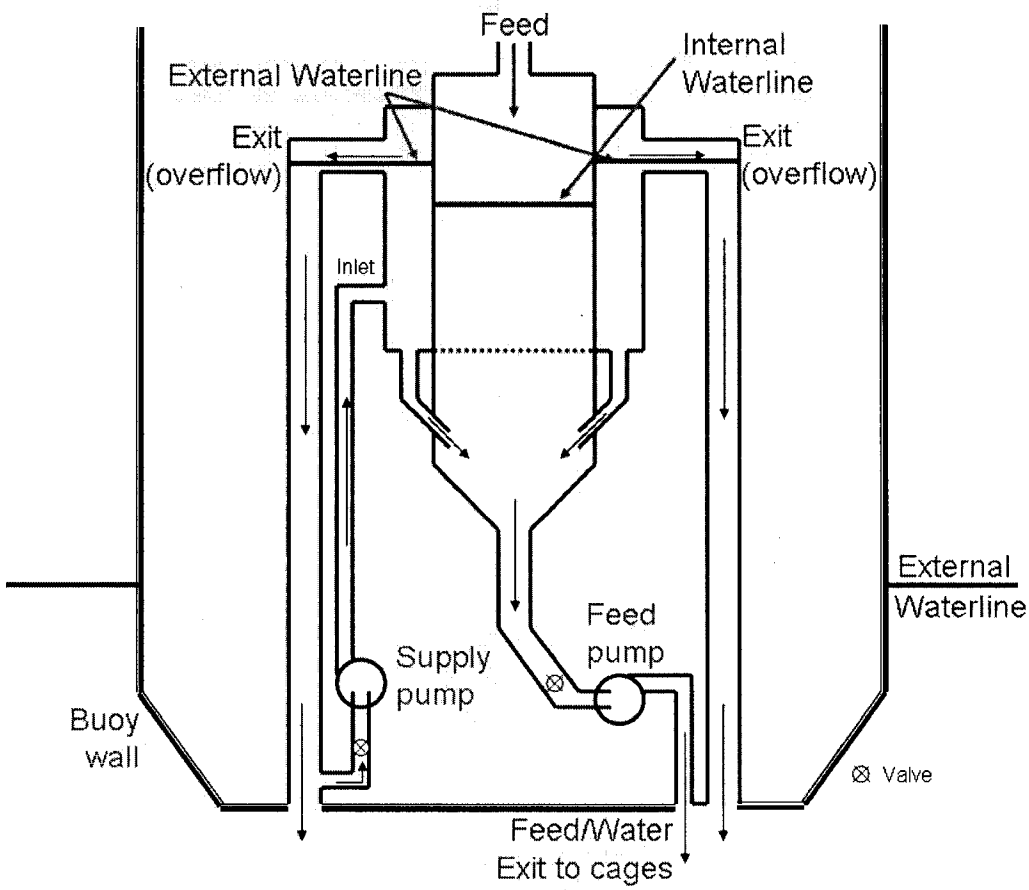

Figure 3.2: Schematic diagram of external feeding system concept including the mixing chamber.

The mixing chamber is one large diameter (approximately 24 inches) tank with one smaller diameter tank (approximately 18 inches) inside it (see Figure 3.3). The interior tank has a conical bottom that protrudes from the bottom of the large diameter exterior tank. The interior tank is taller than the exterior tank to allow for the mounting of hardware to control the feed being introduced to the system. The exterior tank has one water inlet and four exit connections. Two exits from the exterior tank connect to the interior tank, becoming inlets to the inner tank, while the two remaining exits are overflow exits. Any water that does not enter the inner tank is discharged through the overflow exits.

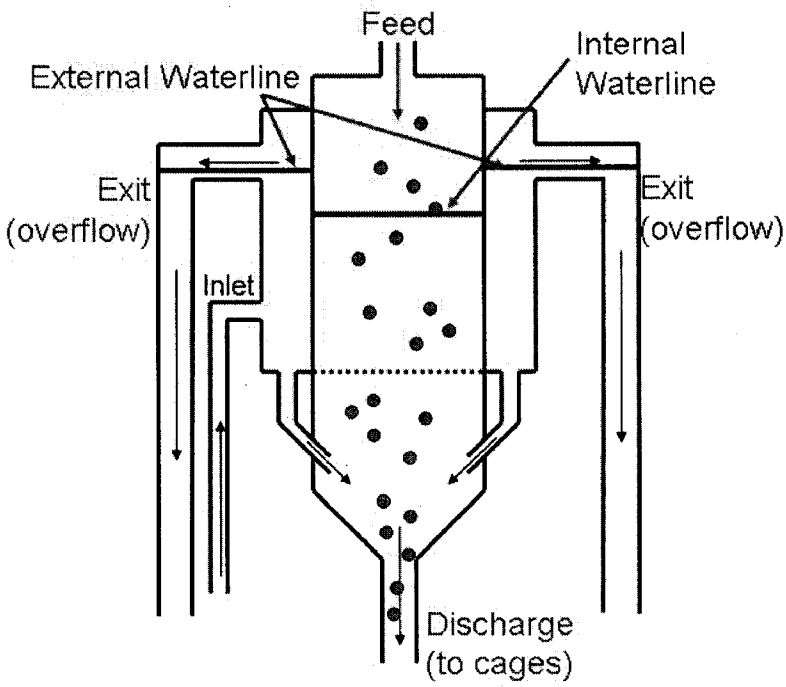

Figure 3.3: Schematic diagram of Mixing Chamber concept.

b. Concept Testing

The three major components of the external feeding system are the feed and supply pumps as well as the mixing chamber. The supply pump is not a problem because it is a standard pump that only needs to move water at the desired rate. The feed pump needs to be able to handle feed passing through the pump with little to no damage.

Pumps that were investigated included: trash centrifugal, centrifugal, fish, diaphragm, and positive displacement pumps. Positive displacement, diaphragm, and centrifugal pumps were dropped for various other reasons including: size, cost, power requirements, and safety. Initially a trash centrifugal pump was investigated that appeared to meet the criteria.

A trash pump evaluation experiment was conducted on 16 November 2004. A water/feed pellet mixture was run through a trash pump similar to the desired pump to view the effects on the feed. The results of the experiment were not favorable. The feed

had a high breakage rate that was not acceptable. A picture of the conveyed feed is shown below in Figure 3.4. Fish transfer pumps were subsequently investigated based upon the poor test results of the trash centrifugal pump as well as the fact that they are designed to transfer live fish without damage. Fish transfer pump evaluation tests were combined with mixing chamber experiments as described in the *Mixing Chamber Testing* section below.

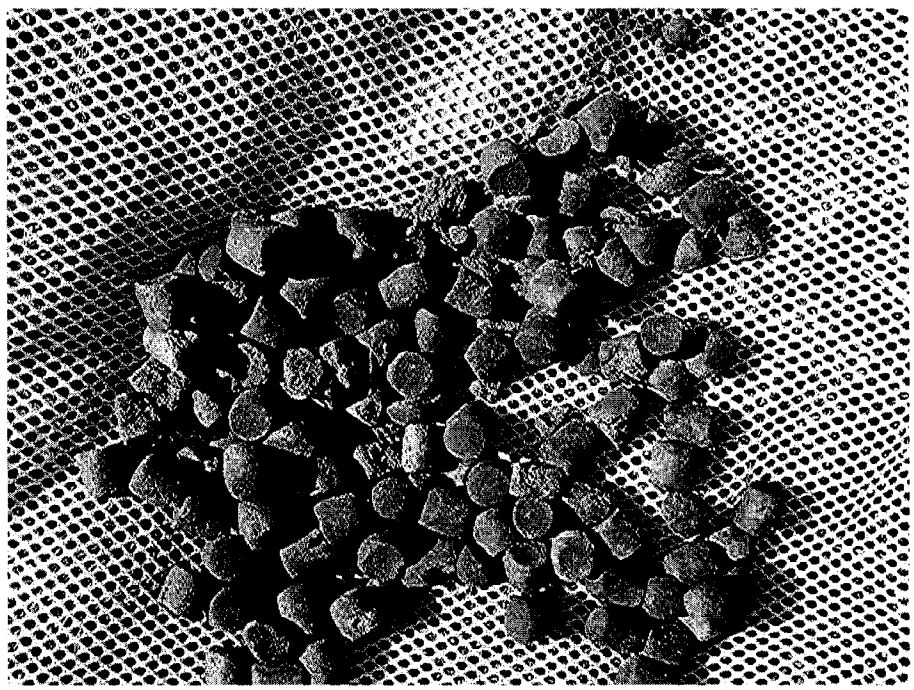

Figure 3.4: Picture of 13 millimeter feed after being pumped through a 3 inch centrifugal trash pump.

The mixing chamber is a vital component in the design of the 20-ton feed buoy. This is where fish feed pellets will be introduced into water and pumped to the submerged net pens. Since this mixing chamber concept is new, a prototype was needed for testing to prove the concept.

Mixing Chamber Prototype

A full scale mixing chamber prototype (see Figure 3.5) was constructed at UNH. The main components of the mixing chamber prototype were fabricated from large,

medium-density polyethylene tanks (MDPE). Construction involved the use of typical hand tools including: electric drill, reciprocating saw, and assorted screwdrivers.

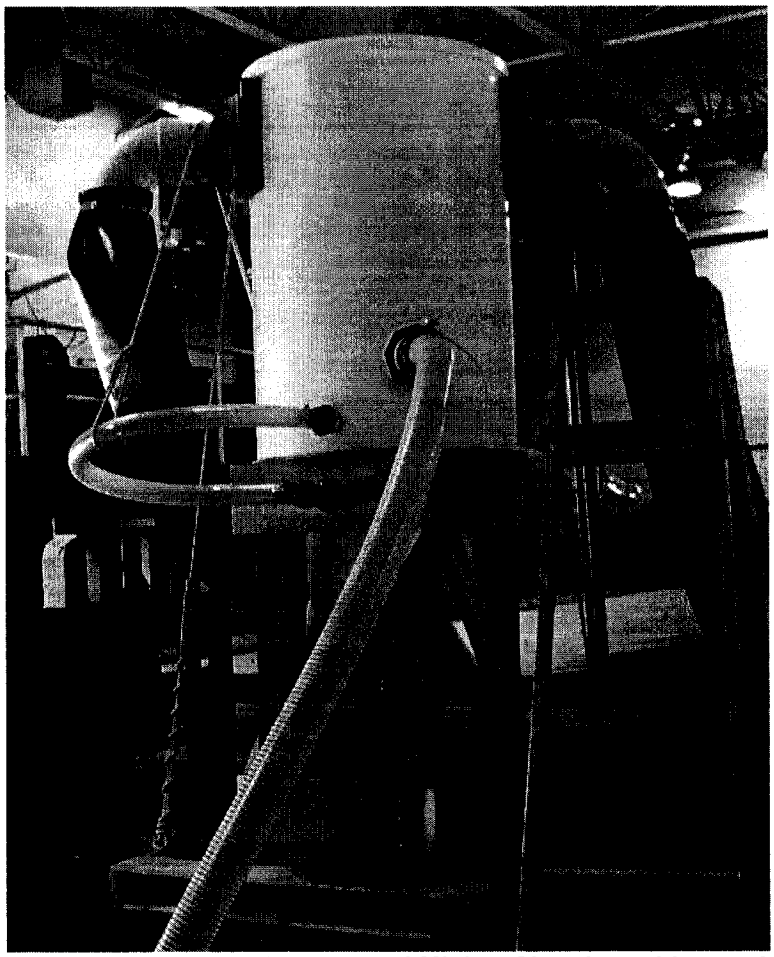

Figure 3.5: Picture of completed Mixing Chamber with stand.

The exterior tank was purchase as one piece, while the inner tank had to be build up of many smaller tanks. All MDPE was joined using a plastic welder and low density polyethylene (LDPE) welding rod. A stand, made of wood, was also fabricated to hold the mixing chamber during testing.

Mixing Chamber Testing

A series of four mixing chamber/feed pump tests were conducted. The initial test was to verify the concept of the mixing chamber. The next three were to investigate

modifications to the mixing chamber, a result of the first test, and to test different feed pumps.

Concept Verification

The first test was conducted at the Ocean Engineering facility at UNH on 19 January 2005. No feed was used; water levels, as well as flow directions and approximate flow rates were observed. The test used the mixing chamber, two pumps – a supply (3 inch Tsurumi trash pump) and feed pump (2 inch Pacer pump), hoses and the UNH's 20 foot deep Engineering Tank. Figure 3.6 is a photograph of the test set-up.

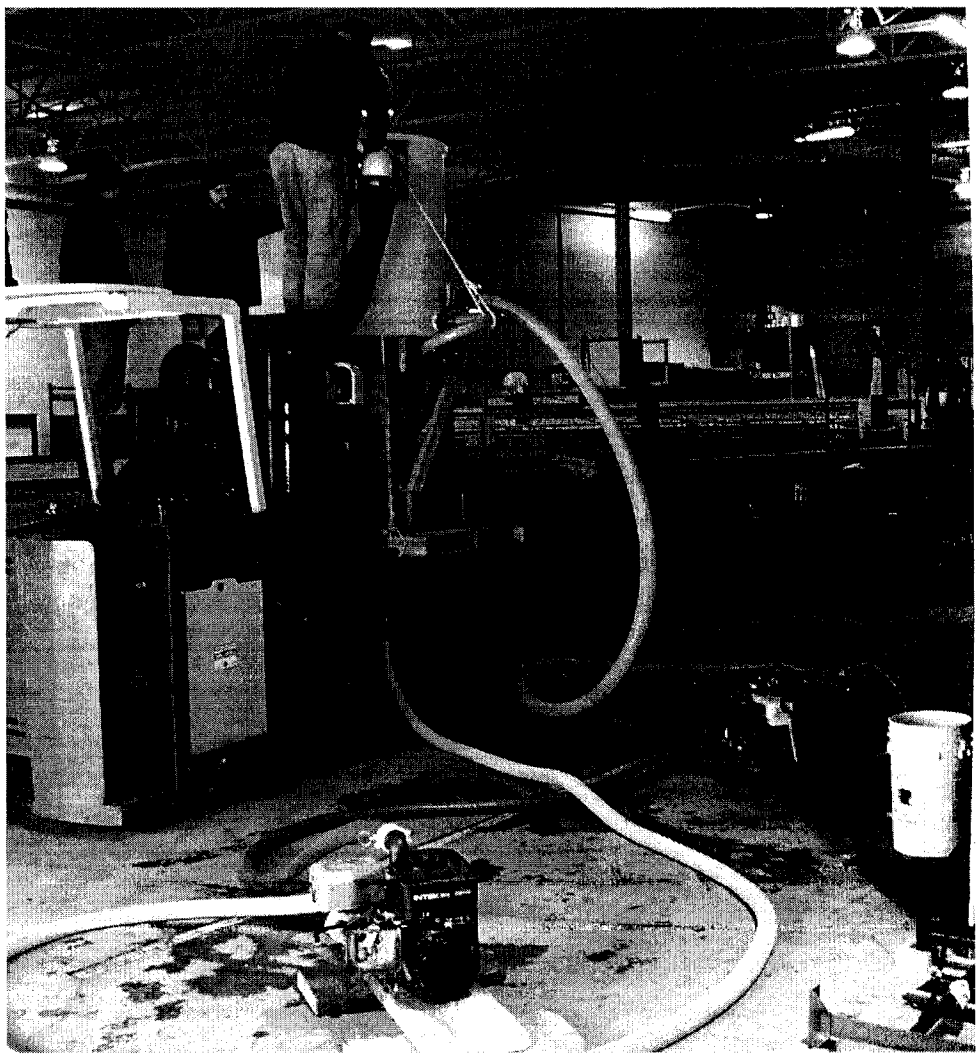

Figure 3.6: The first mixing chamber test. The mixing chamber is being held up by a forklift. Supply and discharge pumps are shown in foreground. The UNH Engineering Tank is shown in the background.

The 3 inch Tsurumi trash pump (pump shown on the right) was used as the supply pump. The supply pump drew water, maximum flow rate of 290 gallons/minute, from the Engineering Tank and pumped it into the mixing chamber exterior tank. Any water that did not enter the inner tank was directed back into the Engineering Tank via the overflow pipes. The 2 inch Pacer pump (pump shown on the left) was the "feed pump" and drew water from the mixing chamber inner tank, maximum flow rate of 130 gallons/minute, and discharged back into the Engineering Tank.

The test was a complete success. The free surface of the exterior tank was created at the height of the overflow/discharge pipes. The interior tank free surface was created below the exterior free surface height. This difference in height confirmed that water was flowing only into the inner tank.

Some modifications that were decided upon after the initial tests are listed below:

- Add small cross-section vertical slits with directional control (to induce swirling) to the upper section of the tank interface. This would eliminate the stagnant area of water at the top of the inner tank and lower air entrainment with a more gentle swirling action.
- Add bulk of cross-sectional area, into inner tank, well below waterline.
- Increase total cross sectional area connecting the inner and outer tanks to an amount corresponding to 2 to 3 inch diameter holes.

Feed Pump Testing

As a result of the preliminary trash pump testing it was decided that a fish pump would be the best option for a pump. Two specific types of fish pumps were under consideration: a PRAqua and Wemco-Hidrostal fish pump. Great Bay Aquaculture (GBA), located in Newington, NH, was gracious enough to let us use their PRAqua fish pump for the mixing chamber feed tests. Two tests were conducted at the GBA facility. A

final test was conducted at UNH using the Wemco-Hidrostal fish pump. In all three tests, feed pellets were introduced to evaluate transport and damage.

The experimental set-up was similar to the test conducted at UNH. Components consisted of the mixing chamber, two pumps – supply and feed, hoses and a reservoir to draw water from. The differences in the tests at GBA were the supply pump used. For the first test, conducted on 4 March 2005, a 2 inch Pacer pump was used (same one as used for the test at UNH), while the second test, conducted on 10 March 2005, used a 3 inch Tsurumi trash pump. There were different supply pumps used because the design flow rates could not be achieved with the 2 inch Pacer pump used in conjunction with the PRAqua pump. The PRAqua pump was used as the feed pump (exit from mixing chamber) and is shown in Figure 3.7.

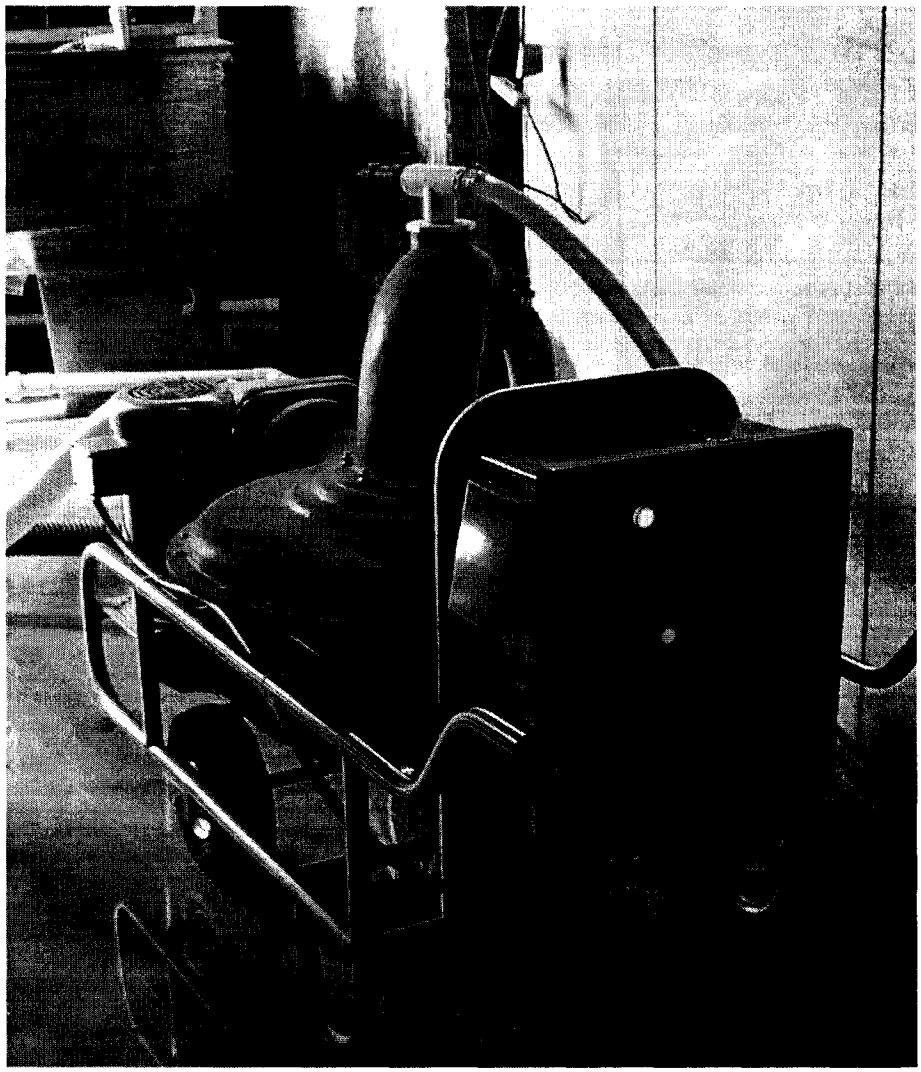

Figure 3.7: PRAqua pump under testing at GBA.

With the system in operation, fish feed pellets were introduced into the mixing chamber. The feed exited the mixing chamber quickly, was pumped through the feed pump, and was discharged into the water reservoir and caught in a net basket. Examples of the two different size feed pellets after going through the system are shown in Figure 3.8. The feed passed through the system with excellent results. The amount of damaged feed was minor. This verified the decision that a fish pump is necessary for the final feeding system design.

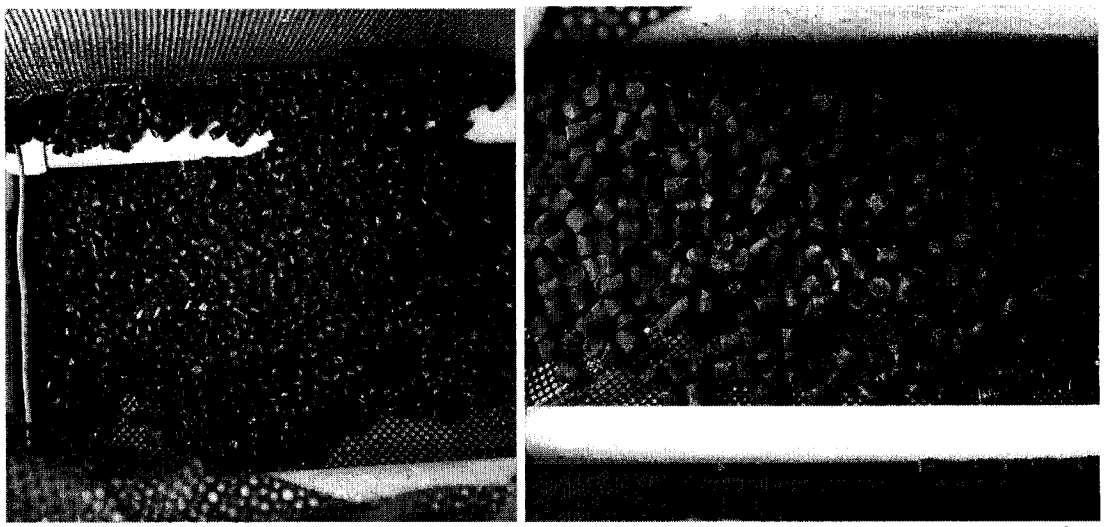

Figure 3.8: Feed after being pumped through mixing chamber and PRAqua pump (8 millimeter – left, 13 millimeter – right). Results show minimal damage to feed pellets.

After the testing at GBA using the PRAqua pump, it was decided to obtain the other pump under consideration – a Wemco-Hidrostal fish pump. This was due to the PRAqua pump barely obtaining the desired flow rates under the design conditions. The pump reached the design goals as tested, but there was no reserve power to work against a head pressure increase. Head pressure is likely to increase in actual operational conditions based upon previous experience.

A Wemco-Hidrostal pump and Toshiba variable frequency controller were purchased for testing and eventual use in the final buoy. After fabricating pump fittings and completed electrical wiring, a test was planned. The test was performed on 12 May 2005 at the Ocean Engineering facility at UNH. This test was to verify the performance of the pump and observe how the feed would pass through the pump and mixing chamber system.

The test set-up was similar to the previous mixing chamber tests. Figure 3.9 is a picture of the Hidrostal pump test (water reservoir and 3 inch Tsurumi trash pump not visible). The pump performed up to design specifications. Feed pellets were introduced into the mixing chamber and pumped through the feed pump. Figure 3.10 shows feed after being pumped through the system. Minor pellet damage is visible. The overall

result of the test, however, was favorable. The external feeding system design, with the tested components, was acceptable.

Figure 3.9: Hidrostal pump test conducted at UNH Ocean Engineering facility.

Figure 3.10: Feed, 8 millimeter, after being pumped through the mixing chamber and Hidrostal fish pump.

c. Mixing Chamber Design

The mixing chamber design (see Figure 3.11) was altered after pump testing in an effort to allow easier access to the internal section of the mixing chamber. These design changes include the addition of two screw-out deck plates, with clear windows, as well as modifications to the top cap. The screw-out deck plates allow visible access to the internal section of the mixing chamber. The feed-water interaction can be observed while feeding operations are being conducted. The deck plates will allow viewing of different flow inlet control plates that are to be used during testing. The top cap diameter was increased to allow access, once removed, to both internal and external sections of the mixing chamber. Having access to both sections will allow easier maintenance and cleaning operations.

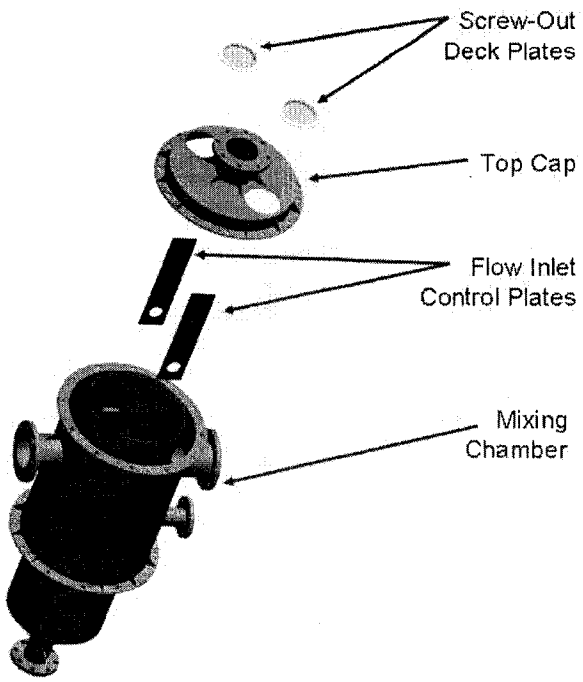

Figure 3.11: Exploded view of Mixing Chamber assembly.

3. Control and Power

The buoy will house all equipment necessary to control the feeding and operational systems. While a detailed description of these systems is beyond the scope of this document, however, a short description is provided.

All electrical power will be generated at the buoy with minimal external input. This will be accomplished by utilizing a 20 kilowatt marine diesel generator as well as a small amount of solar generation.

Buoy operation and feeding systems will be controlled via computer. Monitoring of the buoy's systems will be done mainly on shore (as well as on board) using telemetry data sent via radio.

CHAPTER IV

PHYSICAL MODELING

1. Scale Model Considerations

In order to investigate the expected motion of the buoy at UNH's OOA site physical scale model tests were performed. A 1:20.738 Froude scaled model and mooring were constructed and used for testing. The scale model testing included free-release and wave testing. These types of tests provide insight into the expected buoy dynamics of motion in reaction to wave energy input. Also, physical model testing can reveal dynamics not apparent in numerical testing.

Froude scaling was implemented for the construction of the buoy model and mooring since the buoy will be located in an oceanic environment with water waves. In wave systems, inertia and gravity are the predominant forces involved in the system. Other types of scaling could have been used for this model including Reynolds number scaling. However, Froude scaling is most applicable for this type of system. The Froude number is defined as the ratio of the inertia force to the gravitational force in a fluid medium (Chakrabarti, 1994). The Froude number is defined as

$$Fr = \frac{U}{\sqrt{gL}}, \qquad [4.1]$$

where U is the water velocity, g is the gravitational constant, and L is the characteristic length dimension.

The scale factor was determined by using a depth based approach. The ratio of the depth of water at the expected buoy location (50.6 meters) over the depth of the UNH wave/tow tank (2.44 meters) was used resulting in a scale factor (α) of 20.738. Using Froude scaling and requiring geometric similarity, the scaling factors for length, force, and time could be determined. All length dimensions (including diameter) were scaled as

$$\alpha = \frac{L_{fs}}{L_m}, \qquad [4.2]$$

where subscript *fs* denotes full scale length and subscript *m* denotes model length. Force values (including weight) are scaled as

$$\alpha^3 = \frac{F_{fs}}{F_m}, \qquad [4.3]$$

where F_{fs} is the full scale force and F_m is the model scale force. Another scale of importance for wave testing is the time scale, defined as

$$\alpha^{\frac{1}{2}} = \frac{T_{fs}}{T_m}, \qquad [4.4]$$

where T_{fs} is the full scale time and T_{fs} is the model scale time. Other scale factors of interest can be found similarly as described in Chakrabarti (1994).

With the dimensions of the full scale buoy specified, the model scale dimensions could be determined using the above equations and procedures. All dimensions were determined using a Froude scale approach. A model and mooring were constructed.

2. Scale Model Construction

With the scale factor determined, the sizes and weights for the physical model were calculated. This resulted in a model that was 16.13 inches tall (not including mast), 13 inches in diameter and weighted 19.7 pounds (load condition) or 15.2 pounds (light condition). The load condition corresponds to the buoy with full feed levels, while the light condition is without feed and fuel. The completed model is shown in Figure 4.1 and was constructed during June 2005. The mooring system was completed during the same time period.

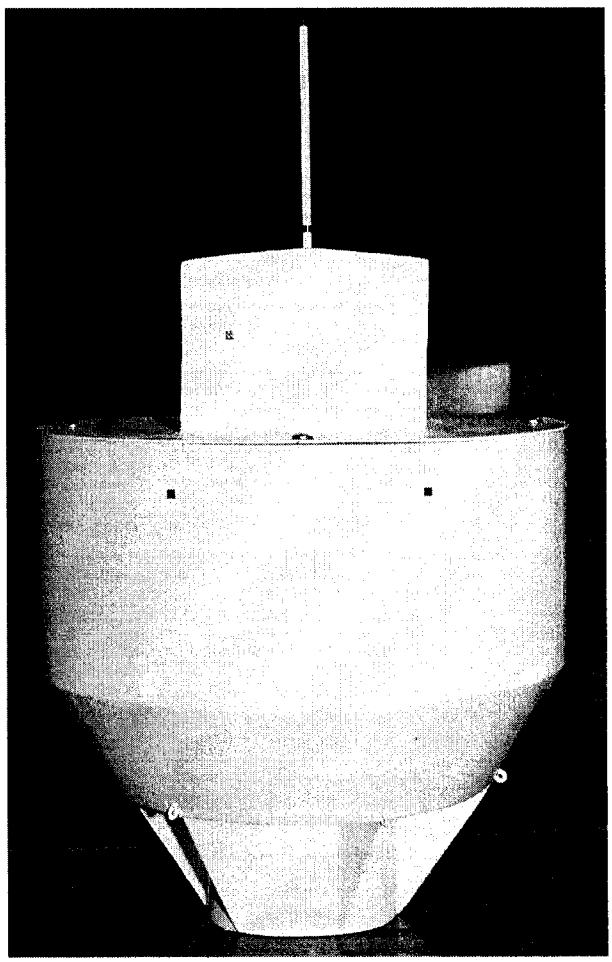

Figure 4.1: Completed 1:20.738 buoy scale model.

This model was constructed in four separate parts: house, hull, ballast can, and a moveable added weight. The added weight is necessary to insure that the overall model weight and center of gravity (CG) match with the full scale buoy properties. Table 4.1

shows the weights and centers of gravity for an ideal model as well as the actual finished properties. The mooring system was constructed using chain, line (non-stretch) with an elastic portion to simulate the line's elastic properties.

Table 4.1: Values used for the creation of the buoy model. Full scale values are shown in addition to the calculated model scale values. Additionally, the actual values are included. VCG refers to the vertical center of gravity. All length dimensions are coaxial with the vertical axis, with zero corresponding to the absolute bottom of the buoy. The buoy is symmetrical about the vertical axis.

	Full Scale		Model Scale		Actual	
Component	**Weight (lb)**	**VCG* (in)**	**Weight (lb)**	**VCG* (in)**	**Weight (lb)**	**VCG* (in)**
Overall (load)	175400	138.0	19.67	6.656	19.7	6.7
Overall (light)	135300	130.9	15.17	6.31	15.2	6.0
House	**	**	**	**	0.7	13.1
Hull	81510	186.1	9.65	8.93	1.1	7.8
Ballast Can	49200	35.93	5.12	1.731	5.6	1.9
Added Weight (load)[a]	n/a	n/a	11.54	8.22	12.5	8.2
Added Weight (light)[b]	n/a	n/a	7.04	8.45	8.0	8.1

* Length dimensions are given relative to absolute bottom of buoy.
** Values were included in the Overall component.
[a] Load refers to buoy with feed.
[b] Light refers to buoy without feed and fuel.

The house was constructed using extruded polystyrene closed cell foam and 1/16 inch thick LDPE sheet (see Figure 4.2). The upper foam section was cut to shape, using a vertical band saw, following the dimensions scaled from the full scale buoy. Bolts (total of four) were put into the bottom of the house foam, bolt head first, and attached using epoxy. Holes were drilled into the LDPE sheet to mate with the bolts. The sheet and foam were then bolted together to complete the house sub-assembly.

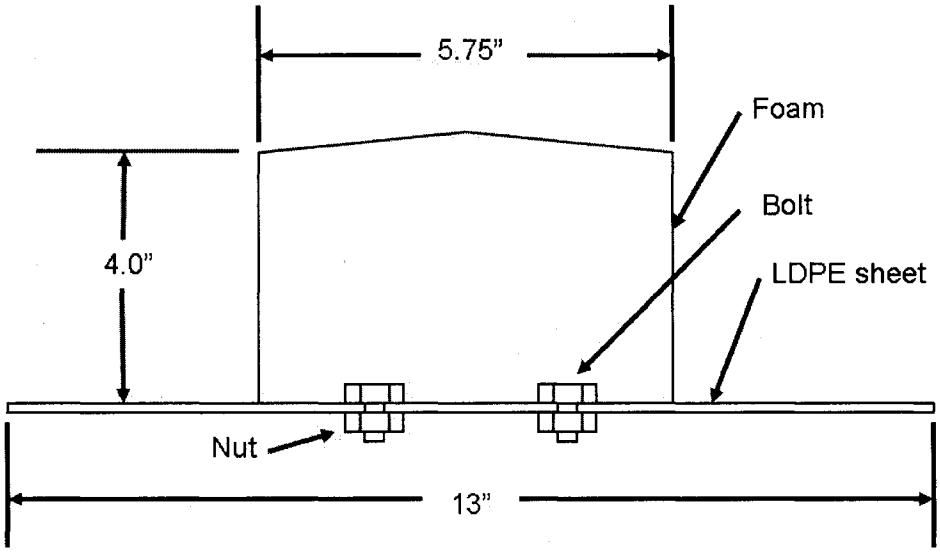

Figure 4.2: Cross-section sketch showing the construction detail of the house.

The hull was constructed of the same extruded polystyrene closed cell foam used in the house as well as 1/4 inch thick HPDE sheet (see Figure 4.3). The main vertical section was cut out as a cylinder using a vertical band saw and then the inner section was hollowed out using hand tools. The lower angled section was cut to height and then the angle was cut using a band saw. The two pieces were then joined using Liquid Nails™ adhesive. Nuts (quantity four) were recessed into the top rim of the hull section and affixed using epoxy. Cap screws could then be used to attach the house component to the hull. This was necessary to allow for access inside the buoy to alter weight configurations to test the varying load conditions.

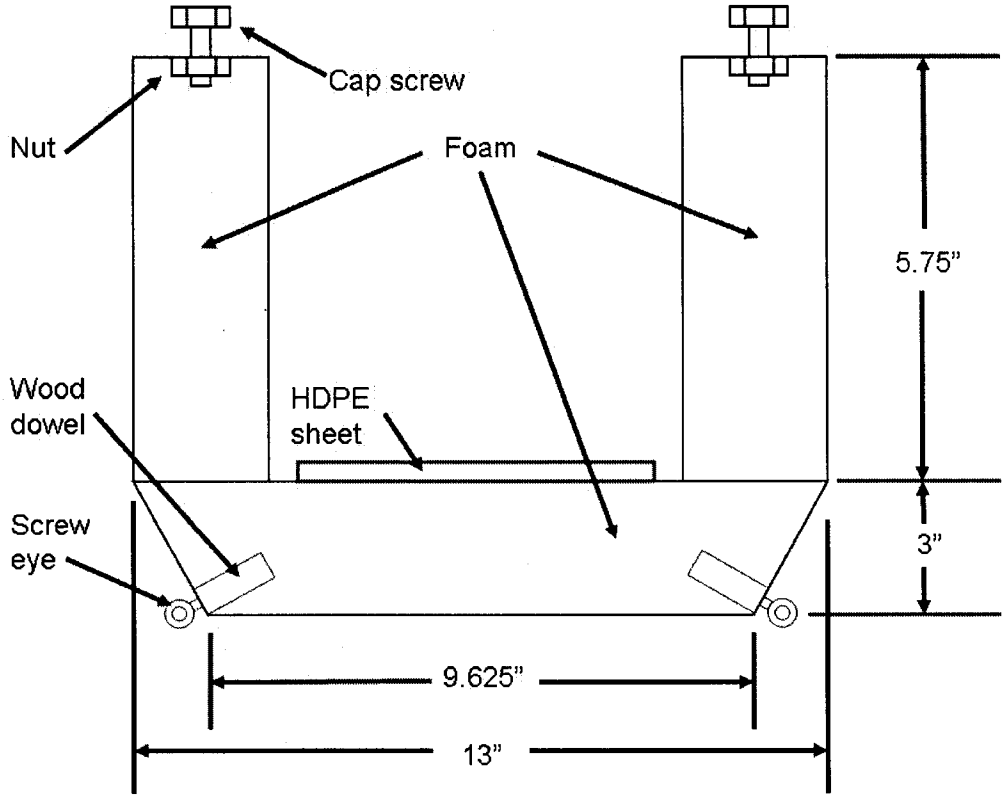

Figure 4.3: Cross-section sketch of the body/hull construction detail.

The mooring attachments were incorporated into the hull section. They consisted of a one inch section of wood dowel (3/8 inch diameter) material with a screw eye screwed into the end of the dowel. Holes were drilled into the lower angled section normal to the angled surface. The attachment points, total of six, were then secured using epoxy. They were spaced at angle increments of 60 degrees, as in the full scale buoy.

With the house and hull sections complete, a thin layer of Evercoat® Universal Repair Filler (a contractor grade filler infused with glass fiber for strength) was applied. This was necessary to produce a smooth surface for painting as well as give the model a strong waterproof outer layer.

The ballast can was constructed using concrete, threaded rod, nuts, washers, and LDPE sheet (see Figure 4.4). A mold was made to the appropriate dimensions using paper, tape, plywood, and screws. The paper was rolled into a cylinder and placed on a

plywood sheet. Tape was placed on the paper protect it from moisture. The paper was supported on the sides by blocks of plywood that were screwed to the plywood base. Concrete was mixed and poured into the mold. While the concrete was wet, threaded rods (washers and nuts attached) were inserted to allow for attachment of the ballast can to the hull of the model. After the ballast can was fully cured a layer of Evercoat® Universal Repair Filler was added. This was done to fill small imperfections in the concrete and provide protection from damage.

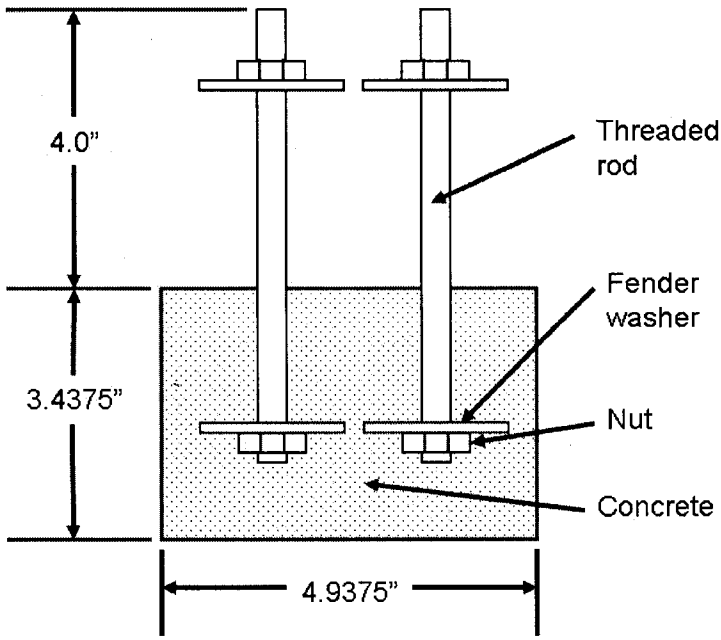

Figure 4.4: Cross-section sketch of the ballast can model construction detail. Threaded rod (quantity two) was used for attachment of the ballast can to the hull of the model.

The ballast can was then attached to the hull component. Threaded rod was passed through holes in the hull component and secured using nuts and washers (see Figure 4.5). A layer of Liquid Nails™ adhesive was also used between the ballast can and hull to provide watertight integrity to the model. With the two components assembled six LDPE gussets were added between the sides of the ballast can and bottom of the hull. LDPE sheet was cut to shape and then attached using epoxy.

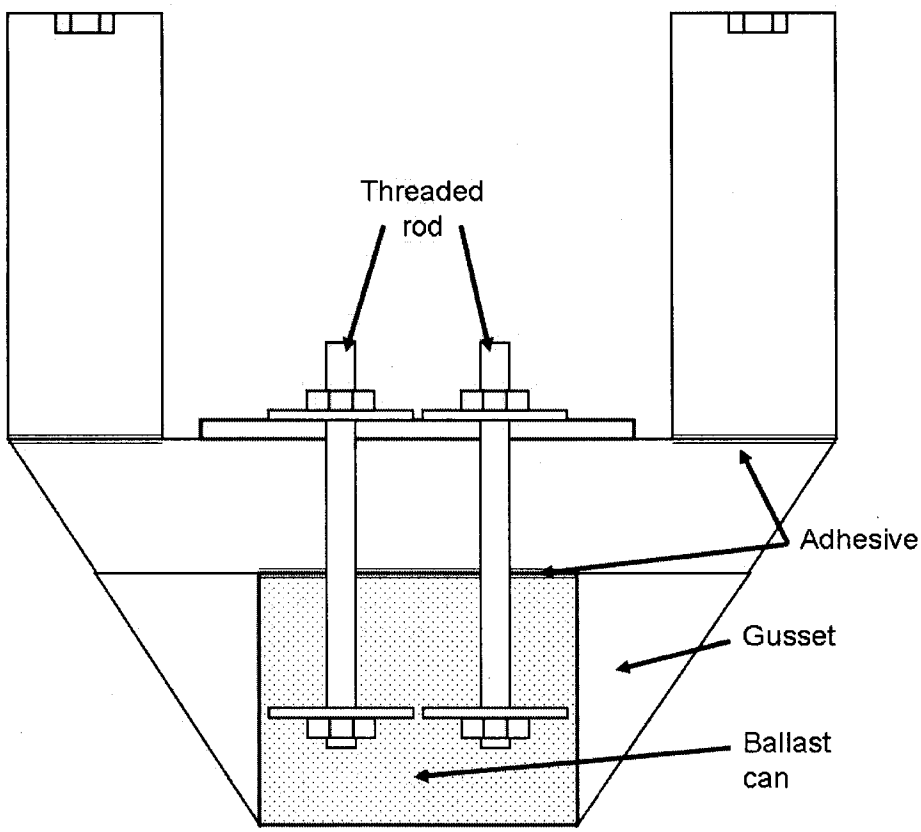

Figure 4.5: Cross-section sketch showing the construction details for the hull and ballast can assembly with gussets.

The buoy model was purposely constructed as light as possible to ensure that weight could be added to control the total buoy weight and center of gravity. The weight was added in the form of 1/16 inch thick lead sheet with a container to securely mount the weight inside the buoy (see Figure 4.6). Since the buoy was to be tested in two different loading conditions it was necessary that the weight could be added or removed to ensure the final model weight and center of gravity were correct.

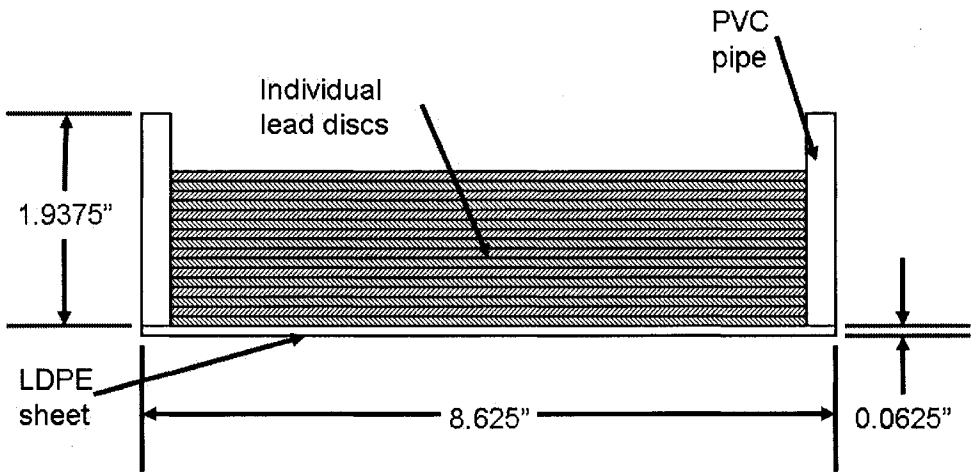

Figure 4.6: Cross-section sketch showing the construction details of the added movable weight.

The added weight container was constructed of a short length of eight inch PVC pipe. The pipe cylinder was sealed on the bottom by using a disc of LDPE sheet that was secured to the PVC using clear packing tape. Individual lead discs were then placed into the container. The location, inside the buoy, and total weight of the added moveable weight were altered to generate the desired testing condition: load or light. This was accomplished by using a variety of foam disc spacers, for vertical adjustment, as well foam block spacers, for horizontal adjustment. The disc spacers had holds to allow the threaded rod to pass through the spacers, allowing the discs to rest on the flat HDPE sheet inside the model.

Before the components could be assembled into a final model, all exterior surfaces were painted. This was done to provide an adequate target for the data collection system described later in this chapter, as well as to provide an additional layer of waterproofing. The individual components used in the final construction are shown in Figure 4.7.

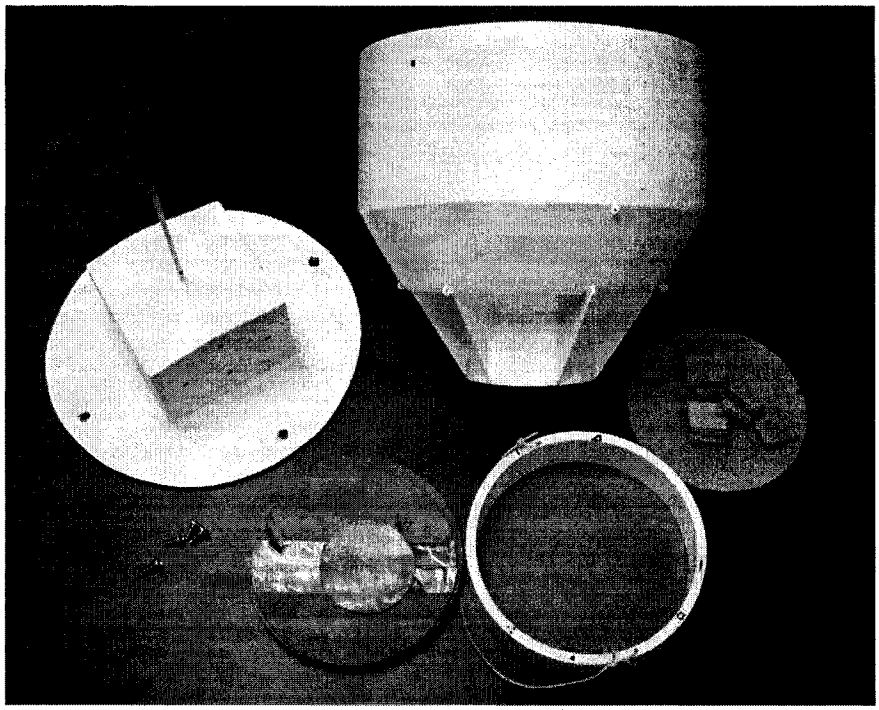

Figure 4.7: Individual model components. Clockwise from the top the components are: the main hull, spacing discs and blocks, lead ballast container, lead ballast discs, cap screws, and the deck.

Due to the physical width limitations only one mooring leg attachment could be utilized for the wave testing. This was acceptable given that the worst case dynamic response of a buoy typically coincides with a single mooring leg attachment and wave direction being coaxial. A typical mooring was used for model testing that includes an anchor, steel chain, and line. The schematic in Figure 4.8 shows the arrangement of the mooring leg attachment in relation to the buoy and wave/tow tank used for testing.

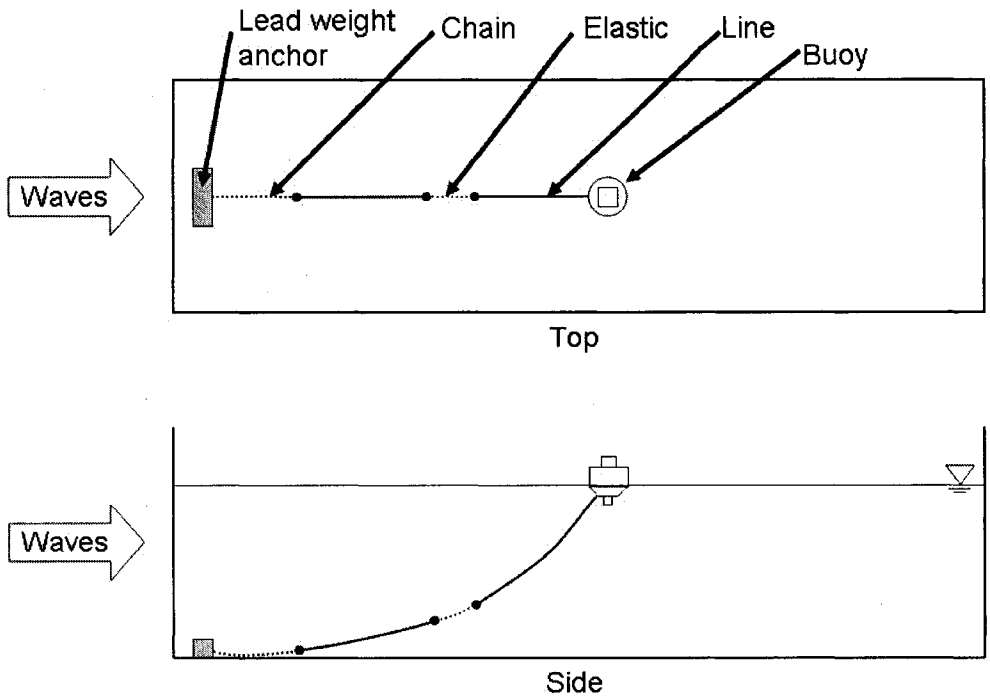

Figure 4.8: Top and side view schematic of the mooring leg arrangement.

The mooring was made of a deadweight anchor; chain, line, and an elastic tether (see Figure 4.9). A typical anchor for use in the full scale system of this type is a plow embedment type anchor. Since the wave/tow tank has a smooth concrete bottom, a plow embedment anchor was modeled as a 25 pound lead weight. The weight of the lead deadweight anchor was sufficient to allow testing without the anchor moving along the bottom of the tank. A typical chain for this full scale application is a shot (90 feet) of 1 inch steel stud link chain. Chain of the appropriate weight per unit length could not be found, in model scale, so small rectangles of lead sheet were added to provide the appropriate weight. The line type selected for use in the mooring of the full scale buoy system is 2 inch Spectra™ line. The desire mooring line scope was specified to be 1:6, a typical value for the expected buoy location water depth. The scope then allowed determination of the length of line needed for a mooring leg. The mooring leg line has a spring constant (k) of 497.3 pounds/foot, however the line used for the model testing has no elastic properties. In order to simulate the elasticity of the mooring line, the line was

cut into two equal lengths and an elastic compliance member was added between them. The resulting section of rubber had a spring constant of 1.22 pounds/foot. Table 4.2 provides lengths and weight for an ideal mooring as well as actual quantities.

Table 4.2: Values used for the creation of the buoy model mooring.

	Full Scale		Model Scale		Actual	
Component	**Length (ft)**	**Weight (lb)**	**Length (in)**	**Weight (lb)**	**Length (in)**	**Weight (lb)**
Chain[a]	90	7650	52	0.86	52	0.85
Line	933.6	*	528.25	*	*	*
Elastic Compliance[b]	n/a	n/a	12	*	11.90	**

* Negligible weight added to system.
** Values were included in the Overall component.
[a] Only chain physical properties were used here. The anchor used was a dead weight lead brick anchor that did not impact testing. The full scale buoy will use plow type anchors that are appropriate for the bottom conditions at the site.
[b] A 12 inch elastic section was added to the mooring line to model the elastic compliance distributed by the line used in the full scale mooring.

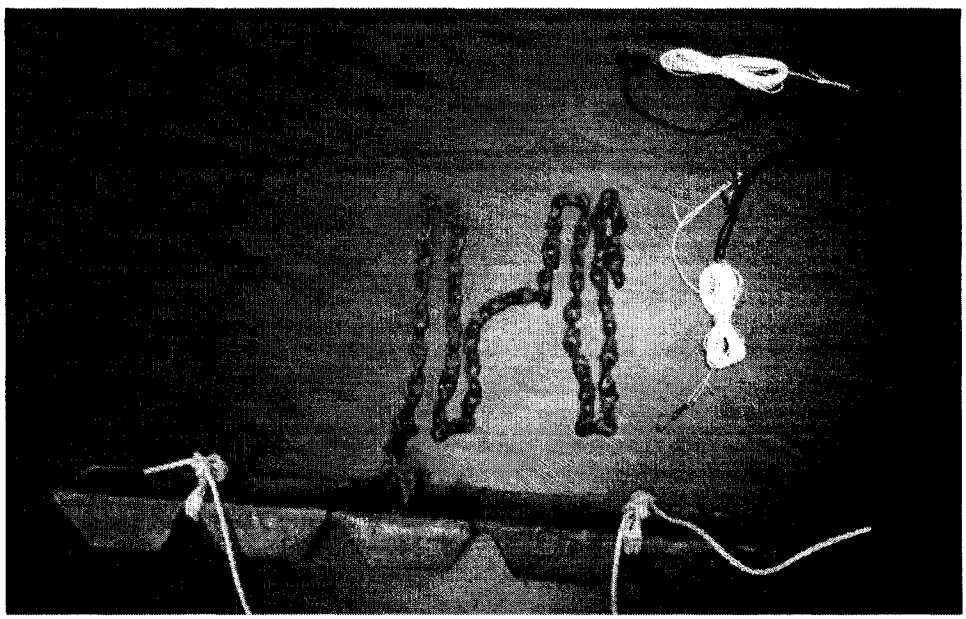

Figure 4.9: Mooring components used for the physical model testing. From left to right the components are: lead dead weight anchor, chain, and the mooring line with the elastic section.

A final component that was needed was a wave measurement device. The waves used during testing need to be measured to verify that the waves desired are being generated. It consisted of a foam cylinder with hemisphere affixed to the bottom of

the cylinder (see Figure 4.10). The float was constrained to vertical motion by a section of vertical monofilament line running from above the water's surface to the tank floor. A hole was created through the vertical axis of the float through which the line was run. The line was held securely by a deadweight anchor on bottom and rigidly attached to a tie-down above the water's surface.

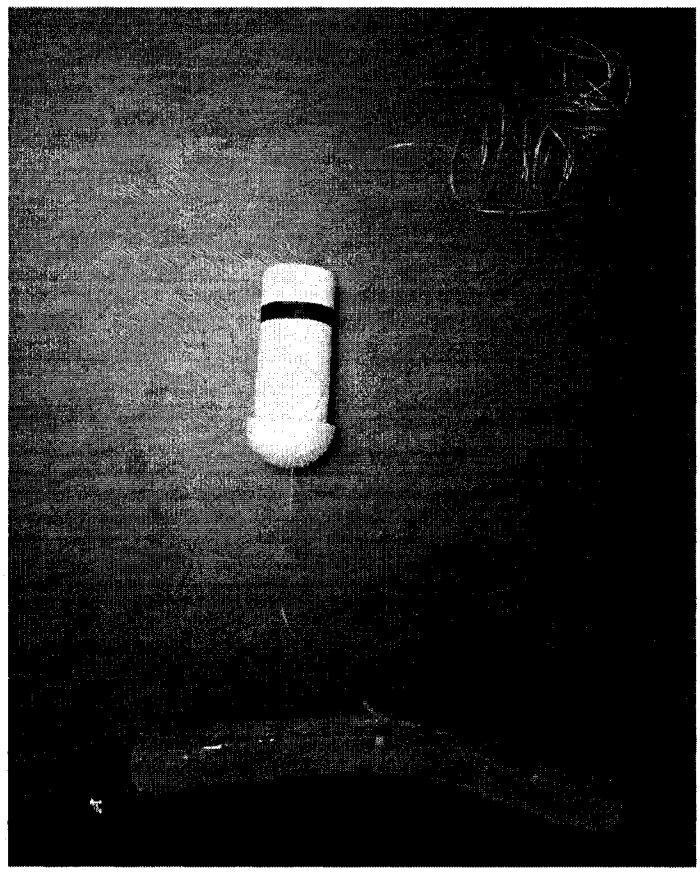

Figure 4.10: Wave height float with lead weight and monofilament line.

3. Experimental Methodology

Free-release tests were conducted to determine the heave and pitch natural frequencies/periods of the buoy. The natural frequencies/periods provide insight into the buoy motion in response to a variety of sea states as well as the overall stability of the buoy.

To determine the natural periods, the buoy is displaced from an equilibrium position. The time response motion of the buoy is observed. The buoy oscillates about

an equilibrium position: vertical motion for the heave case, angular motion for the pitch case. The time between the crest to crest and trough to trough is measured. That time is the damped natural period. The natural frequency is the reciprocal of the natural period.

Free-release tests were conducted at UNH in the Ocean Engineering wave/tow tank from 30 June to 1 July 2005. Heave and pitch tests were performed under two different loading conditions: load and light. The load case corresponds to a buoy with full feed and fuel, while the light case is strictly permanent structures on the buoy.

Wave testing was also conducted to determine the Heave, Surge, and Pitch Response Amplitude Operators (RAOs) or transfer functions. Heave is motion in the vertical direction, surge is motion in the horizontal direction, and pitch is angular motion of the buoy. The RAOs are defined as the ratio of the buoy response to the wave forcing. The *Heave RAO* is defined as

$$HeaveRAO = \frac{HeaveAmp_{buoy}}{HeaveAmp_{wave}}, \qquad [4.5]$$

where $HeaveAmp_{buoy}$ is the buoy heave amplitude and $HeaveAmp_{wave}$ is the wave heave amplitude. The $HeaveAmp_{wave}$ is defined as

$$HeaveAmp_{wave} = \frac{H}{2}, \qquad [4.6]$$

where, *H* is the wave height. The *Surge RAO* is defined as

$$SurgeRAO = \frac{SurgeAmp_{buoy}}{SurgeAmp_{wave}}, \qquad [4.7]$$

where $SurgeAmp_{buoy}$ is the buoy surge amplitude and $SurgeAmp_{wave}$ is the wave surge amplitude. The $SurgeAmp_{wave}$ could not be measured experimentally in this test set-up. The value was calculated based upon the wave heave amplitude (which was measured experimentally) as

$$SurgeAmp_{wave} = HeaveAmp_{wave} \cdot \left[\frac{\cosh\left(\left(\frac{2\pi}{\lambda}\right) \cdot h\right)}{\sinh\left(\left(\frac{2\pi}{\lambda}\right) \cdot h\right)} \right], \quad [4.8]$$

where λ is the wavelength and h is the water depth (Dean, 1984). Similarly, the *Pitch RAO* is defined as

$$PitchRAO = \frac{PitchAmp_{buoy}}{HeaveAmp_{wave} \cdot \left(\frac{2\pi}{\lambda}\right)}, \quad [4.9]$$

where $PitchAmp_{buoy}$ is the buoy pitch amplitude (in radians) and λ is the wavelength.

Wave tests were conducted at UNH in the Ocean Engineering wave/tow tank from 14 July to 19 July 2005. The same two loading conditions (load and light) were tested, as with the free-release tests. A total of 10 different regular wave inputs were tested. The wave inputs bracketed the waves observed at the buoy's expected deployed location.

a. Optical Positioning and Instrumentation Evaluation Software (OPIE)

The data for both the free-release and waves tests were collected using UNH's optical positioning instrumentation and evaluation (OPIE) measurement system (Michelin & Scott, 1996). The OPIE system uses a digital camera, computer and processing software. Images were recorded by the OPIE system at a user set frequency (see Figure 4.11). Software tracks the motion of black dots located on the buoy. The calibration circle is used to determine the magnitude of movement for the tracking dots. Figure 4.12 is a screen capture that was taken by OPIE for a heave test under load conditions. Further analysis was performed on the data collected by OPIE.

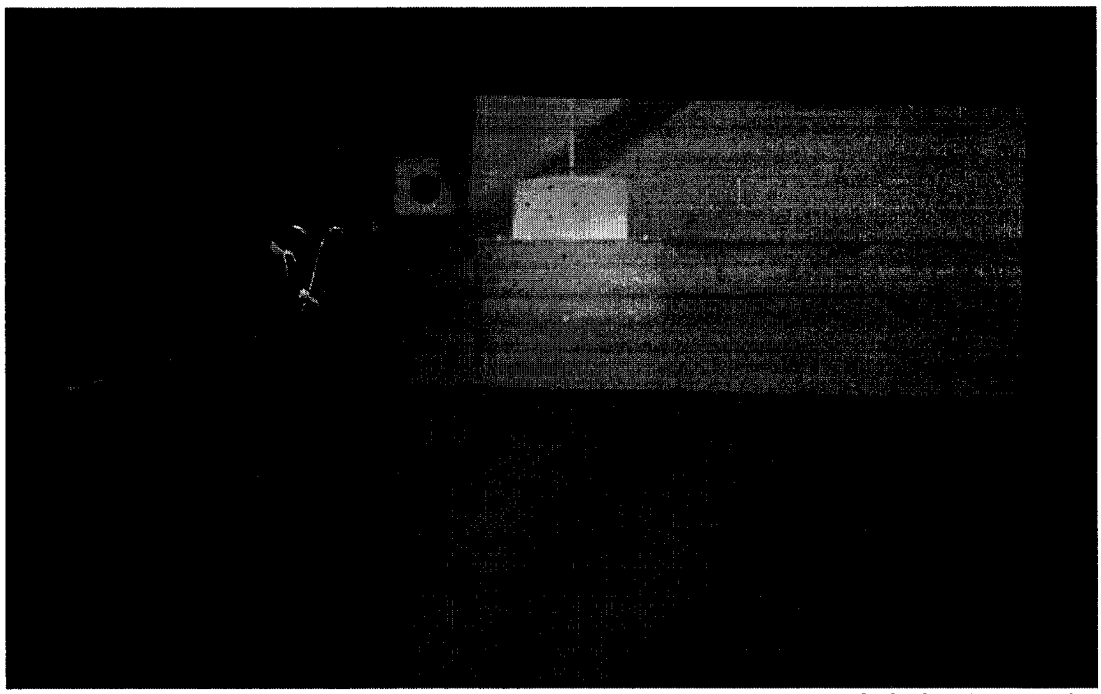

Figure 4.11: Picture of OPIE camera with buoy and calibration circle in background.

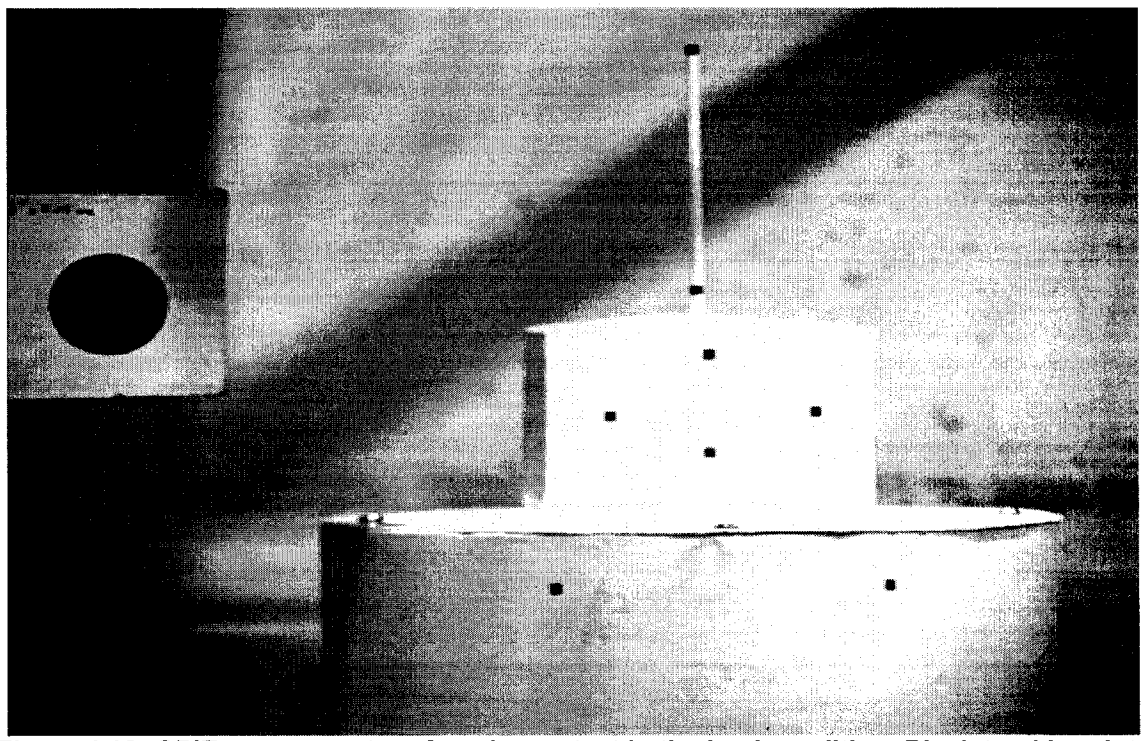

Figure 4.12: OPIE screen capture for a heave test in the load condition. Black tracking dots are visible on the buoy.

b. Procedures

Free-release

For both types of free-release tests and loading conditions, a set of at least six tests were performed. A test consisted of placing the buoy in the wave/tow tank in the OPIE video collection area, displacing it from equilibrium, and then releasing the buoy. The OPIE system would monitor and record the motion of the buoy. To have an initial equilibrium position recorded during testing, data collection began prior to displacement of the buoy.

To displace the buoy for a heave test, the buoy was lifted vertically a small amount (less than 2 inches) and then released. For a pitch test, the buoy was rotated about a horizontal axis a small angle (less than 15 degrees) and then released.

Regular waves

Two additional modeling components were added to the system for testing in a wave environment: a mooring system and a wave float. The mooring system was added since the motion of the waves will tend to move the buoy in the direction of the wave train, resulting in the model being moved out of the OPIE viewing area. Due to the physical size limitations of the testing facilities, the full mooring configuration could not be tested. A single mooring leg, described in the previous section, was used for testing. The wave float was added to measure the generated wave.

Waves are generated in UNH's wave/tow tank by a paddle type wavemaker. The paddle is hinged at the bottom and horizontal displacement is generated by a hydraulic ram connected at the top of the paddle. Waves are generated based upon a user determined wave period and wave height.

The wave parameters that were used are shown in Table 4.3. A wave slope of 1/15 was chosen to specify the wave height where possible. For wave periods longer

than 1.5 seconds, however, the wavemaker could not generate the necessary wave heights and lower slope waves were used. Wave periods/frequencies bracketed common wind generated, storm, and sea swell waves found at the expected location for the buoy.

Wave generation was started a small period of time before data collection began. This was done to ensure that a steady state condition was reached. After data was collected for each wave train, the water in the wave/tow tank was allowed to settle before starting the next test. After the water was calm, testing proceeded.

Table 4.3: Regular wave input parameters into UNH's wave/tow tank. Subscript m indicates model scale; fs indicates full scale. T is period; H is wave height; f is frequency, and λ is wavelength.

	Inputs$_m$		Inputs$_{fs}$						
#	T_m (sec)	H_m (m)	T_{fs} (sec)	H_{fs} (m)	f_m (Hz)	f_{fs} (Hz)	λ_m (m)	λ_{fs} (m)	Slope^{-1} (λ/H)
1	0.50	0.026	2.28	0.54	2.000	0.439	0.39	8.1	15.0
2	0.65	0.044	2.96	0.91	1.538	0.338	0.66	13.7	15.0
3	0.80	0.067	3.64	1.39	1.250	0.274	1.00	20.7	14.9
4	0.95	0.094	4.33	1.95	1.053	0.231	1.41	29.2	15.0
5	1.17	0.143	5.33	2.97	0.855	0.188	2.14	44.3	14.9
6	1.50	0.24	6.83	4.85	0.667	0.146	3.51	72.8	15.0
7	1.93	0.270	8.79	5.60	0.518	0.114	5.78	119.9	21.4
8	2.20	0.230	10.02	4.77	0.455	0.100	7.43	154.0	32.3
9	2.63	0.170	11.98	3.53	0.380	0.083	10.18	211.2	59.9
10	3.00	0.110	13.66	2.28	0.333	0.073	12.54	260.1	114.0

4. Data Processing Techniques

a. Free-release

The data collected by OPIE was then imported into the software package MATLAB®. The vertical displacement locations (heave) and angular displacement (pitch) of the two tracked points on the buoy were plotted versus time. The analysis for heave and pitch free-release testing is identical except the pitch values are angles instead of linear displacements.

A typical heave free-release plot is shown in Figure 4.13. The two points were averaged and then used for subsequent analysis. Displacement and time values were collected for crest and trough positions for the averaged data.

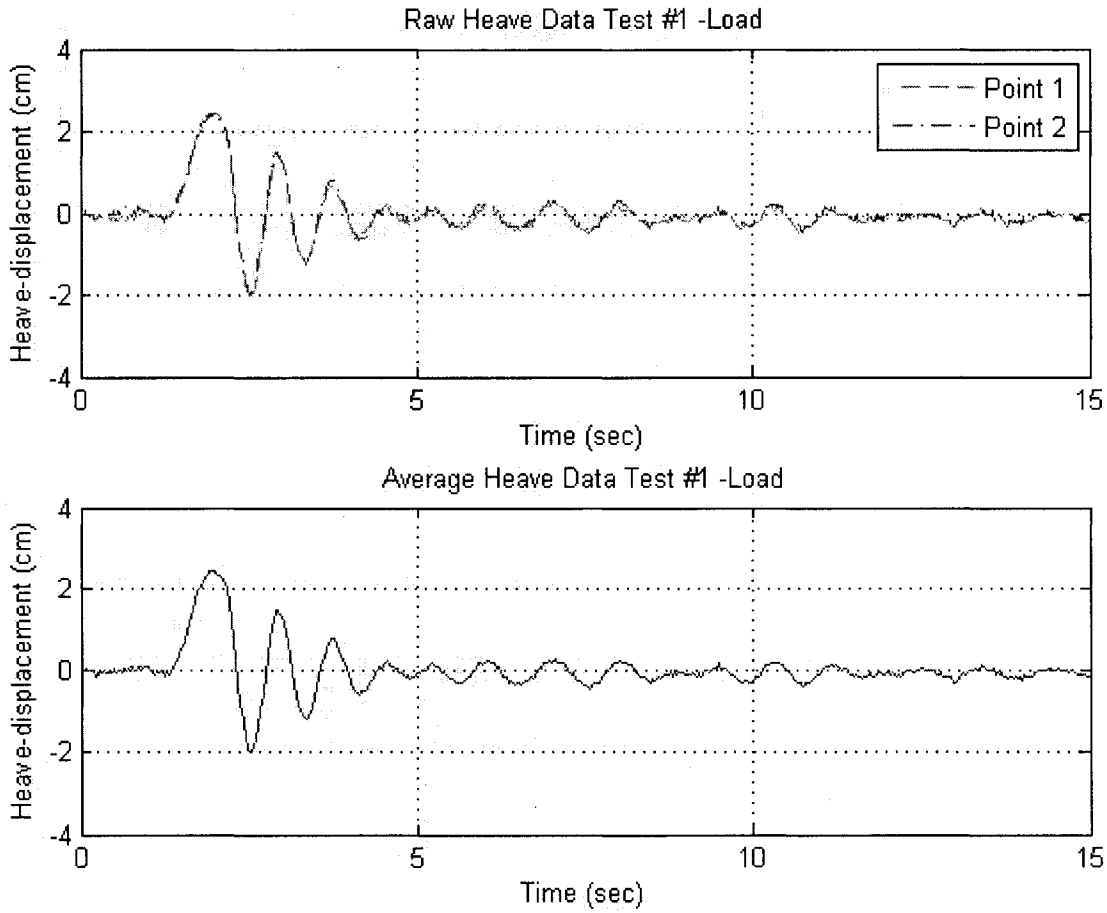

Figure 4.13: Plot of heave displacement versus time for load condition test number one. The raw data for the two points is shown in the upper plot, while the averaged data is shown in the lower plot. The averaged data was used for analysis.

From the collected points, the time differences between a crest to crest and trough to trough location were determined. The initial peak, not used for analysis, represents the initial displacement of the buoy from equilibrium. The time differences (periods) between the cycles are the damped natural periods (Td) desired. The six or seven trough and crest values after the initial displacement were used to determine the period. The periods for each individual test were averaged yielding a single value. After

analyses of all test replicates for each loading condition were performed, those results were averaged to yield the final damped natural period.

b. Regular waves

The data collected from OPIE was imported into MATLAB®. The linear and angular displacements of the wave float and buoy tracked points were plotted versus time. The analysis for heave, surge, and pitch RAOs is identical except the pitch values are angles instead of linear displacements.

A typical heave wave plot is shown in Figure 4.13. The maximum and minimum values, from the plots, were used to determine the amplitudes of motion. These values were then used to calculate the RAO values.

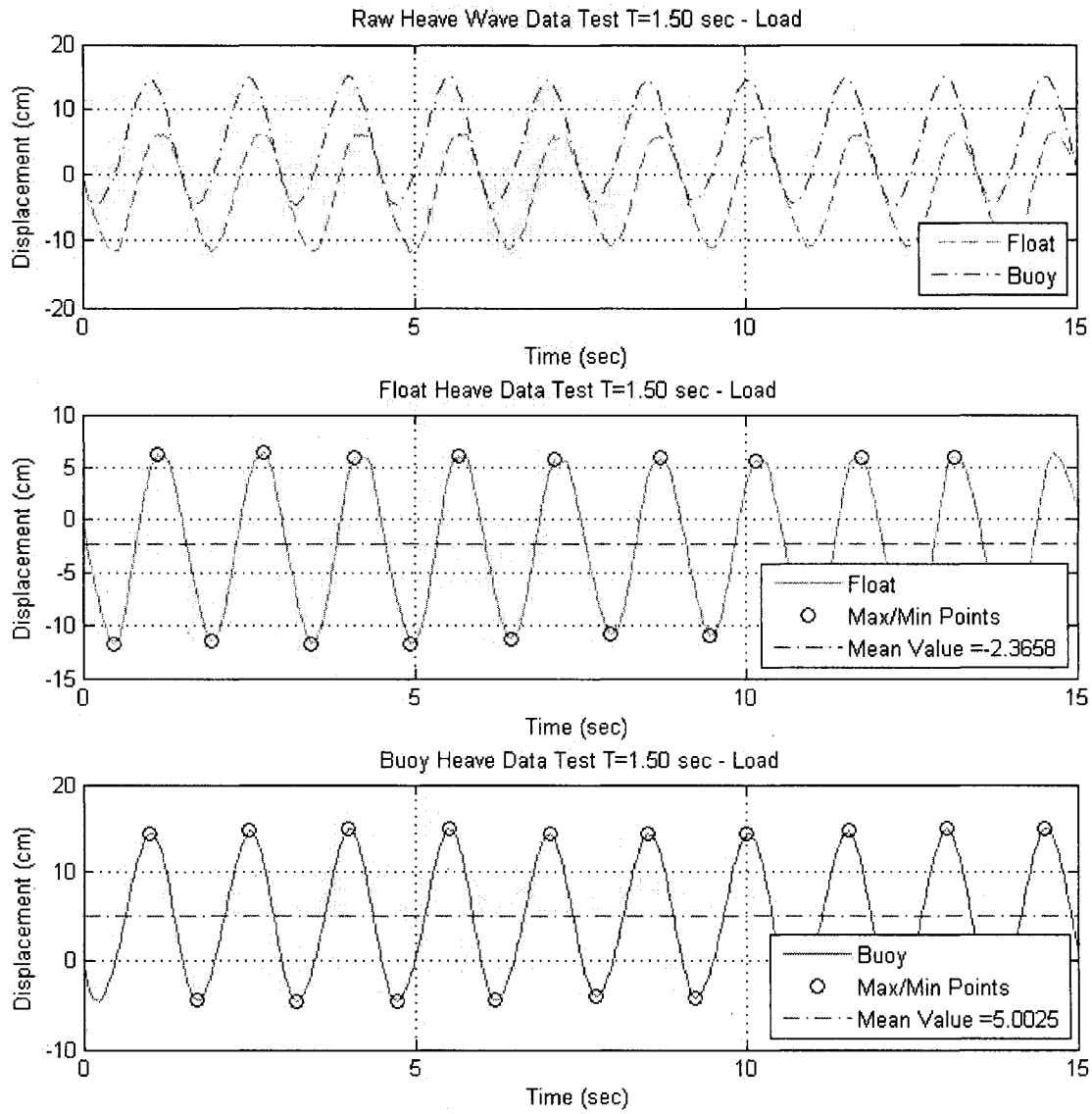

Figure 4.14: Plots showing the data collected from OPIE for a typical wave test. The upper plot is the raw data for the wave float and the buoy. The middle plot is data for the wave float with the maximum and minimum points labeled. The lower plot is the data for the buoy with the maximum and minimum points labeled.

5. Free-release Results

The damped natural period in heave and pitch for the two loading conditions are shown in Table 4.4. The measured model scale values were then scaled up to full scale values.

Table 4.4: Damped natural period (Td) values for the model (m) and full scale buoy (fs).

	Td_m (sec)	Td_{fs} (sec)
Heave (Load)	0.8018	3.651
Heave (Light)	0.7492	3.412
Pitch (Load)	1.0607	4.830
Pitch (Light)	1.0196	4.643

6. Regular Wave Test Results

The Heave, Surge, and Pitch RAOs were calculated for the buoy and are shown in Figure 4.15 through Figure 4.17. The physical model testing heave, surge, and pitch testing results were scaled up to full scale values. The full scale values were used in the calculation of the RAOs.

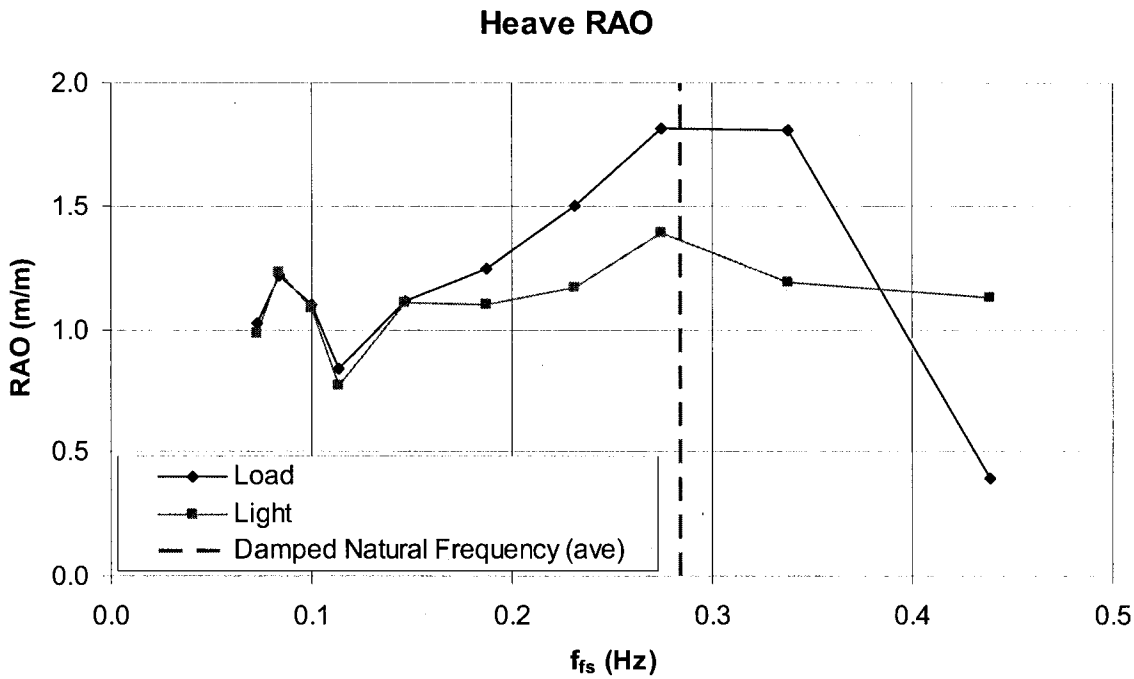

Figure 4.15: Heave RAO for load and light case. Heave RAO is heave amplitude normalized by wave amplitude.

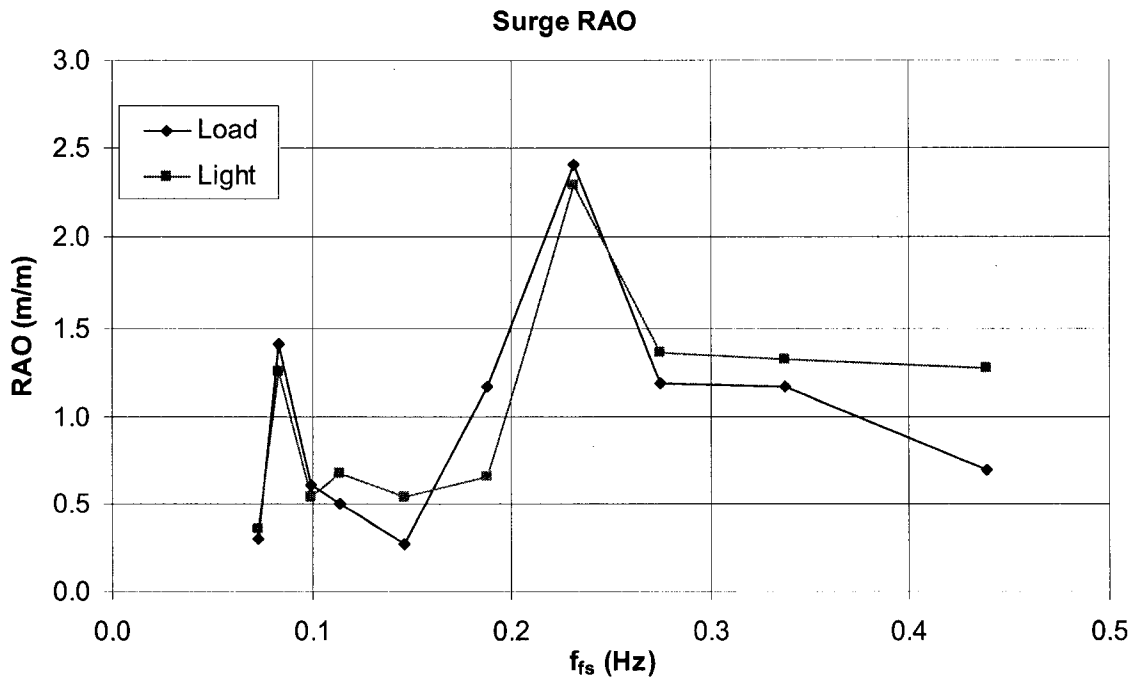

Figure 4.16: Surge RAO for load and light cases. Surge RAO is buoy's horizontal amplitude normalized by fluid particle horizontal amplitude at the mean surface.

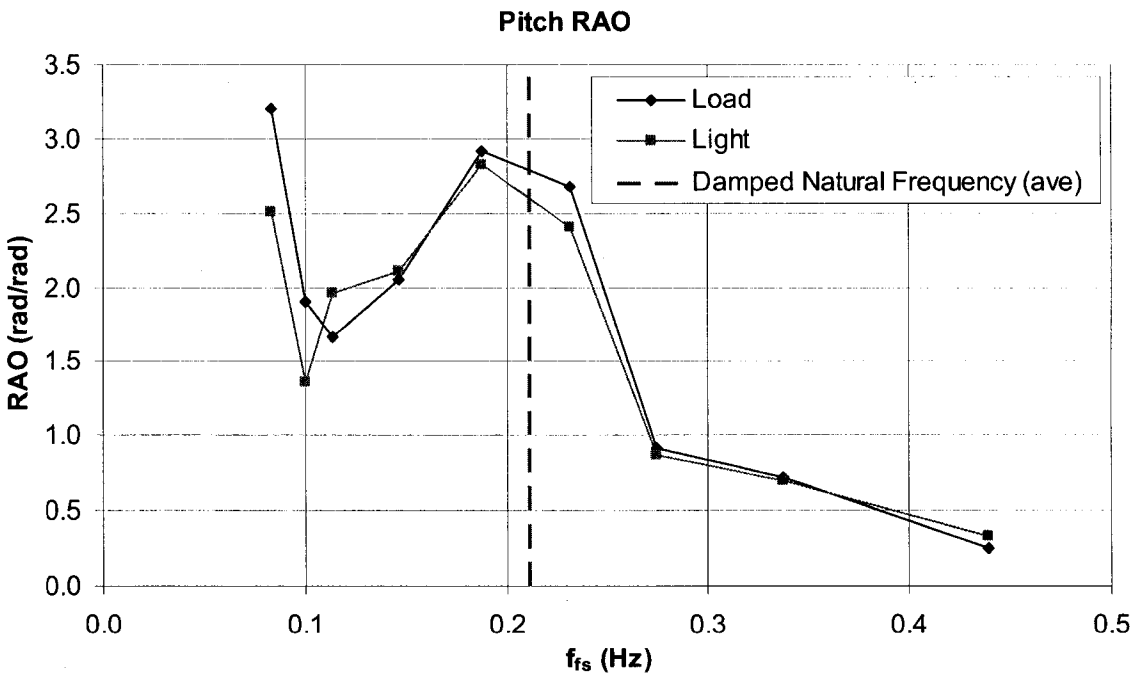

Figure 4.17: Pitch RAO for load and light case. Pitch RAO is buoy's pitch amplitude (in radians) normalized by maximum wave slope.

7. Wave Response Discussion

At low frequencies, the buoy will follow the wave vertical motion, as can be seen in the Heave RAO plot (Figure 4.15). In the frequency range for which the buoy has a large Heave RAO (greater than 1.5) the energy present in the waves is manageable. The average heave natural period of 3.561 seconds, frequency of 0.274 Hz, is visible in the plot. The peak Heave RAO value matches up well with the damped natural frequency determined by the free-release heave test.

The Surge RAO plot (Figure 4.16) shows two peaks at 0.083 Hz and 0.231 Hz, with greater RAO values at the higher wave frequency peak. Thought the highest surge RAO value of 2.40 for the load case is not desirable, surge motion does not directly put the deck underwater. Thus surge motion of the buoy is a secondary concern compared to heave and pitch motion. At higher wave frequencies the Surge RAO values are still close to unity.

The Pitch RAO plot (Figure 4.17) also shows two peaks. One is, as expected, located close to the pitch natural period of 4.74 seconds (average value), frequency of 0.2112 Hz, with Pitch RAO values greater than 2.5. The second peak is at the lowest frequency tested of 0.073 Hz, with RAO values of similar magnitude. Although these values are not ideal, the lower peak is attributed to the mooring system and could not be avoided.

In an effort to minimize the pitch response that was observed from these model tests, a second set of tests were conducted. This series of wave tests used a higher "Upper" mooring attachment location, closer to the center of gravity of the buoy. Information about this set of tests can be found in *Appendix: "Upper" Mooring Attachment Physical Model Testing*. The higher mooring point, however, did not improve

the pitch response significantly. The lower mooring point, therefore, was used in the final design.

Based upon all physical model tests, the buoy is a wave follower with respect to vertical motion for large, long period waves that occur during storms. Heave resonance occurs of higher frequencies associated with small, fair-weather waves. The wave response in general should not have severe reactions to the wave spectra that are normally observed at the expected buoy location.

CHAPTER V

NUMERICAL MODELING

1. Aqua-FE Model

A numerical model of the buoy was generated in Aqua-FE to investigate the buoy's response to a variety of different ocean conditions (see Figure 5.1). Aqua-FE is a finite element analysis program that has the ability to investigate objects in a wave environment (Tsukrov et al., 2002). The Aqua-FE model was generated based upon the same full scale buoy physical properties that were used for construction of the physical scale model. The Aqua-FE model was subjected to similar free-release and wave tests that the physical model underwent. As with the physical model, the tests were performed for two loading conditions: load (full feed) and light (no feed or fuel). The results of the Aqua-FE testing were compared to the physical model test results. The purpose was to optimize and validate an Aqua-FE model of the large, solid feed buoy using an array of truss elements (the basic "element" used by Aqua-FE). Upon successful evaluation, using the feed buoy model to analyze mooring designs (described in Chapter VI) could be done with confidence.

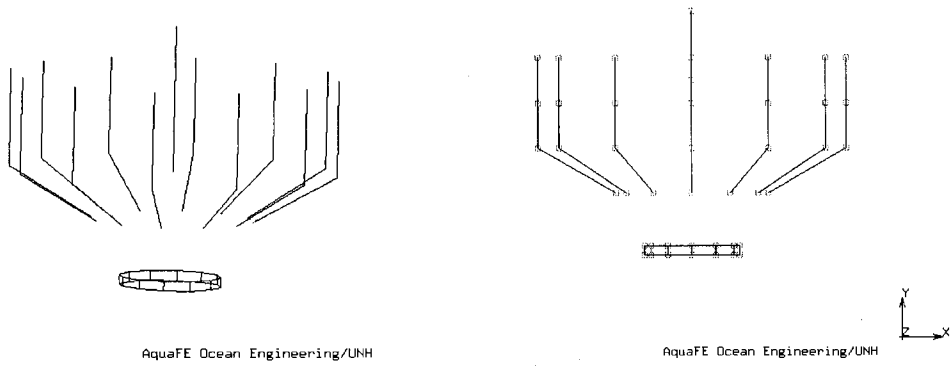

(a) (b)

Figure 5.1: Aqua-FE model of 20-ton feed buoy. (a) Isometric view of model. (b) Front view of model with nodes shown.

It is important to note that the Aqua-FE, feed buoy model was constructed with the proper weight(s), center of gravities (load and light), and volume; however the projected area of the hull model is increased. This is a result of utilizing truss elements, used by Aqua-FE, to represent flat plates. The extra projected area results in an increased drag of the system.

2. Numerical Testing Methodology

Free-release

With the numerical model complete, free-release tests were performed, similar to tests performed on the buoy physical model (see Chapter IV). Heave and pitch tests were conducted at two different displacement conditions: load and light. The load condition corresponds to the buoy with full feed levels, while the light condition is without feed and fuel.

The numerical model tests began with the buoy at a non-equilibrium position. For heave tests the buoy was displaced vertically, while for pitch tests, the buoy was rotated from its vertical axis a small angle. The simulations were run, and positions of two nodes on the buoy (x-axis, y-axis, and z-axis values) were recorded.

Regular waves

Wave tests using the Aqua-FE model were performed using the same regular wave profiles (full scale) that were used in the physical model wave tests (see Table 4.3 for wave parameters). As in the physical model wave testing, a mooring system was required to constrain the buoy's position. To ensure that a steady state condition was reached, the simulations were performed for at least 300 seconds while data was recorded.

The full description of the mooring system design can be found in Chapter VI. However, similar to the scaled physical model testing, only one anchor leg was needed for the wave tests. This mooring, consisting of an anchor, chain, and line (details can be found in Chapter IV), was constructed in Aqua-FE, with the anchor having a fixed position.

3. Data Processing Techniques

Free-release

The data was exported from Aqua-FE and analyzed in a fashion similar to the physical model data. Unlike the physical testing, only one test for each loading condition was necessary for the numerical analysis. The recorded vertical displacement locations (heave) and angular displacement (pitch) of the two tracked points on the buoy were plotted versus time (see Figure 5.2). The time differences (periods) between the cycles are the damped natural periods (Td) desired. The first nine trough and crest values, after the buoy passed through the equilibrium displacement position, were used to determine the period. The periods for each test were averaged yielding a single value, resulting in the final damped natural period for the buoy's numerical model.

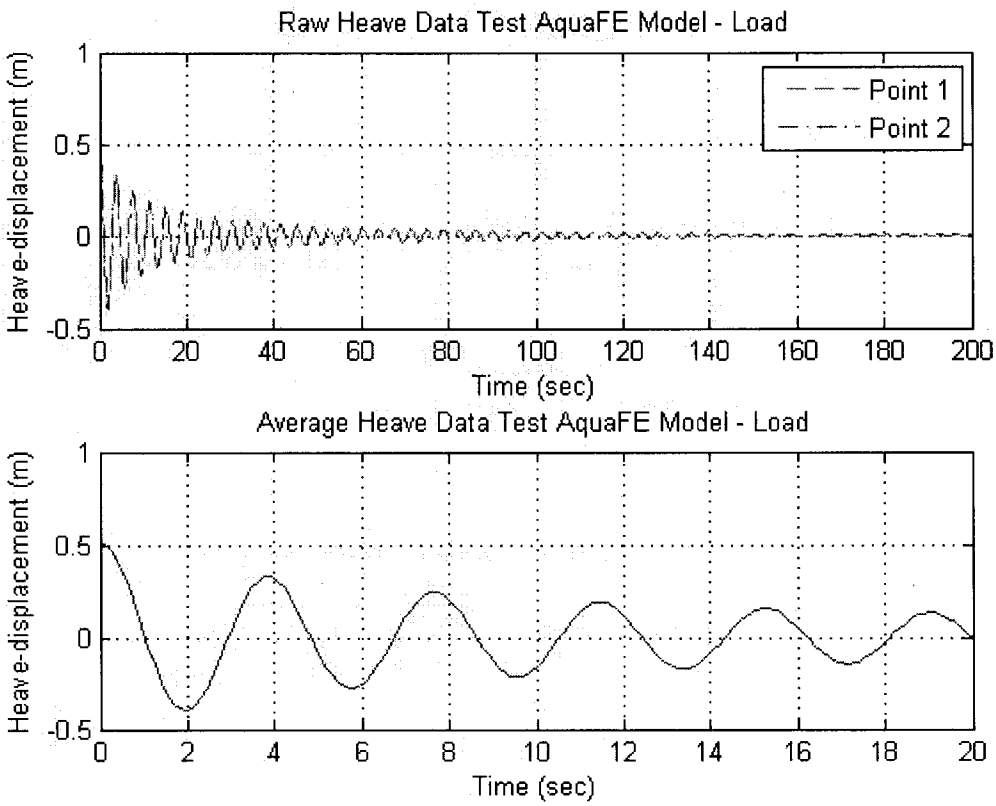

Figure 5.2: Plot of heave displacement versus time for load condition. The raw data for the two points is shown in the upper plot, while the first 20 seconds of the averaged data is shown in the lower plot. The averaged data was used for analysis.

Regular waves

The data collected from Aqua-FE was imported into MATLAB®. The linear and angular displacements of the buoy's tracked nodes were plotted versus time. The analyses for heave, surge, and pitch RAOs are identical except the pitch values are angles instead of linear displacements.

A typical heave wave plot is shown in Figure 5.3. The maximum and minimum values, from the plots, were used to determine the amplitudes of motion. These values were then used to calculate the RAO values.

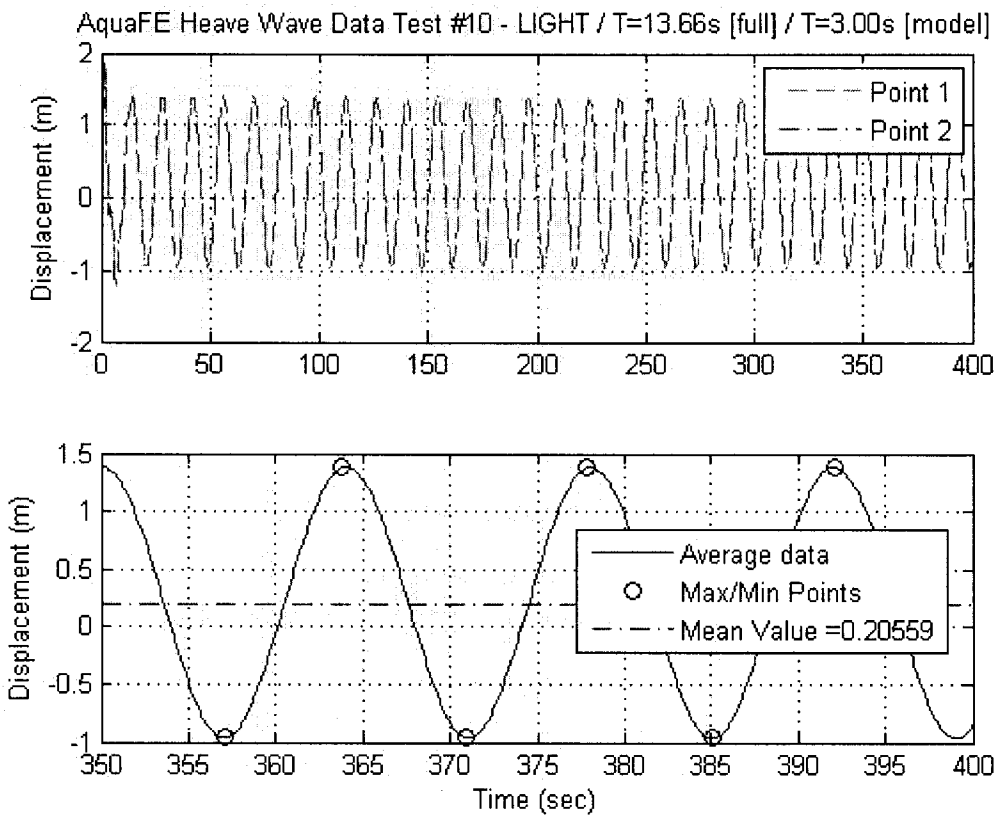

Figure 5.3: Plots showing the data collected from Aqua-FE for a typical wave test. The upper plot is the raw data for the two points tracked. The lower plot is the data for the buoy with the maximum and minimum points labeled.

4. Numerical and Physical Free-release Results and Comparison

The results of the free-release analysis are shown in Table 5.1. The physical model and Aqua-FE model had similar damped natural periods with a maximum 13.3% difference. In general, the numerical model results are similar to the physical model results, giving confidence in the 20-ton capacity feed buoy model in Aqua-FE. With small differences in values, the numerical model supports the results obtained from the physical model.

Table 5.1 Comparison between Free-Release tests: Physical scale model and Aqua-FE computer model.

	Physical Model		Aqua-FE Model		
	Td_{fs} (sec)	f_{fs} (Hz)	Td_{fs} (sec)	f_{fs} (Hz)	% diff. (%)
Heave (Load)	3.651	0.2739	3.814	0.2622	4.5
Heave (Light)	3.412	0.2931	3.357	0.2979	1.6
Pitch (Load)	4.83	0.2070	5.471	0.1828	13.3
Pitch (Light)	4.643	0.2154	4.714	0.2121	1.5

5. Regular Wave Test Results

The Heave, Surge, and Pitch RAOs were calculated for the buoy and are shown in Figures 5.4 through 5.6. The numerical model testing heave, surge, and pitch test results are shown for the load and light conditions. The damped natural frequency is also plotted for comparison. (Comparison with physical model wave tests is done is section 7. below.)

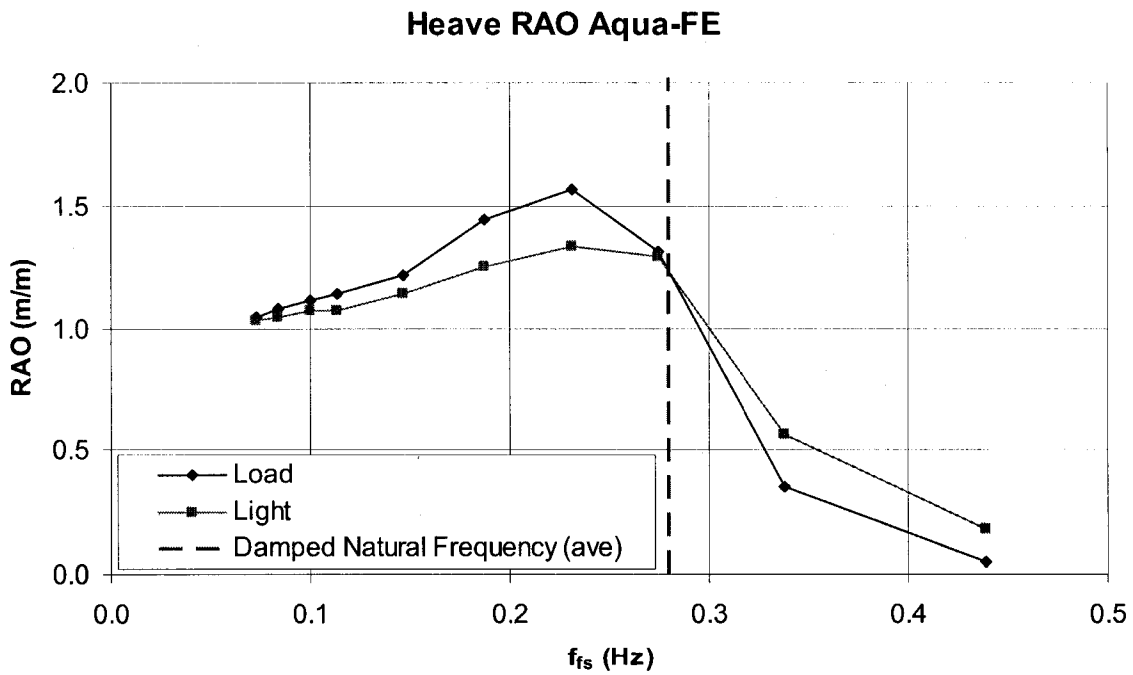

Figure 5.4: Aqua-FE analysis Heave RAO for load and light case. Heave RAO is heave amplitude normalized by wave amplitude.

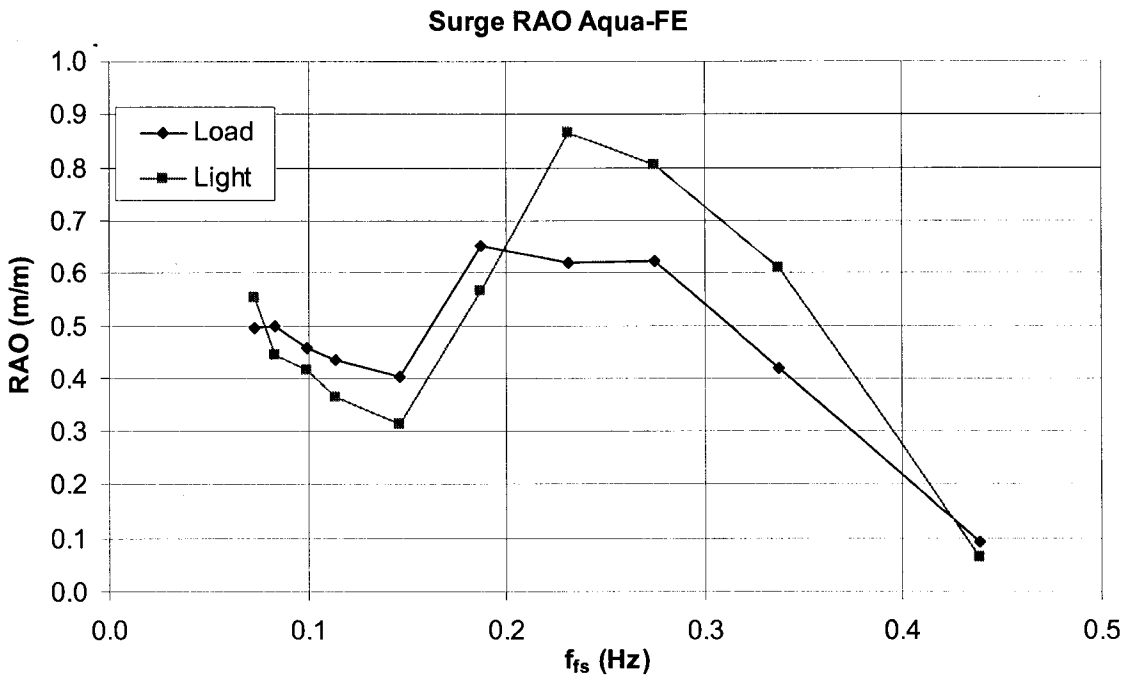

Figure 5.5: Aqua-FE analysis Surge RAO for load and light cases. Surge RAO is buoy's horizontal amplitude normalized by fluid particle horizontal amplitude at the mean surface.

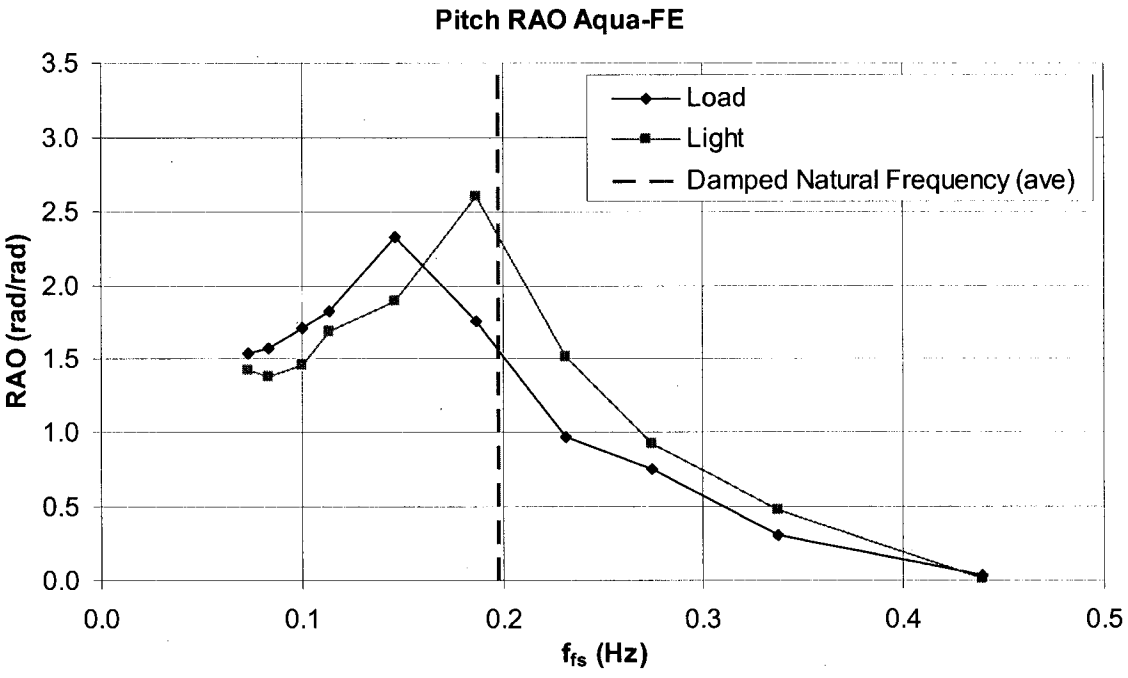

Figure 5.6: Aqua-FE analysis Pitch RAO for load and light case. Pitch RAO is buoy's pitch amplitude (in radians) normalized by maximum wave slope.

6. Wave Response Discussion

At low frequencies, the buoy will follow the wave vertical motion, as can be seen in the Heave RAO plot (Figure 5.4). In the small frequency range for which the buoy has a large Heave RAO (greater than 1.5) the energy present in the waves is manageable. The average heave natural period of 3.59 seconds, frequency of 0.279 Hz, is visible in the plot. The peak Heave RAO value is found to be at a slightly lower frequency than the damped natural frequency determined by the free-release heave test. This phenomenon is most likely the result of Aqua-FE inaccurately representing the drag forces on the buoy. This frequency shift has been seen in previous comparisons between physical and numerical tests using Aqua-FE. However, this slight discrepancy is not of critical importance to the response of the buoy.

The Surge RAO plot (Figure 5.5) shows one peak at 0.231 Hz. However, the RAO value at that peak is close to unity and as such is not a concern to the motion of the buoy.

The Pitch RAO plot (Figure 5.6) also shows one peak. It is, as expected, located close to the pitch natural period of 5.09 seconds (average value), frequency of 0.196 Hz, with Pitch RAO values greater than 2.5.

Based upon all numerical tests, the buoy is a wave follower with respect to vertical motion for large, long period waves that occur during storms. Heave resonance occurs of higher frequencies associated with small, fair-weather waves. The wave response in general should not have severe reactions to the wave spectra that are normally observed at the expected buoy location.

7. Numerical and Physical Wave Response Comparison

The Heave, Surge, and Pitch RAOs for both the numerical and physical model wave testing is shown in Figures 5.7 through 5.9.

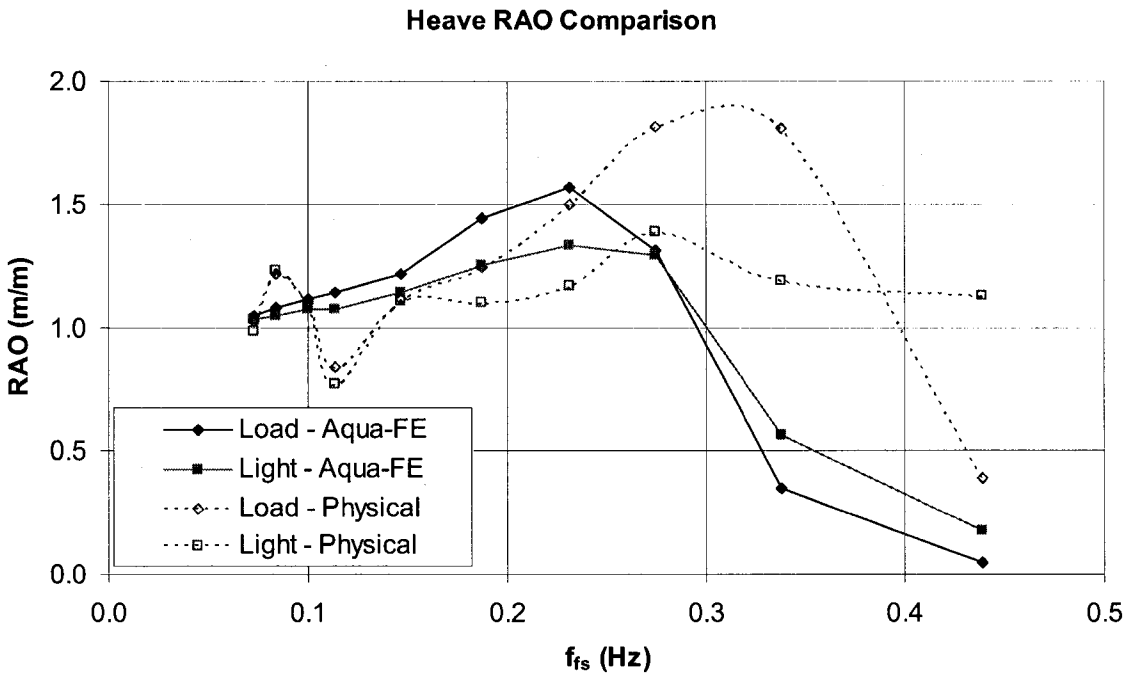

Figure 5.7: Comparison plot showing the Aqua-FE and Physical model Heave RAO analysis results.

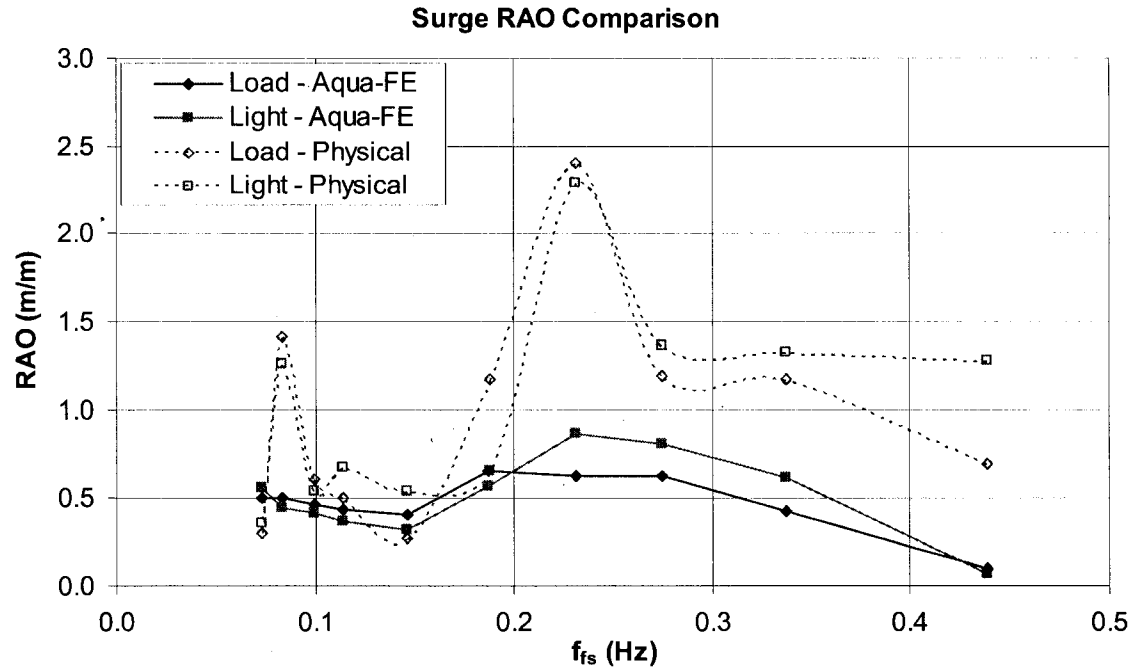

Figure 5.8: Comparison plot showing the Aqua-FE and Physical model Surge RAO analysis results.

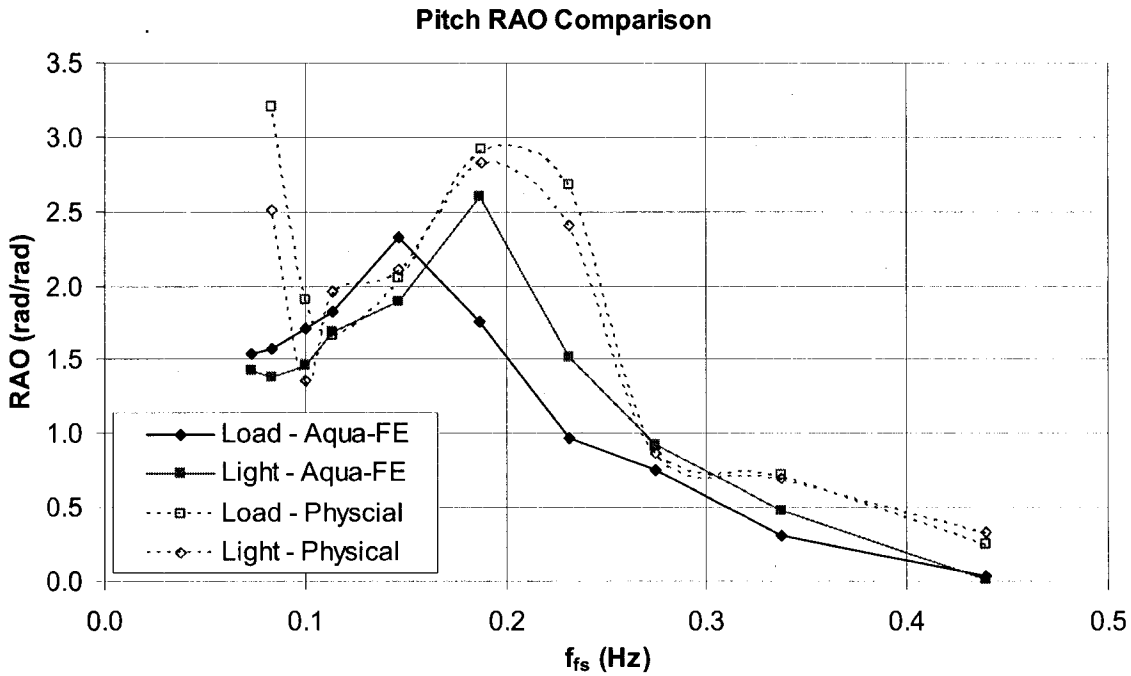

Figure 5.9: Comparison plot showing the Aqua-FE and Physical model Pitch RAO analysis results.

With the exception of the Surge RAO plot, the curve shapes between the numerical and physical models are similar. The Aqua-FE Surge RAO plot is flat in comparison to the physical model Surge RAO plot. One possible reason for this is the increased projected area of the Aqua-FE model buoy. In Aqua-FE, the buoy will, in general, initially set back more against the mooring, but have reduced oscillations. While a slight shift in peak RAO values can be seen between the Aqua-FE and physical model heave and pitch testing, which can also be seen in the free-release damped natural frequency results, the differences are minor. This leads to the conclusion that the numerical model captures the basic physics of vertical and rotational oscillations but my over predict the effects of drag and hence, mooring loads. For mooring design purposes, Aqua-FE is conservative and therefore acceptable.

CHAPTER VI

MOORING SYSTEM DESIGN

1. Mooring Design Using Aqua-FE

The numerical modeling program, Aqua-FE, was utilized to design the mooring system, in conjunction with the previously constructed feed buoy finite element model (see Chapter V). Aqua-FE is a finite element analysis program that has the ability to investigate objects in a wave environment (Tsukrov et al., 2002), and was used to design the mooring system for the Isles of Shoals site. Aqua-FE numerical analysis was applied to the full UNH aquaculture system (see Figure 6.1), including the cages and mooring grid, to predict the response of the buoy and nearby gear to large amplitude storm waves combined with current.

While four mooring designs were initially investigated, the final design for the feed buoy mooring has four anchor legs, separate from the UNH OOA grid system (see Figure 6.1). The feed buoy mooring was not incorporated into the grid system for two reasons: the grid was not designed to hold a large surface buoy, and the grid was to be maintained as an independent scientific/engineering platform. Also, the buoy could not be located inside the grid due to the interference of the buoy mooring with cage surfacing operations. The buoy was situated off the northeast (NE) grid corner in order to minimize the feed hose lengths as well as have the mooring legs that exit the site be as

parallel as possible to the navigation LORAN lines. (Lobster trap trawl lines are set parallel to LORAN lines to minimize interference.)

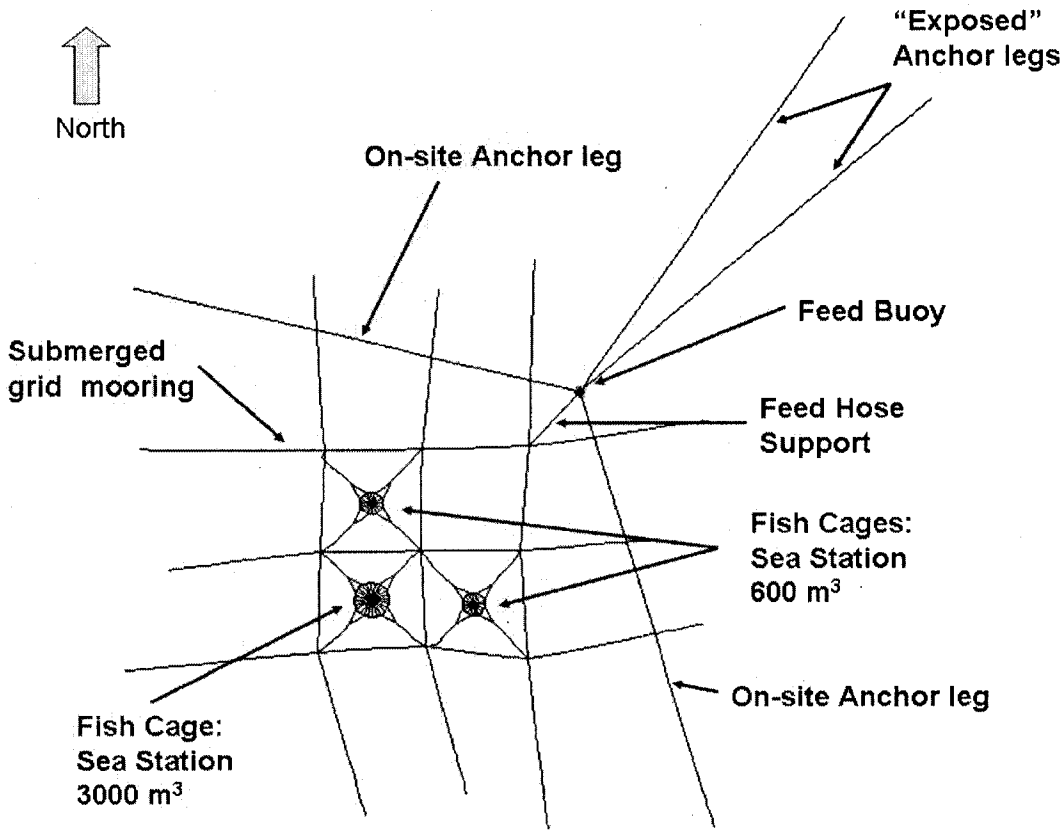

Figure 6.1: General layout of the UNH OOA submerged grid system (as deployed) with the current design of the 20-ton feed buoy mooring.

The ratio of mooring line length to water depth (scope) was selected to be 6:1. Although this scope does place two anchors off the site, it allows: (1) standard seamanship practice of mooring surface vessels, (2) minimize the downward force that would be exerted on the buoy with a mooring line under tension, enabling the buoy to ride up and over a large wave as opposed to being forced through it, and (3) the line to provide adequate compliance to the system.

a. Mooring Leg Details

The mooring legs (see Figure 6.2), that have a scope of 6:1, two run approximately NE, one runs south-southwest (SSW), and another runs west-northwest

(WNW) (see Figure 6.1). The anchor legs consist of a 1650 pound (750 kilogram), plow embedment anchor, with a holding power ratio of 55.2:1, a shot (90 feet) of 2 inch stud link anchor chain, and approximately 830 feet of 3 inch line. This first (lowest) length of line is terminated approximately 100 feet from the buoy. Two separate lines continue from the termination, one to the surface (and located via a float for vessel tie-up purposes) and the other line attached to the feed buoy.

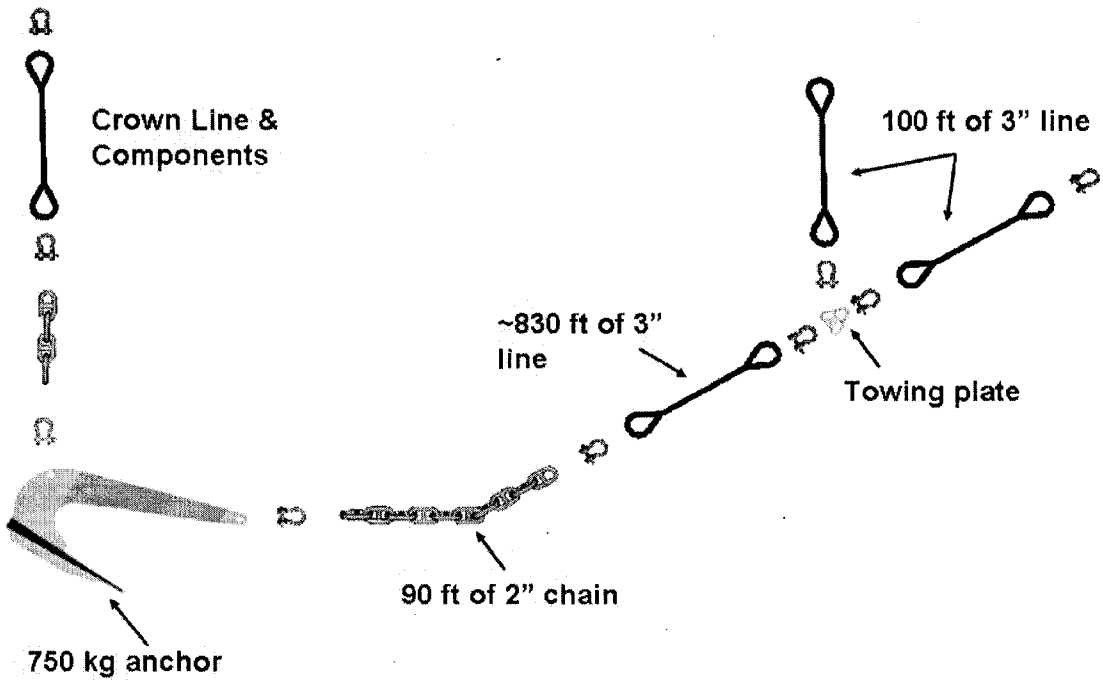

Figure 6.2: Exploded view of a single mooring leg attachment. Each anchor leg consists of 1 anchor, a shot of chain, and 2 lengths of line.

b. Aqua-FE Analysis & Results

The Aqua-FE analyses were performed using multiple wave heights, periods, and currents. All analyses were performed with the buoy in the load condition (full of feed). This was done assuming the larger buoy weight would produce the greatest tensions and buoy motions. The majority of the analyses were done using UNH's design wave that has the following parameters: 9.0 meter wave height, 8.8 second period, and

1 meter per second current that is constant with depth and in the direction of the wave train.

Using UNH's design wave and a worst-case scenario, one mooring leg taking the entire load of the wave forcing, the maximum tension that was found in a single anchor leg was 282 kilo-newtons. This compares with a single anchor pull-out force of 405 kilo-newtons and a mooring line maximum breaking load of 800 kilo-newtons. With the present mooring design the buoy's watch circle will be a maximum/minimum straight line distance of 72/33 meters from the NE grid corner. The expected operating distance of the buoy from the NE grid corner is 49 meters. The buoy was subjected to the design wave and current from various directions to generate the final watch circle (see Figure 6.3).

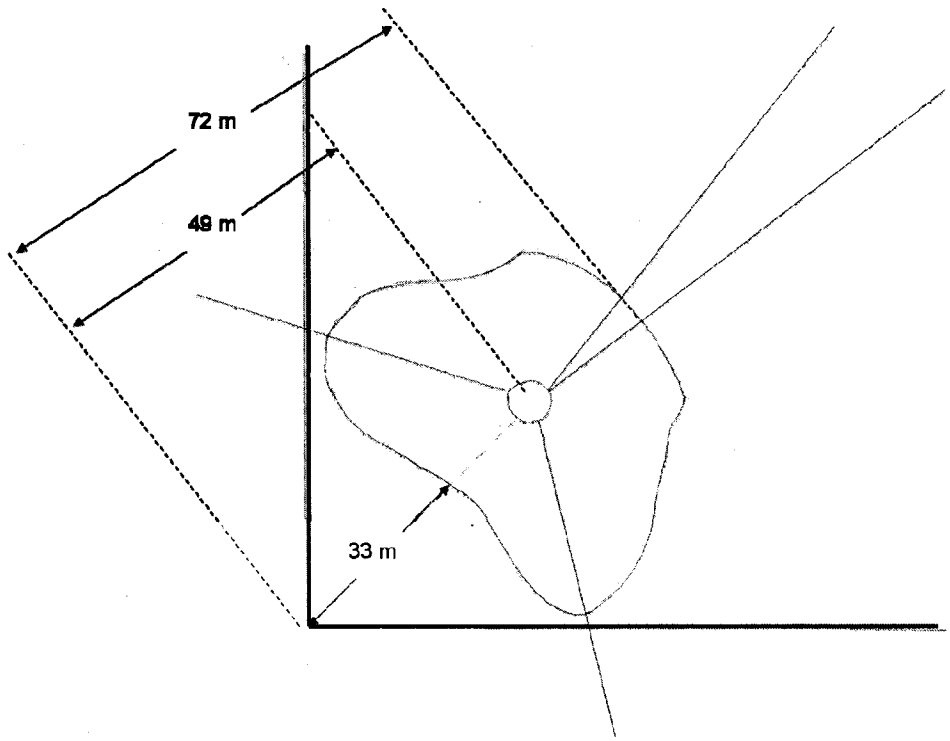

Figure 6.3: The final watch circle of the feed buoy mooring.

c. Mooring System Discussion

With the buoy properly moored in the northeast corner of the UNH OOA grid, buoy operations should not interfere with the grid. In the unlikely event that the mooring

leg loading is higher than the Aqua-FE analyses predicted, the anchor will drag before the line will fail. Based upon this analysis, however, the buoy will be securely held in location, even under extreme environmental loading.

CHAPTER VII

CONSTRUCTION

1. Builder Selection

The first step in construction was to locate organizations that had the capability to manufacture and assemble the feed buoy. Due to the buoy's large steel structure, the construction had to be performed outside of UNH. The next step was to complete the construction documents, followed by a bidding process and awarding the buoy construction project to the desired organization.

a. Potential Builder Site Visits

Site visits to potential builders were conducted to confirm their interest in the project as well as gather information concerning their approach to the actual construction process. Meetings were held with the following companies:

- Rockland Marine at Rockland, ME on 16 December 2004
- Cianbro at Pittsfield, ME on 17 December 2004
- Stommel Fisheries Services at Durham, NH on 10 January 2005.

In addition, the meetings also provided insight of the builder's possible customer relationship with UNH such as frequent site visits during construction by UNH personnel. At then end of each meeting, the organizations were informed that they would be

involved in a competitive bid process. The company with the best overall bid would be awarded the contract.

b. Request For Proposal

With the scope of the design and the expected cost for the buoy determined, the University System of New Hampshire (USNH) Purchasing and Contract Services was brought into the project. Jackie Nyberg, Purchasing Agent, was selected by USNH to aid with the contract process. A meeting with representatives from the Engineering and Operations Teams, as well as USNH Purchasing, was held in early April to discuss the project. It was decided that a Request for Proposal (RFP) was the best choice for the project because of the flexibility it provided.

There were two main components involved with the RFP package for the buoy. One was the engineering drawings that define the specifics of the buoy while the other was the text description for the design of the buoy. After the engineering drawings were complete at the end of May 2005, the RFP text description and proposal procedures document was written.

The RFP package was completed and an announcement posted on the USNH Purchasing web site on 10 June 2005. All proposals from potential builders were due on 8 July 2005. Proposals were received from: Stommel Fisheries Services and Cianbro. Stommel Fisheries Services had a base price of $400,000 while Cianbro had a base price of $350,000. Both of these proposals were considerably more than the amount that was originally budgeted for the construction of the buoy shell (less than $100,000). The rapid rise in steel prices and associated fabrication costs since the original budget was made accounts in large part for the discrepancy. The UNH Open Ocean Aquaculture program had some contingency reserves, but they were insufficient to cover the difference. After the proposals were received, alternate sources of funding were

investigated. No additional funds could be located in a short amount of time, and no contract was awarded on 5 August 2005.

An expanded search for potential builders was carried out after the first RFP process was unsuccessful. The UNH Open Aquaculture program re-allocated internal funds enabling a second RFP process to begin on 30 November 2005.

All proposals from potential builders were received by 9 January 2006. Proposals were submitted from: Aquaculture Engineering Group Inc. (AEG), Rockland Marine Corporation and Gladding-Hearn Shipbuilding. Base bids were evaluated and negotiations undertaken. AEG's bid was accepted by UNH on 13 February 2006. Construction began in early March 2006 at AEG's fabrication facility located in Hillsborough, NB, Canada.

2. Aquaculture Engineering Group

Aquaculture Engineering Group Inc. (AEG) is a Canadian organization devoted to the advancement of aquaculture equipment and systems. AEG's development and construction of a 100-ton capacity feed buoy, of their own design, demonstrated their experience dealing with large construction projects. Their experience and familiarity with the aquaculture industry were important assets for the construction of the 20-ton buoy.

3. Fabrication Procedure/Methods

The construction of large steel structures is typically done in stages. Smaller components, fabricated individually, are assembled into a larger finished product. The buoy was constructed in a similar fashion. The smaller components consisted of the Ballast Can, Main Hull (including the Chine Level), Main Deck, and the Machine House. Detailed information about the listed components can be found in Chapter II.

The Ballast Can (see Figure 7.1) was constructed out of a rolled steel cylinder. The bottom plate, gussets, and mooring attachments were then incorporated into this component.

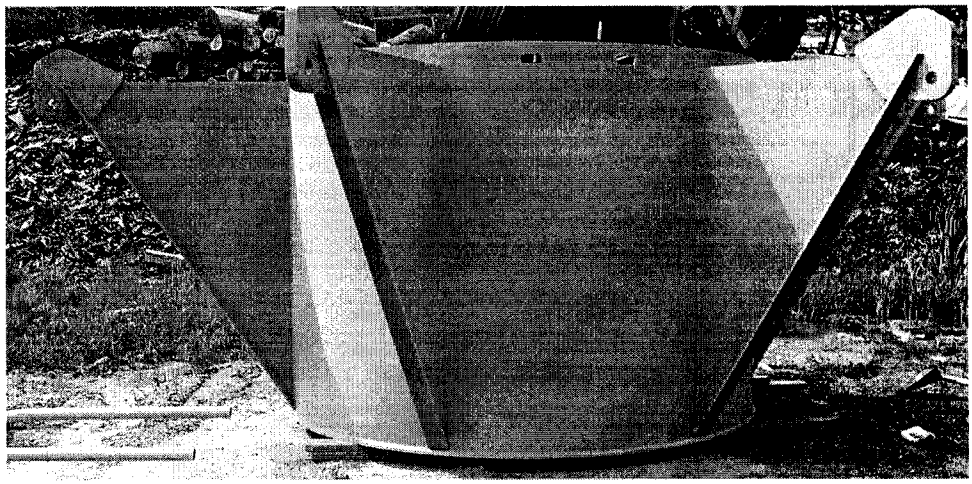

Figure 7.1: Ballast Can after complete welding and painting.

The main body of the buoy is an assembly of the Chine Level and the Main Hull sections (see Figure 7.2). To ease the transport of this large component, wheels and a towing attachment were welded directly to the structure. After the main hull was assembled, subsequent internal framing was welded in place. Figure 7.3 shows the interior of the Main Hull with scantlings, internal decks, and the silo support structures.

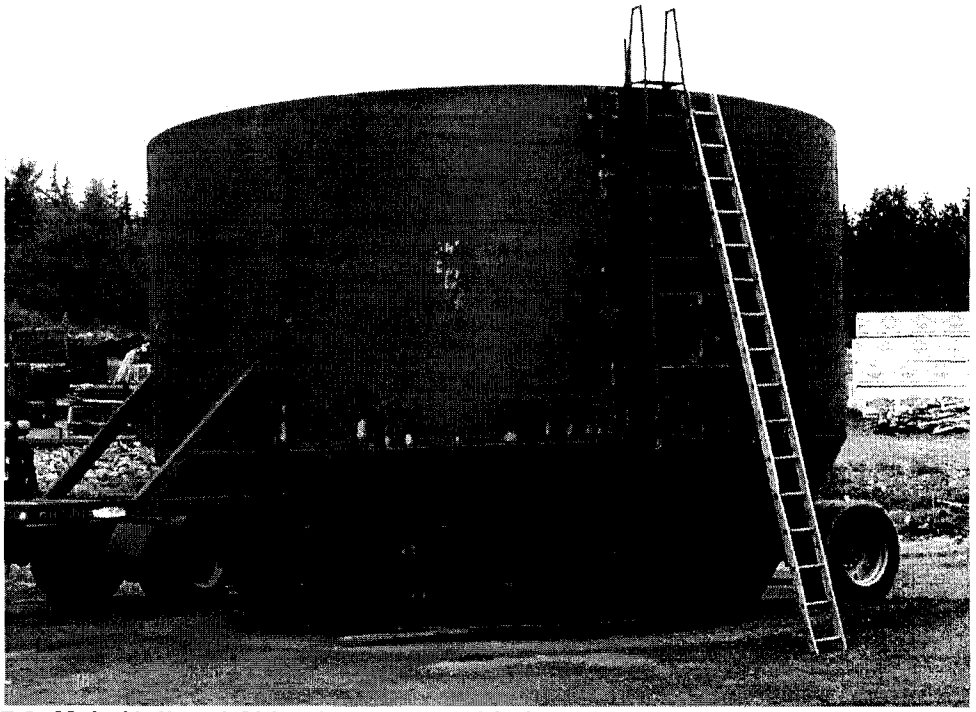

Figure 7.2: Main Hull and Chine Level assembled together. Wheels are welded to the Chine Level to facilitate transport during construction.

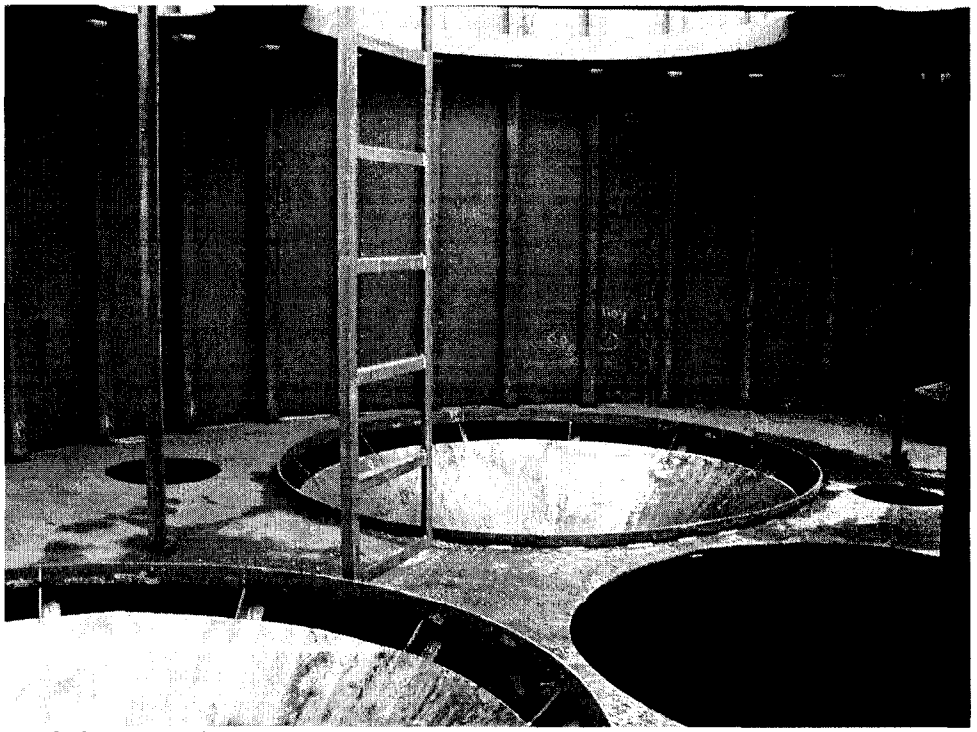

Figure 7.3: Interior of Main Hull. Scantlings as well as the silo support structures. Sub-Main Deck (upper level) and Chine Deck (lower level) are visible.

The Main Deck was fabricated upside down to allow for easier welding of scantlings. After the scantlings were attached, the deck was flipped over, and other features were added (see Figure 7.4) such as the handrail, lifting attachments, and cleats.

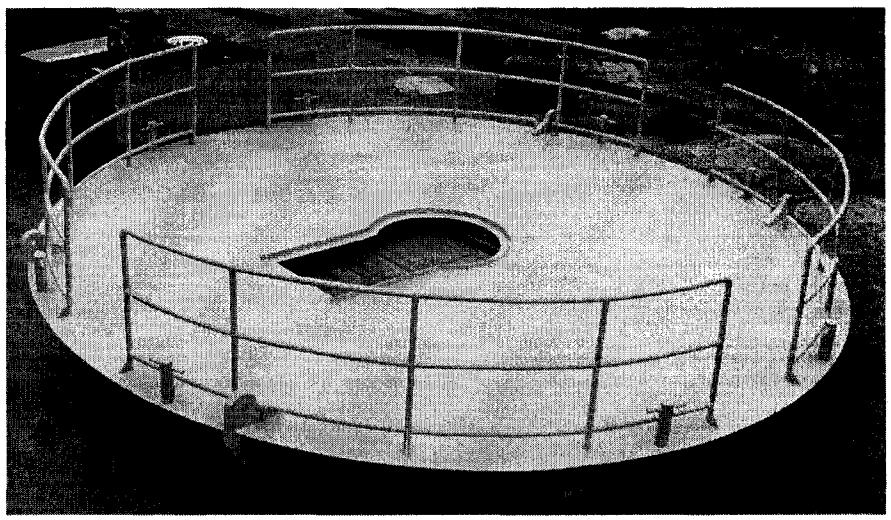

Figure 7.4: Main Deck complete with railings, lifting attachments, cleats, and scantlings (underneath deck) after painting.

The Machine House walls and roof were cut and then welded together (see Figure 7.5). After the house was formed, the internal scantlings were added. Lifting attachments, not included with the design, were added to the structure to allow the structure to be lifted for transport.

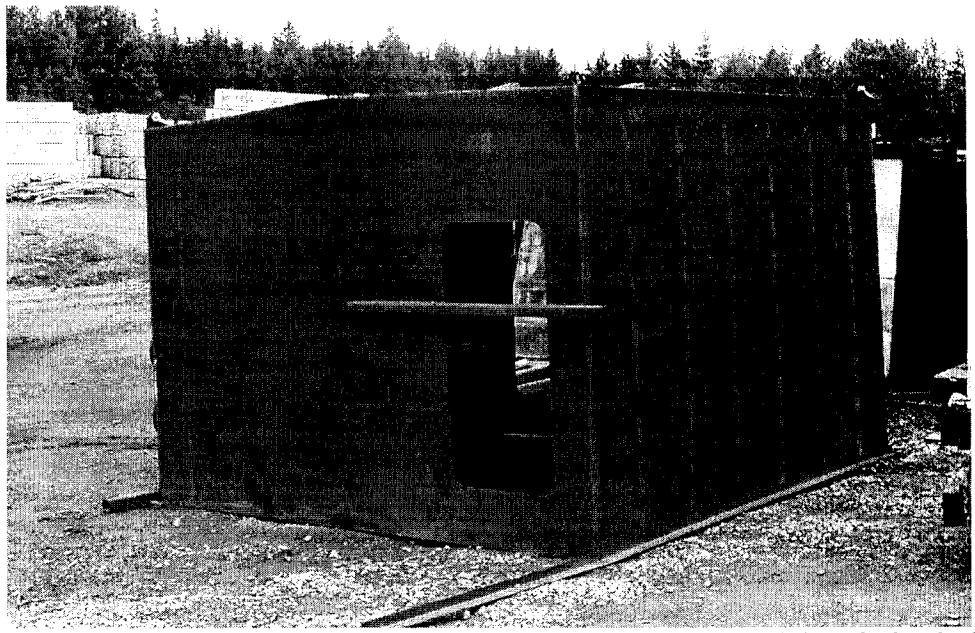

Figure 7.5: Machine House complete with internal scantlings and door holes before painting.

After basic steel fabrication was completed, all major components were sandblasted and painted. Then the large internal components including the feed storage silos and fuel tanks were placed inside the buoy. Figure 7.6 shows the four feed storage bins as well as one fuel tank affixed in the Main Hull subassembly of the buoy. The feed pump was also installed on to the Ballast Can structure before final assembly. This was necessary since the items were too large to be positioned inside the buoy after the main components were assembled into one large structure.

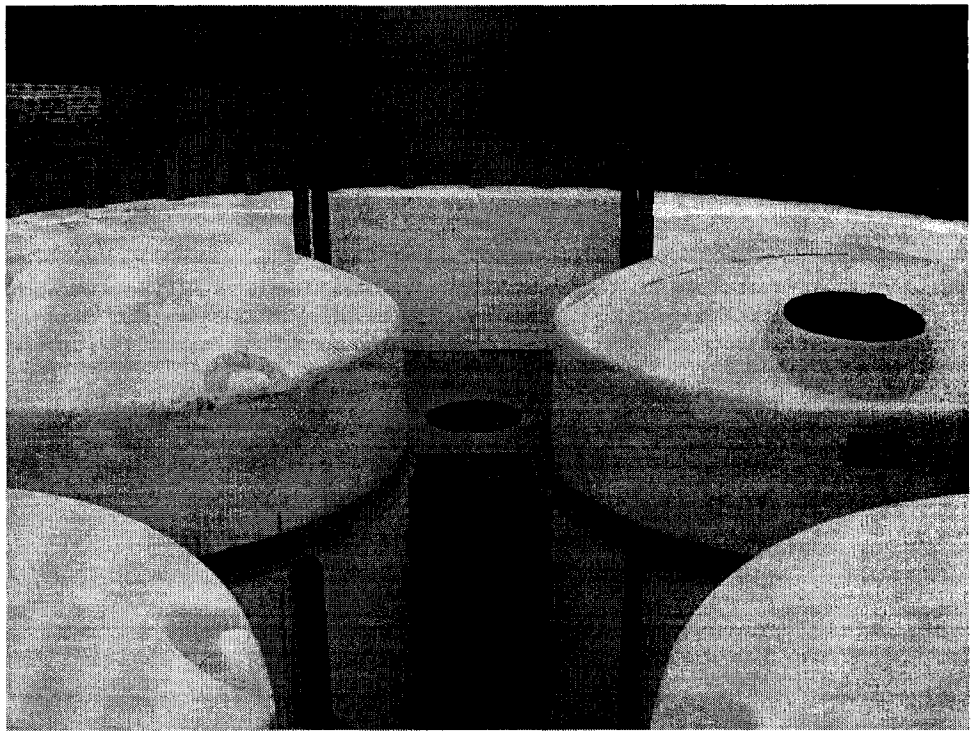

Figure 7.6: Interior view of Main Hull assembly before the addition of the Main Deck. The four feed storage silos are visible as well as one diesel fuel tank (aluminum tank in center) under the Sub-Main Deck.

When the individual components were completed, they were transported to the final assembly/launch site (see Figure 7.7). This was necessary since the buoy would be too large and heavy to move over the roadways after final assembly. The Main Hull assembly was towed to the launch site using the attached wheels and towing attachment. The Ballast Can, Main Deck, and Machine House were all moved separately on flat bed trailers.

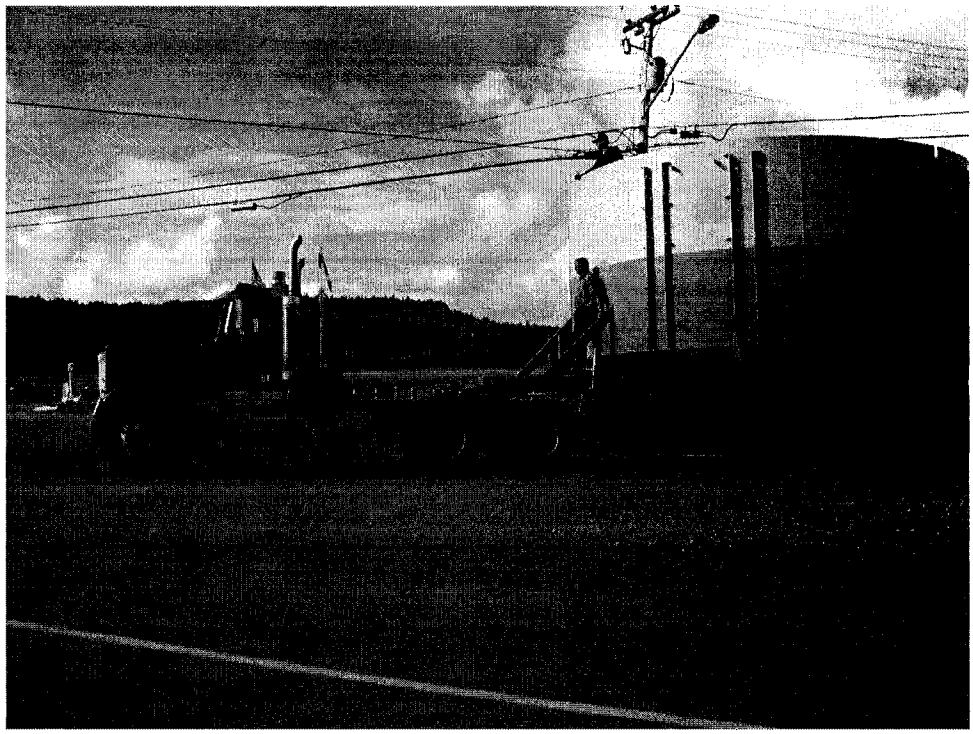

Figure 7.7: Main Hull assembly during transport to the final assembly and launch site.

Once at the launch site, the components were set in place by a crane. The Ballast Can was put into position on top of steel rods that were placed on a large steel sheet (see Figures 7.8 and 7.9). The rods and sheet steel were placed under the buoy to aid in the launching, allowing the buoy to roll into the ocean.

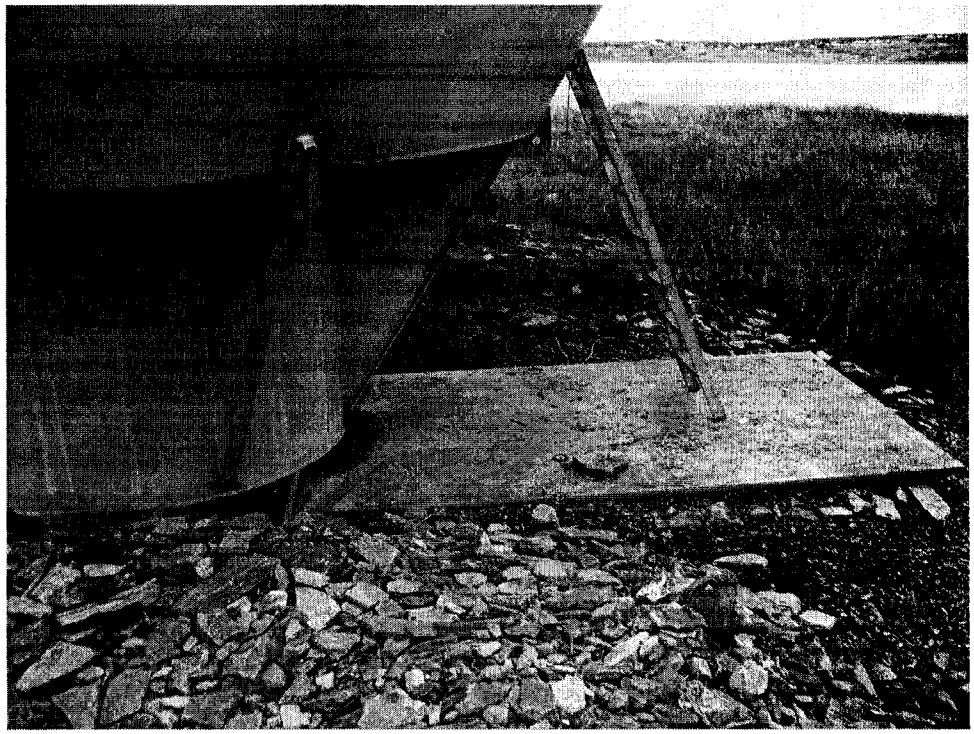

Figure 7.8: Buoy launch plate placed under the buoy. Steel rods shown under buoy are to allow the buoy to roll into the ocean during launch.

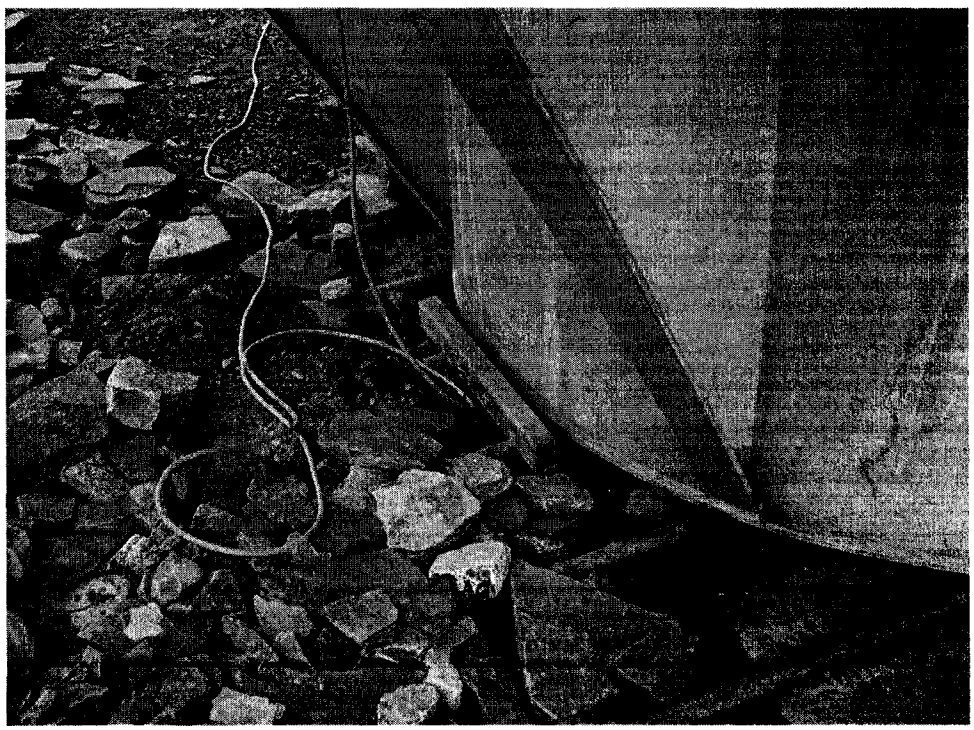

Figure 7.9: Close up of steel rods placed under buoy to allow the buoy to roll into the ocean during launch.

With the Ballast Can in position, the Main Hull subassembly and Main Deck were assembled. Figures 7.10 and 7.11 show the two components being positioned with a

crane. After they were in place, all the components were welded together. With the main components of the buoy's hull assembled, internal components were added to the structure. Figure 7.12 shows the 20-ton buoy with major exterior construction completed.

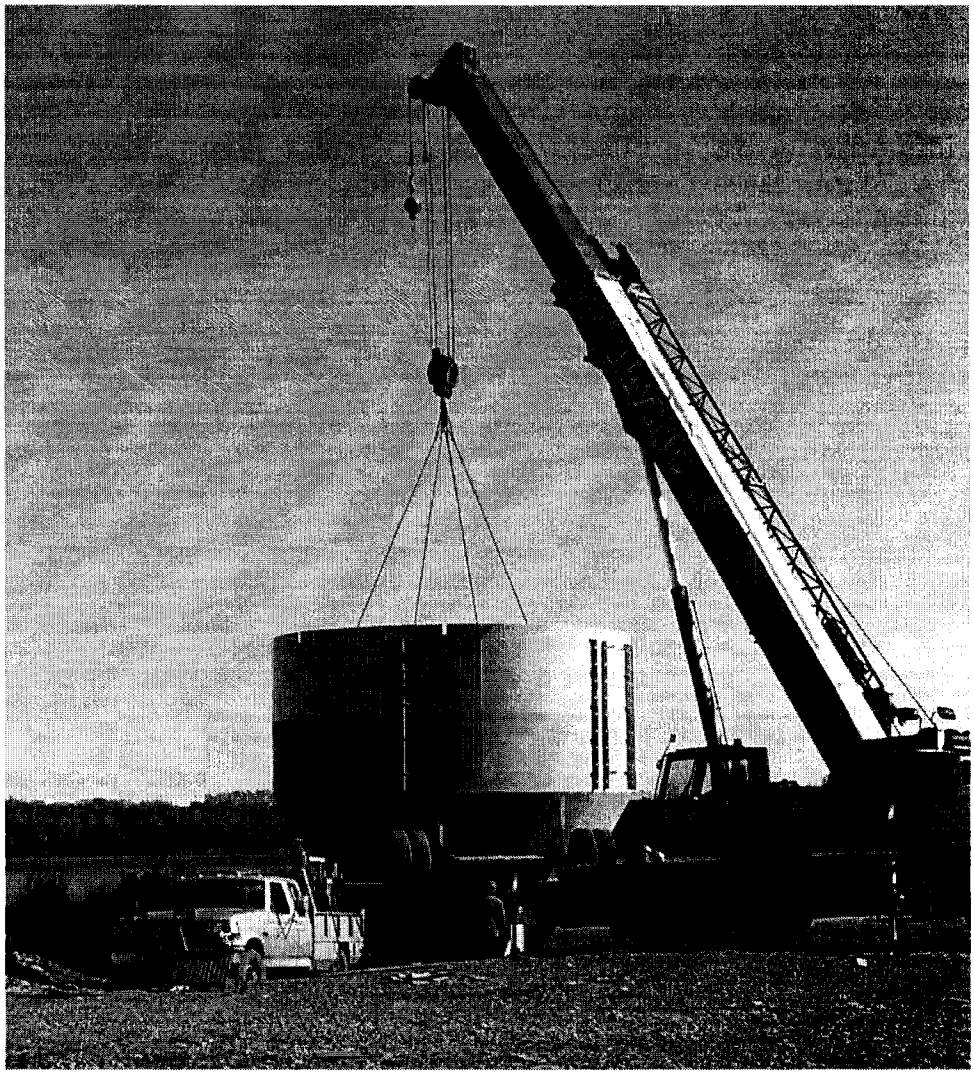

Figure 7.10: Main Hull assembly being lowered into position on top of the Ballast Can at the launch site.

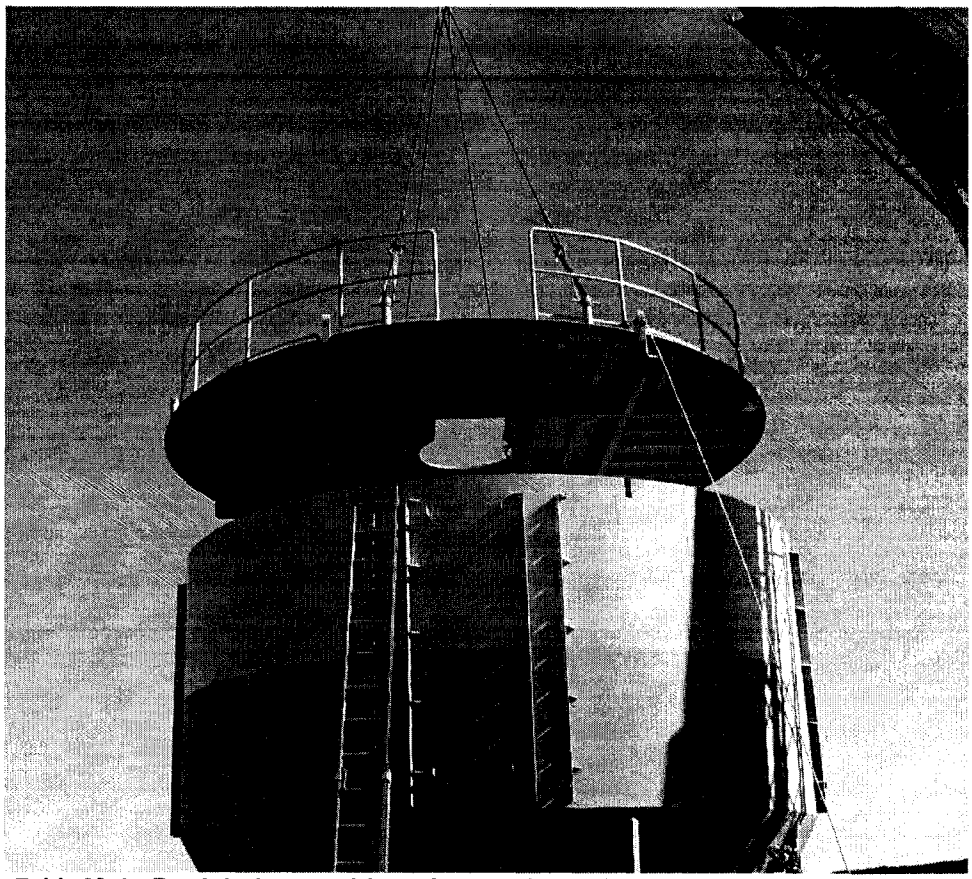

Figure 7.11: Main Deck being positioned upon the Main Hull assembly at the launch site.

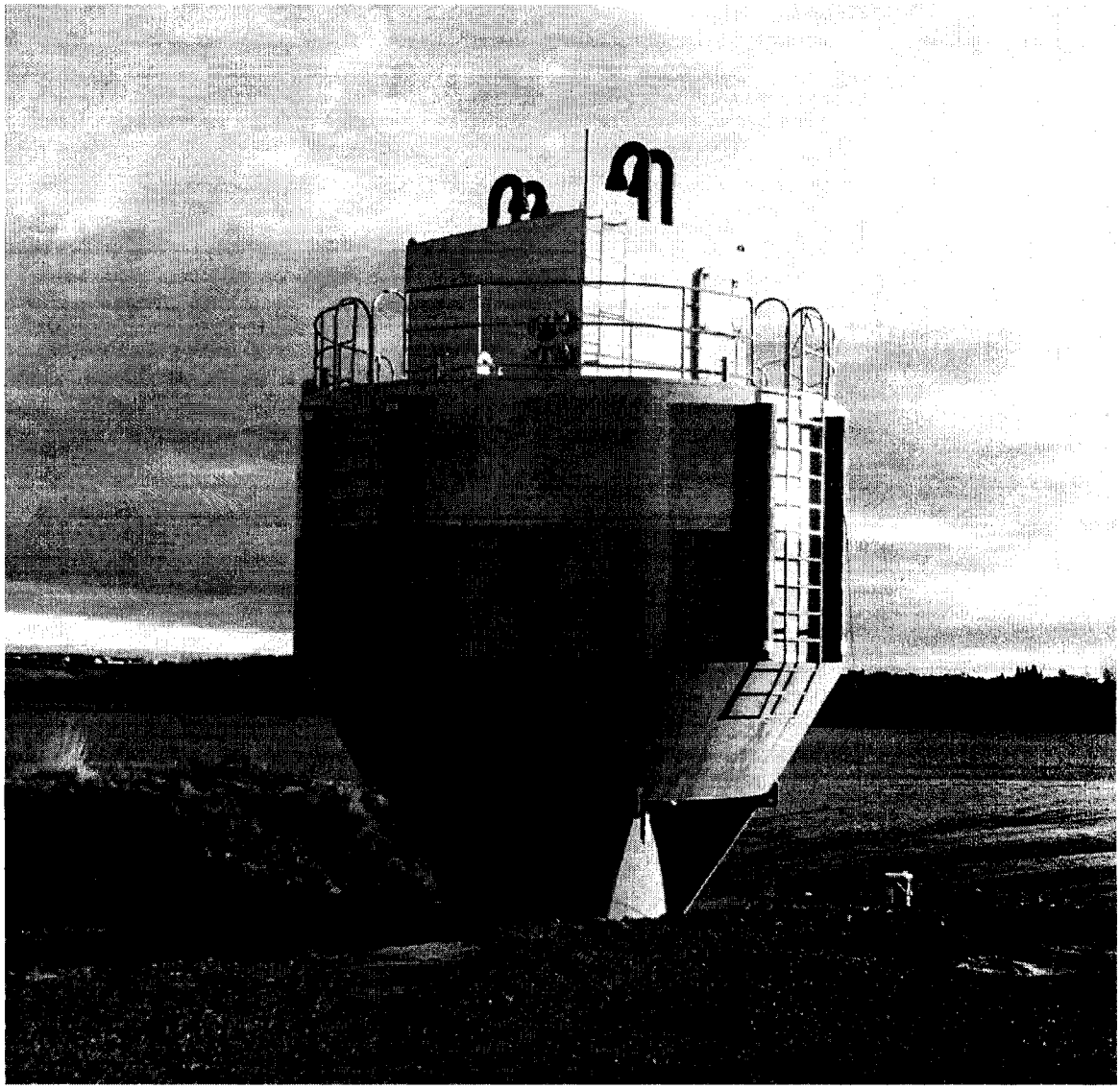

Figure 7.12: Assembled 20-ton buoy at final construction site in Hillsborough, NB, Canada.

Installation of Interior Components

Mechanical components required for the buoy's functioning were purchased and shipped to the fabrication site. These items included major items such as: four feed storage silos, two aluminum fuel tanks, generator, mixing chamber, four flex-augers, and fiberglass piping. Numerous small items were also purchased and delivered to the site. These purchases were made during the major hull construction process.

The first major item installed in the buoy was the concrete ballast that was poured into the Ballast Can (see Figure 7.13). Figure 7.14 shows one flex auger motor

bolted to a support structure welded inside the Machine House. Figure 7.15 shows the lower portion of one flex auger attached to the silo. Figure 7.16 shows the mixing chamber bolted to its support (left), as well as other internal items including: silos, flex augers, supply pump, and piping.

Figure 7.13: Close-up picture of Ballast Can filled with concrete (left), as well as the Chine Level weld interface.

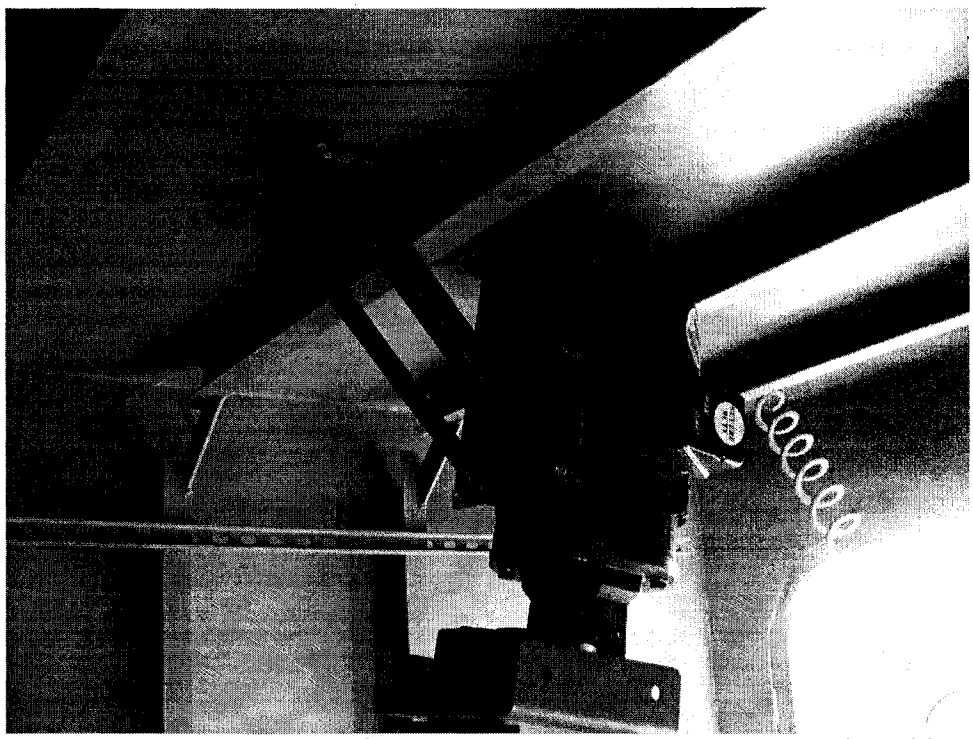

Figure 7.14: Interior feed transport flex-auger motor mounted to ceiling of Machine House.

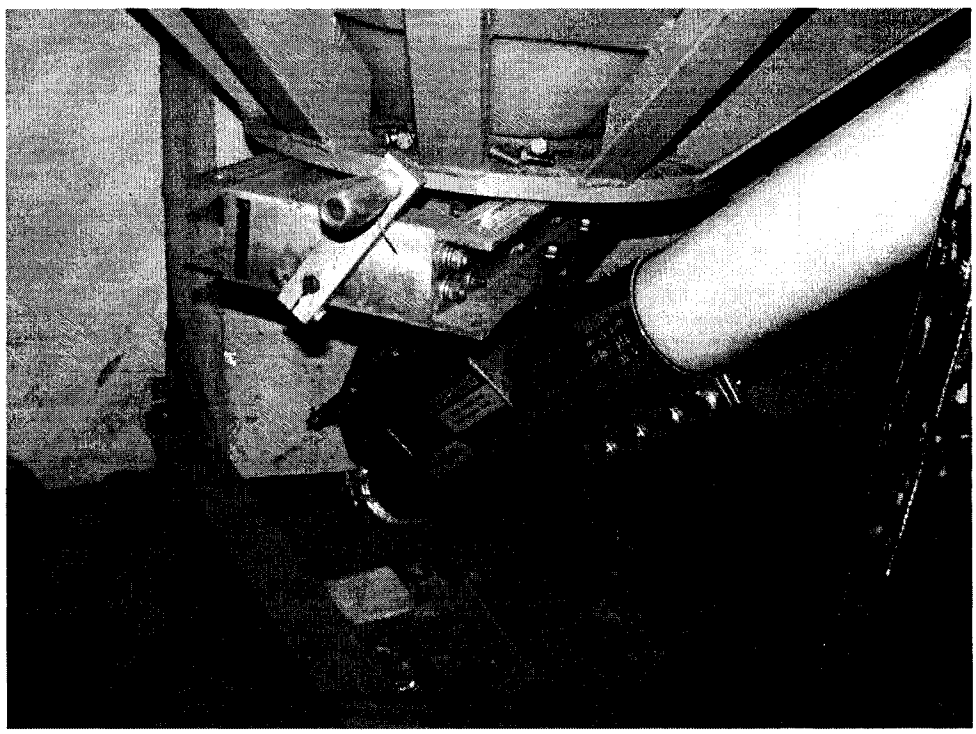

Figure 7.15: Interior feed transport charging adapter bolted to bottom of silo support.

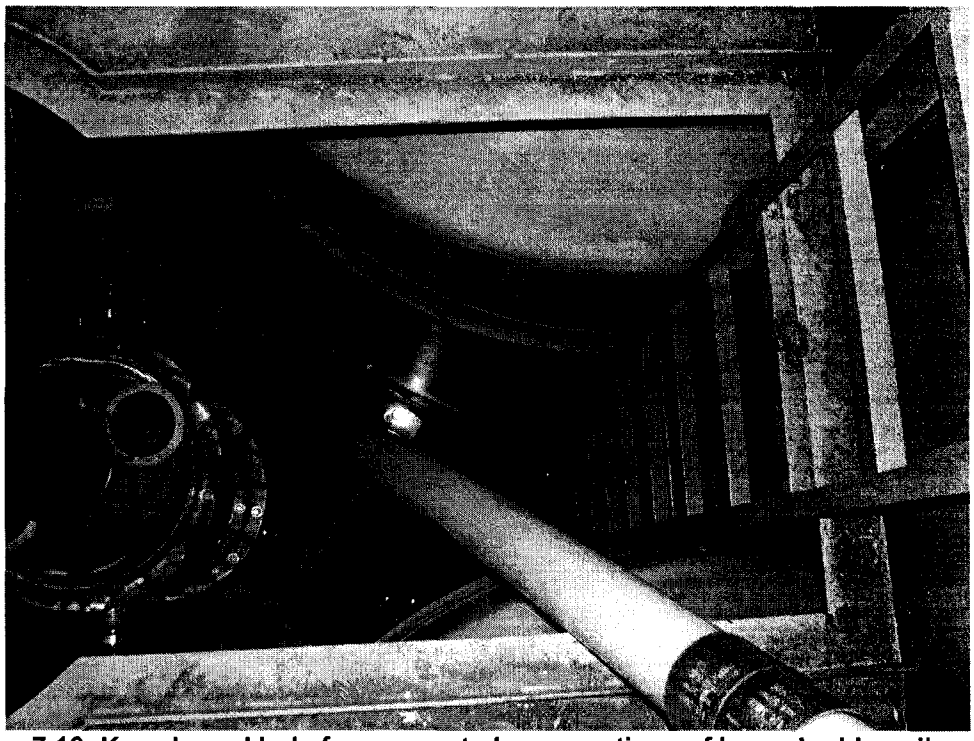

Figure 7.16: Key shaped hole for access to lower sections of buoy. Ladder, silos, flex-augers, and mixing chamber are visible installed in the buoy.

Some other items that were assembled and subsequently bolted inside the buoy are the internal piping system as well as the generator's keel cooler. The fiberglass piping components were bolted into subassemblies and then affixed inside the buoy. Figure 7.17 shows some fiberglass fittings being bolted together. The keel cooler (see Figure 7.18) was also bolted to the exterior of the buoy.

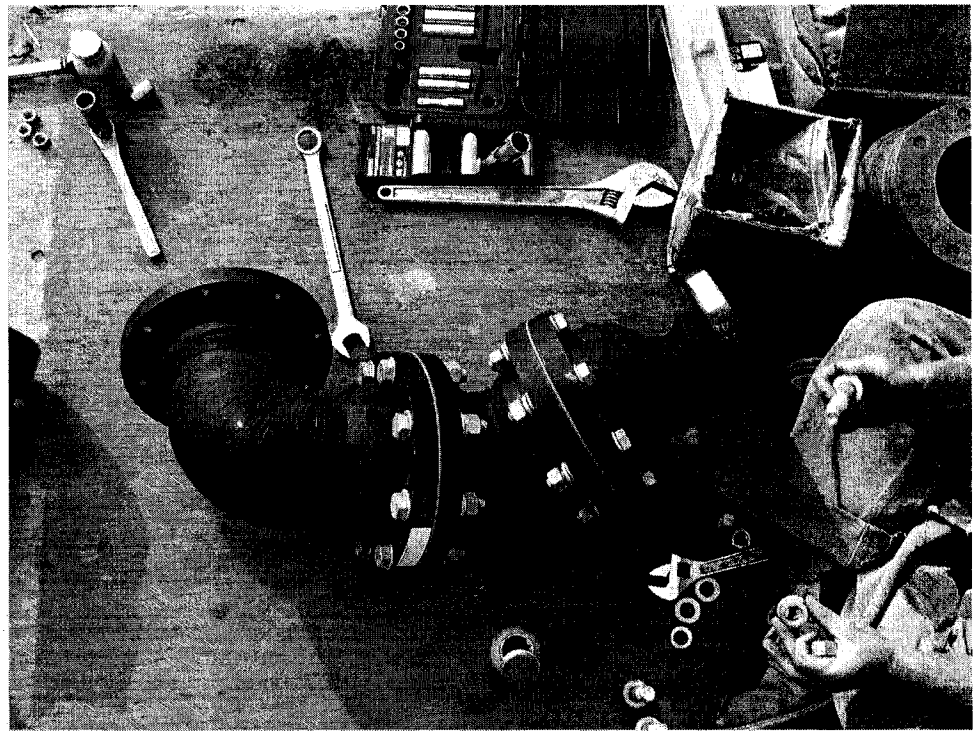

Figure 7.17: Fiberglass piping component being assembled.

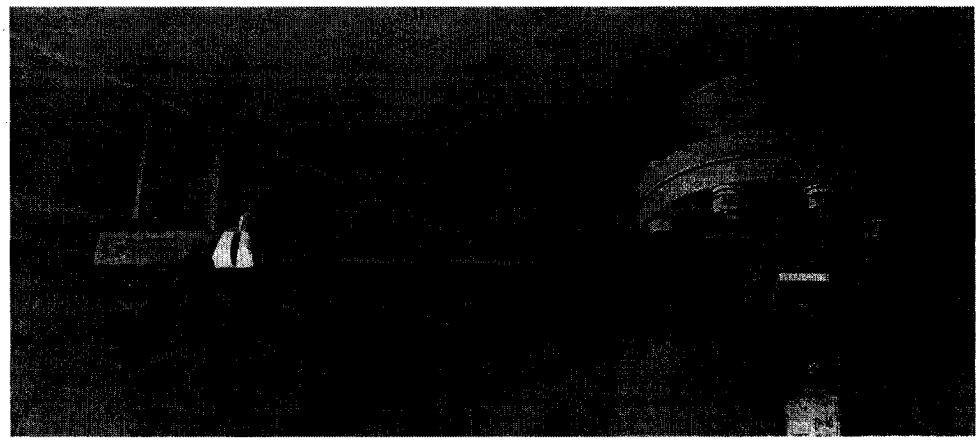

Figure 7.18: Keel cooler mounted to outside of buoy.

Unexpected Construction Problems

The construction progress was slower than anticipated due to internal components not arriving in a timely manner to the fabrication facility. The delays have predominately been the result of component manufactures' late completion of parts. These delays resulted in the completion date for the buoy being pushed back until the spring of 2007.

Aside from components arriving in an untimely manner, the construction was not without problems. One major component, the feed storage silos, was not manufactured to the tolerances that were provided by the manufacturer upon purchase. The silo's diameter was larger than specified and would not fit in the holes that were in the Sub-Main Deck and Chine Deck. As a fix, these holes were enlarged to allow the insertion of the large diameter silos into position.

Other problems were minor and were typical during a construction project of this scale. Most of these problems consisted of parts delayed, due to the manufactures time line. Other delays consisted of construction time for items not planned for during the design phase of the project.

Control and Telemetry

In an effort to expedite the delivery of the buoy to New Hampshire waters, the Control and Telemetry electronics design and installation were outsourced to AEG. This allows the buoy to go straight into service, upon delivery to UNH, instead of having a significant electronic installation and testing time while in New Hampshire. However, significant testing of the internal systems and the electronics will be done by AEG and UNH personnel before delivery.

4. Costs

Aside from the base construction costs of the buoy, numerous parts and internal components were purchased for the buoy. Table 7.1 shows the components and prices for the buoy. All prices and values are current as of 19 March 2007.

Table 7.1: Costs of buoy construction and parts. Prices shown are in US dollars.

	Purchased From	Quantity	Total
Shell/Structure			
Feed Buoy Shell/Structure (including delivery to NH)	Aquaculture Engineering Group (AEG)	1	$266,530.00
		sub-Total	$266,530.00
Silos (Feed Storage)			
Silos	US Plastics	4	$9,879.12
Misc.	N/A	N/A	$473.30
		sub-Total	$10,352.42
Internal Feed transport			
Auger System	Flexicon	1	$31,500.00
Knife gates	Salina-Vortex	4	$2,440.00
Cyclones	Lorenz	2	$2,672.72
Misc.	N/A	N/A	$1,369.50
		sub-Total	$37,982.22
External Feeding system			
Feed pump	Weir Specialty Pumps	1	$14,581.06
Supply pump	Pump Biz	1	$1,093.00
Mixing Chamber	Macy Industries	1	$7,982.50
Rotary Airlock	Prater	1	$5,461.00
Collection Hopper	US Plastics	1	$112.63
Collection Hopper Fitting	Macy Industries	1	$550.00
Piping (fiberglass pipe and fittings)	Conley	1	$7,223.60
Piping (PVC ball valves)	F.W. Webb	1	$8,298.80
Feed pump VFD controller	Stultz Electric Motor & Controls, Inc.	1	$918.49
Fasteners	Fastener Warehouse	N/A	$2,367.12
Misc.	N/A	N/A	$4,301.66
		sub-Total	**$52,889.86**
Fuel system			
Fuel tanks	Luther's Welding	2	$3,900.00
Fuel Tank Fittings	McMaster-Carr	1	$656.82
Misc.	N/A	N/A	$497.03
		sub-Total	$5,053.85

Table 7.1: Continued

Generator/Cooler			
Kohler 20 kW Generator	J&D Power Equipment	1	$14,580.13
	Purchased From	**Quantity**	**Total**
GRIDCOOLER® Keel Cooler	Fernstrum	1	$959.00
Misc.	N/A	N/A	$1,098.02
		sub-Total	$15,678.15
Fenders			
D-Shape Vessel Fenders	Maritime International, Inc.	8	$10,695.20
		sub-Total	$10,695.20
Miscellaneous			
Misc. tools, supplies, and parts	Various	N/A	$2,817.21
		sub-Total	$2,817.21
		TOTAL	$401,998.91
NOTES: Prices shown include shipping charges (where applicable)			

5. Launch Site

Due to the buoy's size and weight, final assembly was performed at a launch site in Hillsborough, NB, Canada on the Bay of Fundy. The site is only a few miles from the main fabrication facility where the buoy components were constructed. Figure 7.19 shows the completed buoy exterior structure at the launch site.

Figure 7.19: Completed buoy at launch site in Hillsborough, NB, Canada.

The launch plan is to make use of the extremely large tidal range of the Bay of Fundy and push the buoy into the ocean on a large spring tide. Figure 7.20 shows the buoy (at an earlier stage of completion) during a weak high tide event. During a spring tide event a portion of the Ballast Can is submerged, including the grasses to the right of the buoy in Figure 7.20. Once the buoy is floating it will be towed to a mooring in St. Andrews, New Brunswick, Canada for testing and evaluation before being delivered to UNH.

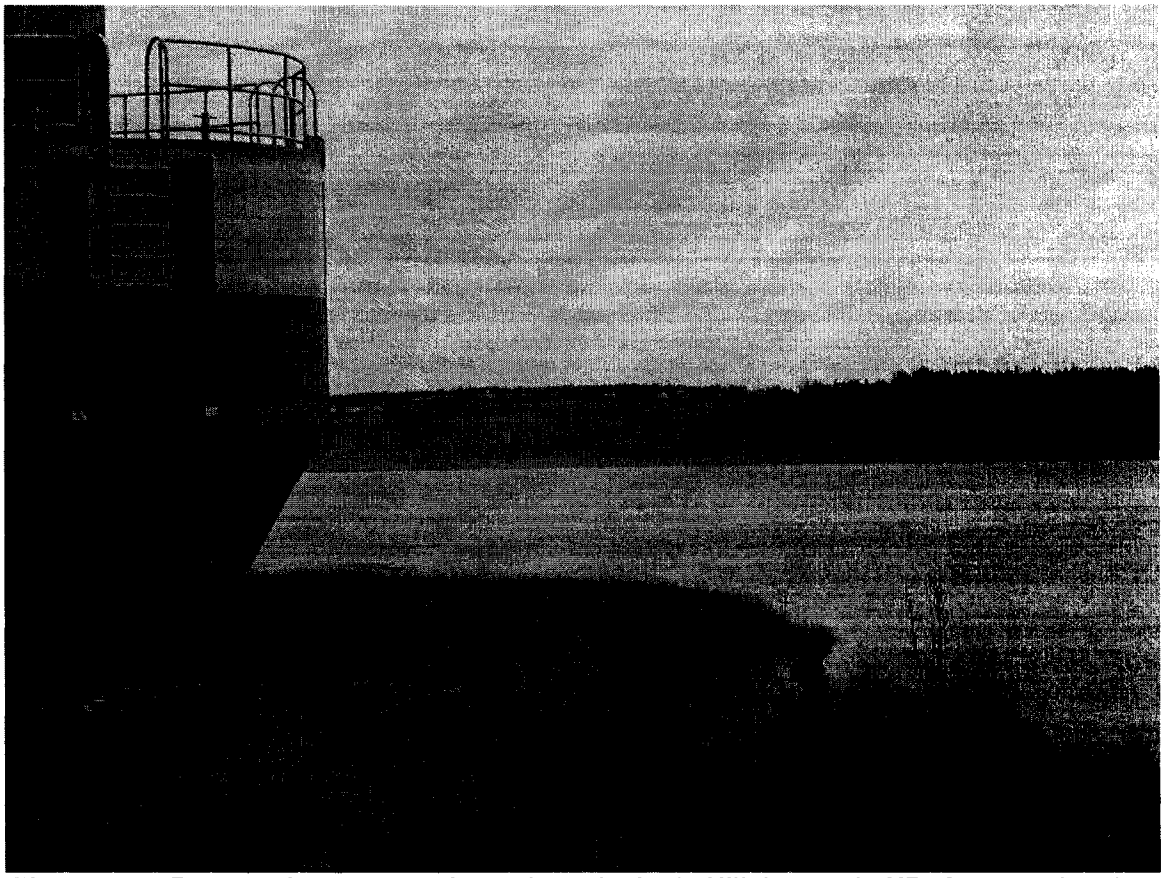

Figure 7.20: Buoy under construction at launch site in Hillsborough, NB, Canada showing the water height at a moderate high tide.

CHAPTER VIII

CONCLUSION

The design, analysis, and construction of an open ocean aquaculture 20-ton capacity feeding buoy was completed. Experimental testing was performed on the feed transfer system designs. Extensive hydrostatic analyses were performed on the hull design to ensure a positive righting moment at all angles of heel. A physical scale model was constructed and subjected to free-release and regular wave testing. A numerical model of the buoy was generated using MARC.Mentat and subjected to the same type of testing as the physical scale model using Aqua-FE. The results of the physical and numerical model were compared. The mooring system for the buoy was designed using the numerical model and Aqua-FE. The buoy was constructed and is scheduled for deployment in the summer of 2007.

All components required for feeding operations were incorporated into the design of the buoy hull. The hull was designed to withstand the harsh environmental conditions expected at the UNH OOA site. Iterative hydrostatic analyses were performed on the hull to ensure the metacentric height (GM) was positive under all loading conditions. These loading conditions consisted of load (full feed and fuel), light (no feed or fuel), and ice (with ice on the exterior surface of the hull). All testing conditions resulted in positive GM values, indicating satisfactory, initial stability of the buoy.

To investigate the buoy's dynamic response in an ocean environment, physical scale model testing and numerical model testing was performed. Based upon the physical and numerical model tests, the buoy is a wave follower with respect to vertical motion for large, long period waves that occur during storms. Heave resonance occurs of higher frequencies associated with small, fair-weather waves. In general, the buoy should not have severe reactions in response to the wave spectra that are normally observed at the expected buoy location.

Comparison between the results of the physical and numerical model testing shows that with the exception of the Surge RAO plot, the curve shapes for the RAO plots are similar. However, the differences between the physical and numerical free-release tests are minor. This leads to the conclusion that the data obtained using the numerical model, and the physical model corroborate one another.

The buoy is scheduled to be deployed in the summer of 2007. With the buoy properly moored in the northeast corner of the UNH OOA grid, buoy operations should not interfere with the submerged grid. Based upon the analysis of the buoy mooring design the buoy will be securely held in location, even under extreme environmental loading.

While deployed at the site, the buoy's feeding systems will be tested. Electrical systems will also be tested extensively. The results of testing of the buoy's systems are vital to determining the future of feed buoy design at UNH. In response to the upcoming results of the buoy's performance at the UNH OOA site, the next generation feed buoy hull design could have a different hull shape and internal configuration.

All goals for the latest UNH feed buoy were met, including developing a new feed delivery system for feed stored low in the buoy. All testing performed on the buoy hull shape demonstrates the buoy should have the hydrodynamic stability for all environmental conditions at the UNH OOA site. Regardless of the location for an

aquaculture site, a semi-autonomous feeding platform that requires less action or input by fish farmers would be beneficial and this buoy should provide valuable insight into the design of such a system.

LIST OF REFERENCES

Baldwin, K., B. Celikkol, R. Steen, D. Michelin, E. Muller, P. Lavoie (2000). Open Aquaculture Engineering: Mooring and Net Pen Deployment. Mar. Tech. Soc. J. Washington D.C. Vol 34, No. 1 pp 53-67.

Celikkol, B., J. DeCew, K. Baldwin, S. Boduch, M. Chambers, D.W. Fredriksson, J.D. Irish, O. Patursson, G. Rice, M.R. Swift, I. Tsukrov, and C.A. Turmelle, "Engineering Overview of the University of New Hampshire's Open Ocean Aquaculture Project," Proc. Oceans06, Boston MA, Sept, 2006.

Chakrabarti, S.K. (1994). Offshore Structure Modeling. World Scientific Publishing Company, Singapore. 470 p

Dean, R.G. and Dalrymple R.A. (1984). Water Wave Mechanics for Engineers and Scientists. World Scientific Publishing Company, Singapore 353 p

Fredriksson, D.W., M.R. Swift, E. Muller, K. Baldwin and B. Celikkol. (2000). Open Ocean Aquaculture Engineering: System Design and Physical Modeling. Mar. Tech. Soc. J. Washington D.C. Vol 34, No. 1 pp 41-52.

Fredriksson, D.W., J. DeCew, M.R. Swift, I. Tsukrov, M.D. Chambers, and B. Celikkol. (2004a). The Design and Analysis of a Four-Cage, Grid Mooring for Open Ocean Aquaculture. Aqua. Eng. Vol 32 (1) pp 77-94.

Fredriksson, D.W., J. DeCew, J. Irish, V. Panchang, D. Li and I. Tsukrov (2004b). SK Progress Report for the period between January 1, 2004 and June 30, 2004. Project Title: Engineering Design and Analysis for More Secure Salmon Net Pen Systems. Grant # NA03NMF4270183.

Fullerton, B. Swift, M.R., Boduch, S., Eroshkin, O. and G. Rice, (2004). "Design and Analysis of an Automated Feed Buoy for Submerged Cages." Aqua. Eng. Vol 95 (1) pp. 95-111.

Michelin, D. and Scott, S. (1996) "Optical Positioning, Instrumentation and Evaluation", Ocean Projects Course Final Report, Tech 797, Sea Grant, Kingman Farm, University of New Hampshire, Durham, NH, 85 p.

Palczynski, M.J. (2000). Fish Cage Physical Modeling. M.S. Thesis, Ocean Engineering, University of New Hampshire, Durham, NH, 111 p.

Principles of Naval Architecture, (1988) E.V. Lewis (ed.), Society of Naval Architects and Marine Engineers, Jersey City, NJ.

Rice, G.A., M.D. Chambers, M. Stommel, O. Eroshkin. (2003). The Design, Construction and Testing of the University of New Hampshire Feed Buoy in C.J. Bridger and B.A. Costa-Pierce, editors. Open Ocean Aquaculture: From Research to Commercial Reality. The World Aquaculture Society, Baton Rouge, Louisiana, United States, 197-203.

Tsukrov, I., Ozbay, M., Fredriksson, D.W., Swift, M.R., Baldwin, K., and Celikkol B., 2000. Open Ocean Aquaculture Engineering: Numerical Modeling. Mar. Tech. Soc. J. 34 (1), 29-40.

Tsukrov, I., O. Eroshkin, D. Fredriksson, M.R. Swift and B. Celikkol. (2002). "Finite Element Modeling of Net Panels Using Consistent Net Element," Ocean Engineering. 30: 251-270.

Tupper, E (1996), Introduction to Naval Architecture. The Society of Naval Architects and Marine Engineers, USA 361 p

APPENDIX

"UPPER" MOORING ATTACHMENT PHYSICAL MODEL TESTING

In an effort to minimize the pitch response that was observed from previous wave model tests, a second set of tests were conducted. This series of wave tests used a higher "Upper" mooring attachment location, closer to the center of gravity of the buoy (see Figure A.1). The original tests were conducted using the "Lower" mooring attachment. The buoy physical model was altered (December 2005) with the addition of two new mooring attachment points.

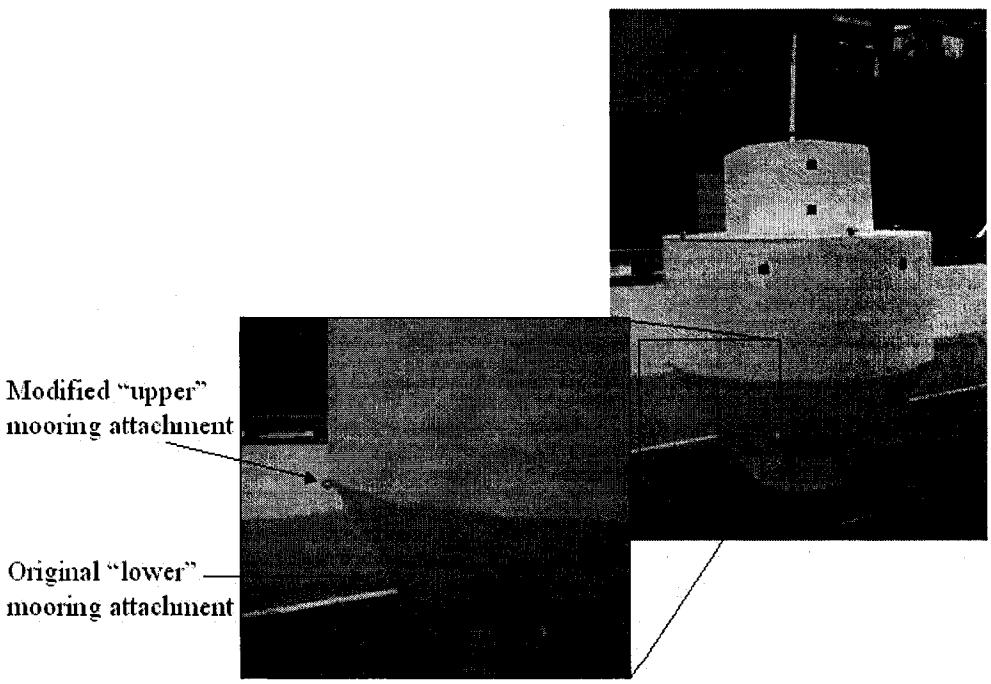

Figure A.1: The physical model used for testing with close-up view of "upper" mooring attachment.

The modified buoy was tested in December 2005 and January 2006 in the UNH wave/tow tank. The wave tests were conducted over the same range of wave profile inputs as that of the original tests (see Chapter IV).

The purpose of the wave testing was to compare the Heave, Surge, and Pitch Response Amplitude Operators (RAOs) between the two mooring attachment locations. The following three figures show the RAOs that were calculated for the buoy in the load and light displacement conditions as well as the "Upper" and "Lower" mooring attachment configurations.

The movement of the mooring attachment location provided similar results compared with the previous buoy analysis (original, lower mooring attachment) as described in Chapter IV. The changes in the RAO values for the different mooring attachment points did not justify the significant design changes that would have arisen from moving the buoy mooring attachment point. The mooring location on the buoy will remain at the "Lower" attachment point.